

Offshore Windfarm

Eneco Luchterduinen

Ecological monitoring of seabirds

T2 report



December 2017

ISO 9001
Management System Certification

BUREAU VERITAS
Certification Denmark A/S



Offshore Windfarm

Eneco Luchterduinen

Ecological monitoring of seabirds

T2 report

Prepared for ENECO
 Represented by Ms. Sytske van den Akker



Photo by Thomas W Johansen

| | |
|--------------------|--|
| Project manager | Henrik Skov |
| Author | Henrik Skov Stefan Heinänen Martin Lazcny Magda Chudzinska |
| Quality supervisor | Ramunas Zydelis |

| | |
|----------------|------------------|
| Project number | 11813060 |
| Approval date | 17 December 2017 |
| Revision | Revised |
| Classification | Confidential |

CONTENTS

| | | |
|----------|---|-----------|
| 1 | Abbreviations | 3 |
| 2 | Executive summary | 4 |
| 3 | Introduction | 5 |
| 4 | Materials and methods | 6 |
| 4.1 | Monitoring approach | 6 |
| 4.2 | Survey design and available data | 7 |
| 4.3 | Seabird counting techniques | 8 |
| 4.4 | Quality control and post-processing of survey data | 10 |
| 4.5 | Distance analysis | 10 |
| 4.6 | Distribution models | 12 |
| 4.7 | Analysis of displacement and number of included surveys | 15 |
| 4.8 | Presentation of data | 17 |
| 5 | Results | 17 |
| 5.1 | Effort and sample sizes | 17 |
| 5.2 | Distance analysis | 20 |
| 5.3 | Species accounts | 20 |
| 5.3.1 | <i>Divers: Red-throated Gavia stellata and Black-throated Divers Gavia arctica</i> | 20 |
| 5.3.2 | <i>Great Crested Grebe Podiceps cristatus</i> | 24 |
| 5.3.3 | <i>Northern Gannet Morus bassanus</i> | 28 |
| 5.3.4 | <i>Great Cormorant Phalacrocorax carbo</i> | 34 |
| 5.3.5 | <i>Little Gull Hydrocoloeus minutus</i> | 38 |
| 5.3.6 | <i>Black-headed Gull Chroicocephalus ridibundus</i> | 42 |
| 5.3.7 | <i>Common Gull Larus canus</i> | 46 |
| 5.3.8 | <i>Lesser Black-backed Gull Larus fuscus</i> | 50 |
| 5.3.9 | <i>Herring Gull Larus argentatus</i> | 54 |
| 5.3.10 | <i>Great Black-backed Gull Larus marinus</i> | 58 |
| 5.3.11 | <i>Black-legged Kittiwake Rissa tridactyla</i> | 62 |
| 5.3.12 | <i>Common Guillemot Uria aalge</i> | 66 |
| 5.3.13 | <i>Razorbill Alca torda</i> | 72 |
| 5.3.14 | <i>Marine mammal observations</i> | 77 |
| 6 | Discussion | 79 |
| 7 | References | 80 |
| | APPENDIX A – Detailed results of species distribution models for the T-1 surveys | 82 |

1 Abbreviations

| | |
|------|---|
| AIC | Akaike Information Criterion |
| AUC | Area Under Curve. Probability of correctly predicting presence of species |
| EEZ | Dutch Exclusive Economic Zone |
| EIA | Environmental Impact Assessment |
| ESW | Effective Strip Width |
| GAM | Generalized Additive Model |
| LUD | Offshore Windfarm Eneco Luchterduinen |
| LAT | Lowest Astronomical Tide |
| MEP | Monitoring and Evaluation Program |
| OWEZ | Offshore Windfarm Egmond aan Zee |
| OWF | Offshore Windfarm |
| PAWP | Prinses Amalia windfarm |
| TOR | Terms of Reference |
| UTM | Universal Transverse Mercator |
| WTG | Wind Turbine Generator |

2 Executive summary

The T2 report provides the results from the second year of the Offshore Windfarm Eneco Luchterduinen (LUD) seabird monitoring program regarding displacement of seabirds from LUD as well as updated results from PAWP and OWEZ. The dynamic modelling and simulation framework, which was tested during LUD-T1 was applied on all available data from the three windfarms including the data collected during the four LUD-T2 surveys. The LUD-T1 report indicated that high power would be achievable after T2 for Common Guillemot (detection of a displacement of 50%), whereas the power of the data for Northern Gannet would be too low to detect reductions of 50% of this species from LUD after T2. The results of the updated power tests and simulations in this report corroborate these findings.

Based on the power simulations the displacement of Northern Gannets at LUD is probably in the range between 50% and 75%. The simulations indicated that a high power (above 0.8) can only be achieved either with 75% displacement or in case of lower displacement with at least one more survey with high numbers of Gannets during LUD-T3. The degree of displacement of Common Guillemots seems to be less than for Northern Gannets. Yet due to the higher sample size the power of the data at hand from the LUD surveys is much higher for Common Guillemot. The simulations indicated that a displacement of 50% can be detected with very high power with the available data after LUD-T2. After LUD-T3 the simulations indicate that even lower levels of displacement of Common Guillemots from LUD may be detected. Based on the model predictions the level of Common Guillemot displacement from LUD is around 45% (around 30% in regards of probability of presence), when comparing prediction with and without the windfarm response level. The level of Northern Gannet displacement from LUD is according to the model predictions higher, around 70% regarding densities and around 55% regarding probability of presence.

The LUD-T2 results are generally in line with the results from LUD-T1 and other studies like Krijgsveld (2014) and Welcker & Nehls (2016), see (Table 0). The LUD-T1 distribution models indicated negative responses of Northern Gannets (2 km avoidance) and Common Guillemot (2-4 km avoidance) to PAWP and OWEZ. The updated results now indicate that a 2 km avoidance zone is more realistic than 2-4 km for Common Guillemot at all three windfarms. Several species including Black-legged Kittiwake and Razorbill showed a significantly lower probability of occurrence at PAWP, while no clear effect was seen at LUD and OWEZ. It seems plausible that this difference in displacement effect is related to the shorter distance between turbines in PAWP as compared to the other two windfarms.

Table 0. Summary of species-specific responses to the LUD, PAWP and OWEZ windfarms, significant displacement/attraction or no significant impact. Significance of both model parts are given for each windfarm (presence-absence/positive model part), ns = not significant. In the last column the results of a review of displacement patterns from several windfarms presented in Welcker & Nehls 2016 are given for comparison with other studies.

| Species | LUD | PAWP | OWEZ | General review (Welcker & Nehls 2016) |
|---------------------|-----------------------------|-----------------------------|--------------------------|---------------------------------------|
| Divers | Out of range (not included) | Out of range (not included) | Displacement, <0.001/- | 10/10 displacement |
| Great Crested Grebe | Out of range (not included) | Out of range (not included) | <0.05/ns | - |
| Northern Gannet | Displacement 0.001/ns | Displacement <0.001/ns | Displacement <0.001/ns | 8/10 displacement |
| Great Cormorant | Attraction <0.001/ns | Attraction <0.001/ns | Attraction <0.001/<0.001 | - |
| Little Gull | (not included) | (not included) | Displacement <0.01/ns | 5/8 displacement |
| Black-headed Gull | Displacement <0.001/ns | No sig. impact ns/ns | No sig. impact ns/ns | - |
| Common Gull | No sig. impact ns/ns | No sig. impact ns/ns | No sig. impact ns/ns | 5/6 no displacement |

| | | | | |
|---------------------------|------------------------------|-------------------------------|---------------------------|------------------------------------|
| Lesser Black-backed Gull | Displacement <0.01/ns | No sig. impact ns/ns | No sig. impact ns/ns | 5/8 no displacement |
| Herring Gull | Attraction <0.05/ns | Attraction <0.05/ns | No sig. impact ns/ns | 6/8 no displacement |
| Greater Black-backed Gull | No sig. impact ns/ns | Attraction <0.01/ns | No sig. impact ns/ns | 5/7 no displacement, 2 attractions |
| Black-legged Kittiwake | No sig. impact ns/ns | Displacement 0.01/<0.05 | No sig. impact ns/ns | 5/7 no displacement |
| Common Guillemot | Displacement <0.001/<0.05 | Displacement <0.001/<0.001 | Displacement <0.001/ns | 9/11 displacement (Alcids pooled) |
| Razorbill | No sig. impact ns/ns | Displacement <0.01/ns | No sig. impact ns/ns | 9/11 displacement (Alcids pooled) |

Based on the LUD-T2 results it seems most likely given the oceanographic variability, mobile behaviour and hence variability of abundance of Northern Gannet and Common Guillemot at LUD that detection of reductions in density of 70% and 45% respectively of these species from this wind farm will require data from LUD-T3. It is therefore recommended to finalise surveys as planned under LUD-T3.

In addition to these results for the two key species, a number of interesting observations were made during the T2 surveys, including relatively large numbers of Red-throated Divers and Great Crested Grebes in coastal waters, large numbers of Common and Velvet Scoter during the December 2016 survey, concentrations of Little Gull at the southern edge of LUD during the March 2017 survey and very large numbers of Lesser Black-backed Gulls during the March survey. The latter observation was a concentration of gulls at a working trawler close by LUD. The T2 surveys also resulted in 90 sightings of 128 harbour porpoise around LUD and PAWP and off IJmuiden. The largest number of animals was observed around and in the periphery of LUD.

3 Introduction

Construction of the Offshore Windfarm Eneco Luchterduinen (LUD) started in 2014, and the 129 MW (43 turbines) were fully operational by summer 2015. The windfarm covers an area of 16 km². The location for the LUD is 17 km south of the existing Prinses Amaliawindpark (PAWP), roughly 23km off the coast of IJmuiden in block Q10 of the Netherlands Continental Shelf (NCS) in the Dutch Exclusive Economic Zone (EEZ). The water depth at this location ranges between 19 m and 24 m relative to LAT. The water depth and composition of the sediment underground allow for steel mono-piles to be used in conjunction with the preferred wind turbine generator (WTG) type which, under these circumstances, is the most cost effective solution. At a water depth of 25 m the WTGs require mono-piles of 51.5 m in length, with a diameter between 4.2 and 4.6 m and a transition piece of 19.1 m in length with a diameter of 4.5 m. Pile penetration in the seabed is approximately 23 m. An offshore high voltage station (OHVS) collects the generated energy at all WTGs and transforms the voltage from MV level to HV level, suited for export to shore. The windfarm is connected to the 150 kV onshore substation in Sassenheim.

OWEZ was constructed between April and August 2006, while PAWP was constructed between October 2006 and June 2008. The two windfarms have very different designs; PAWP has a much higher turbine density than OWEZ (60/17km² [3.5 WTG·km⁻²] and 36/24 km² [1.5 WTG·km⁻²] resp.) and has been built in slightly deeper waters (19-24 m versus 18-20 m) and further offshore (ca 23 km versus ca 15 km) than OWEZ.

As part of the Wbr-permit application an ‘Environmental Impact Assessment’ (EIA) and an ‘Appropriate Assessment’ were carried out. The outcome of these studies resulted in the requirement by the Competent Authority for a ‘Monitoring and Evaluation Program’ (MEP). The MEP is undertaken in conjunction with and for approval by the Competent Authority. Currently the MEP consists of eleven monitoring topics, of which seabirds is one topic. LUD is obliged to carry out a 3-5 year monitoring program on seabirds.

According to the license permit the objective of the Luchterduinen seabird monitoring program is to conduct the seabird monitoring program in a way that location specific and cumulative avoidance behaviour can be measured in LUD and the two existing offshore windfarms (OWEZ and PAWP). For this purpose, a ship-based line transect monitoring program of seabirds focusing on the winter season has been proposed by Clusius CV and approved by the Competent Authority. The program covers pre-construction (baseline), construction and post-construction phases. This report covers the results of the second year of post-construction monitoring with ship-based surveys (T-2) undertaken October-November and December 2016, January and early March 2017. The main aim of the report is to present the results of the T2 surveys and assess to what extent displacement (including cumulative displacements) of seabirds can be detected and whether there are any differences between LUD, PAWP and OWEZ with respect to the displacement of seabirds. The assessments of the LUD-T1 results should include tests, which will indicate the value of additional monitoring (T3).

Pelagic seabirds such as gannets, divers and alcids flying in the vicinity of offshore windfarms consistently show strong avoidance behaviour, with only a few exceptions (Krijgsveld 2014). Evaluations of the habitat displacement of seabirds from OWEZ and PAWP indicated strong avoidance of Northern Gannet and Common Guillemot (although they not fully avoided the windfarms). Other species showing significant avoidance behaviour were divers, Great Crested Grebe, Little Gull, Lesser Black-backed Gull, Black-legged Kittiwake and Razorbill (Leopold et al. 2013). The lay-out of the windfarms seemed to be an important factor, as the widely distributed birds avoided PAWP to a larger degree than the more widely spaced OWEZ (Leopold et al. 2013), which also partly could be due to distance from coast and differences in environmental factors related to this.

4 Materials and methods

4.1 Monitoring approach

The TORs for the seabird monitoring are to study the distribution and abundance of seabirds in the region of the three windfarms before, during and after construction of the LUD windfarm. After the post-construction surveys, the results will be evaluated (once or twice) to determine to what extent the behavioural responses of species of seabirds have been determined, and whether the ship-based surveys can be curtailed. The collected data should be used to assess the avoidance behaviour of seabirds both in relation to the LUD windfarm and as a secondary priority cumulatively to the LUD, OWEZ and PAWP windfarms. The study should be undertaken using three sets of four NE-SW oriented transects traversing the three windfarms. Each of the proposed transects measures approximately 20 km. Results of the monitoring of habitat displacement of seabirds and waterbirds at other offshore windfarms have strongly indicated displacements to a distance of 1-2 kilometers (Petersen et al. 2006, Skov et al. 2012, Welcker & Nehls (2016). Hence, the use of relatively short transect lines in the three windfarms is suitable for detecting gradients in abundance (densities) within a relatively well-defined area around each of the windfarms. Thus, the design allows to detect changes in densities between pre- and post-construction periods which can be attributed to ecological habitats (by integration of hydrodynamic data), shipping activity (by integration of AIS data) and the presence of the windfarms (Skov et al. 2015). This means that the degree of habitat displacement from all three windfarms can be tested statistically by gradient analysis.

In addition to the three series of four 20 km long primary transects through each of the LUD, OWEZ and PAWP windfarms, the monitoring approach includes a number of 30-40 km long secondary transects running east-west through the entire survey region. As habitat displacement of seabirds from offshore windfarms is typically short-scaled, this survey design provides a good basis for determining to what degree the different species of seabirds are impacted by habitat displacement, which can be determined by testing for changes in densities at increasing distances from the windfarms.

4.2 Survey design and available data

The survey design is given in Figure 4.1, showing the three series of four dense primary transects through LUD, OWEZ and PAWP designed to detect habitat displacement and the coarse set of secondary transects covering a larger region surrounding the three windfarms designed to describe distributions over a wider region. Between LUD and PAWP-OWEZ the shipping lane to/from IJmuiden is located. Two anchoring sites are associated with the shipping lane. The study area extends from about 52°30'N (Noordwijk) to about 52°45'N (Hondsbosche Zeewering) and from the shore to circa 18 nm out to sea. The size of the study area is circa 725 km². The primary transects are oriented NE-SW to capture the expected density gradient in seabirds, whereas the secondary transects are largely perpendicular to the main physical and ecological parameters, such as distance from the coast, water depth, temperature and salinity.

Four surveys in winter 2016-2017 were undertaken following the construction of the LUD windfarm. Each survey conducted during a period of five days (if permitted by the weather). The survey strategy has been to cover primary transects during all surveys, and as many of the secondary transects as possible. The primary transects were surveyed first, and surveying of the secondary transects was only initiated once the primary transects had been surveyed. The primary transects measure 209 km (+ 11 km transit) which can be covered in 12-14 hours of survey time. The secondary transects measure 660 km (+ 48 km transits). It was the strategy to achieve as much coverage as possible in the coastal and offshore environment surrounding the Luchterduinen survey area. The coverage of the secondary transects was therefore designed to achieve as much survey effort as possible on the secondary transects in the southern part of the survey region.

When crossing the three windfarms a safety distance of 250 m was kept to the turbines. During crossing of the shipping lane a minimum distance of 1000 m was maintained to all vessels in the shipping lane.

Surveys were initiated only on the basis of a forecasted weather window (less than Beaufort 5, good visibility (≥ 2 km), no heavy precipitation) of at least 2 days. Surveys should only be undertaken during sea states less than or equal to 4 and visibility of 2 km or more. Cancellation of a survey would only take place in situations with adverse weather conditions in relation to surveying (sea state above 4, visibility < 2 km) extending beyond the 5 day period of a survey.

By including the T0 and T1 data from OWEZ and PAWP (Leopold et al. 2013) data from a total of 13 surveys could be included in the analyses of habitat displacement at LUD (Table 1). In the analyses the OWEZ and PAWP T0 and T1 survey data were treated as part of the LUD baseline.

Table 1. List of available surveys included in the analyses of seabird displacement from LUD.

| Year | Survey dates | Reference |
|------|----------------------------|--------------|
| 2007 | 5-6/11 and 20-24/11 | PAWP/OWEZ T1 |
| 2008 | 14-18/1 and 3-7/11 | PAWP/OWEZ T1 |
| 2009 | 19-22/1, 5-9/10 and 2-6/11 | PAWP/OWEZ T1 |
| 2010 | 18-22/1 and 22-26/2 | PAWP/OWEZ T1 |
| 2011 | 3-7/10 and 31/10-4/11 | PAWP/OWEZ T1 |
| 2012 | 9-13/1 and 20-23/2 | PAWP/OWEZ T1 |
| 2013 | 18-22/10 | LUD T0 |
| 2014 | 10-14/1 and 19-23/1 | LUD T0 |

| | | |
|------|--|------------------|
| 2015 | 19-23/10 and 13-17/12 | LUD T1 |
| 2016 | 11-16/2 and 4-8/3 30/10 – 3/11 and 3-7/12 | LUD T1 LUD T2 |
| 2017 | 16-20/1 and 6-10/3 | LUD T2 |

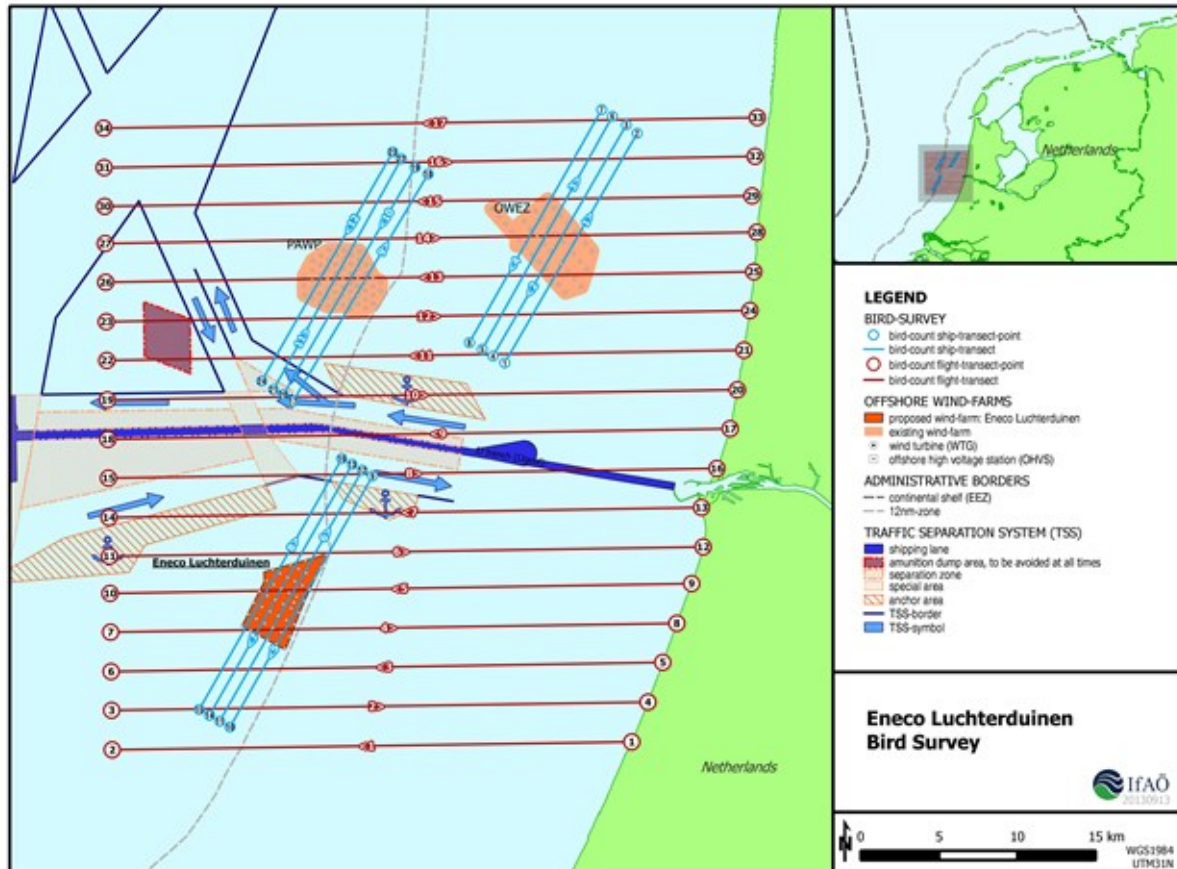


Figure 4.1. Primary (blue) and secondary (red) transects with indications of Luchterduinen, Prinses Amalia and Egmond aan Zee windfarms indicated.

4.3 Seabird counting techniques

Seabirds were recorded according to the method for surveying seabirds from ship by means of the strip-transect method as suggested by Tasker et al. 1984, Camphuysen et al. 2004 and Leopold et al. 2004, and implemented as a standard by the European Seabirds at Sea Database (ESASD). As the search mode used during previous surveys for OWEZ and PAWP was ‘naked-eye’ (Leopold et al. 2013) this mode was also used during the monitoring of seabirds for LUD. The observation height was between 6.5 and 10 m above sea level. The method is a modified strip transect with a width of 300 meter, and five perpendicular distance sub-bands:

- 0-50 m;
- 50-100 m;
- 100-200 m;
- 200 – 300 m;
- ≥ 300 m.

Transect lines were broken up into 1 minute (time) stretches and birds seen “in transect” in each individual 1 minute count were pooled (from $t=0$ to $t=1$ mins and for portside and starboard). At $t=1$ mins, the next count commenced, from $t=1$ mins to $t=2$ mins, etc. Densities were calculated as numbers seen in transect, divided by area surveyed. Area surveyed is the segment length covered in that particular 1 minute period, depending on sailing speed (average 9 knots) and strip width (300 m), which were both continuously monitored, corrected for the proportion of birds that were missed by the observers (see next section: distance sampling). The location of each count was taken as the mid-position between the positions at $t=0$ and $t=1$ mins, for each count, on the ship’s transect line.

Birds were counted from the roof of the survey ship by four bird observers (Table 2), two on each side of the ship (Figure 4.2). Swimming seabirds were counted on both sides of the ship, and snap-shot counts of flying birds were made whereby every minute all birds were counted within an area of 300 by 300 m transverse and directly in front of the ship (Figure 4.3).



Figure 4.2. The ‘Ivero’ used as the survey ship.

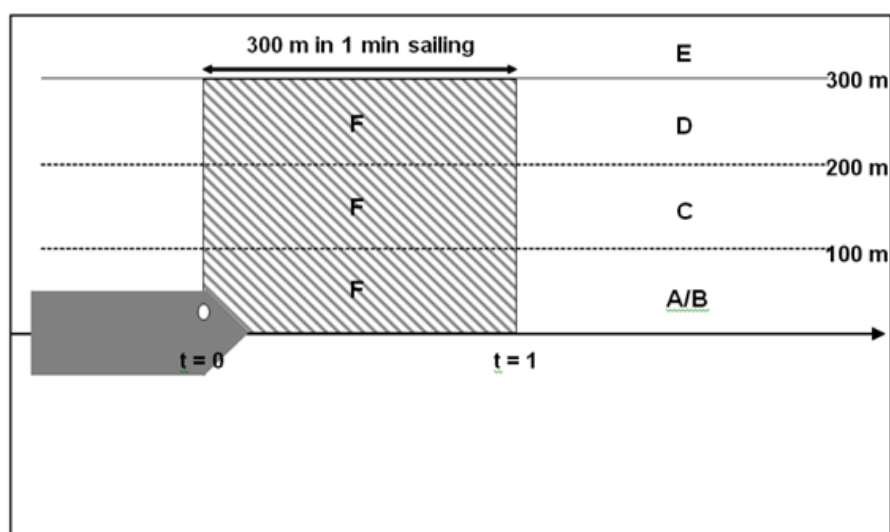


Figure 4.3. Schematic overview of the seabird survey method (see above for definitions of bands A-E).

Table 2. List of observers engaged in the LUD-T2 seabird surveys.

| Survey | Observers |
|----------|---|
| LUD-2-01 | Jörn Hartje*, Thomas Schubert, Michael J. Malinga, Ernst Eric Schrijver |
| LUD-2-02 | Jörn Hartje*, Thomas Schubert, Thomas W. Johansen, Ernst Eric Schrijver |
| LUD-2-03 | Jörn Hartje*, Thomas Schubert, Thomas W. Johansen, Ernst Eric Schrijver |
| LUD-2-04 | Jörn Hartje*, Thomas Schubert, Troels Ortvad, Michael J. Malinga |

*Cruise leader

4.4 Quality control and post-processing of survey data

General quality assurance and management were conducted and documented in accordance with internationally accepted principles for quality and environmental management as described in the DS/EN ISO 9001 standard. Post-processing of the survey data followed Leopold et al. (2013).

Before and after every survey an equipment check was carried out following an approved checklist. On the ship all routines followed strictly briefing rules with the party chief as outlined in the Work Method Statement. All observations of seabirds, marine mammals and ships were recorded on sheets and the ship's position and speed in a GPS. After each survey the GPS-track was downloaded to a computer and checked for completeness. As soon as possible after the survey the sheets were transcribed by one of the observers directly into a special developed database. Unusual data were marked and commented and the observers were asked for clarification or confirmation if needed. This procedure is very important to get rid of erroneous data as soon as possible. Later on, the data sets were run through different automated routines to detect mistyping and other errors.

All observations and GPS positions were stored in a special SQL geo-database (FULMAR) held by IFAÖ for aerial and ship-based surveys, which is linked to ArcGIS, and which exports the results to a Microsoft Access® database. The post-processing chain starts by transcribing the general survey metadata (e.g. date, observer, observation height etc.) from the observation sheets into the database. The next step is to import the GPS-track into the database by using a special extension for ArcGIS, which is started by the database. In ArcGIS the whole track is shown. The start and end points of each transect line are marked and then the track points with their position and time are imported into the database. The user of the database can now view track points, time and the columns for the sightings. Every observation will be sorted by time to the nearest 1 minute count period. Also the weather conditions which are monitored continuously during the survey are stored into the database during this step.

After finishing the data input, different tools are used to visualize the observed seabirds along the transect lines. The next step was the validation of the data by a senior biologist, who also checked the weather conditions along all the transect lines on each side of the ship according to sea state, glare and visibility. If the observations of parts of the lines are affected by strong glare, sea state over Bft 4 or poor visibility, he marks that period as "invalid". After the evaluation, and if necessary by additional confirmation of the observer, the data will be exported to a report-file, which is a Microsoft Access® database file. Here, all common types of results are generated by queries. Two tools are generating the export files for ArcGIS and population estimation in Distance.

4.5 Distance analysis

The term 'Distance analysis' used in this report refers to analyses following standard distance sampling techniques (Buckland et al. 2001) conducted using the Distance package in R (<https://cran.r-project.org/web/packages/Distance>). These analyses were conducted to calculate distance detection functions for swimming seabirds. Sitting seabirds like auks or divers may be difficult to detect in the outer

distance bands (farther away from the ship) and may also respond to the approaching survey vessel, and hence the collected densities of sitting seabirds are biased. As flying seabirds are comparatively easy to detect the collected densities of flying seabirds have been treated as unbiased, and no distance correction was applied. Flying birds were included (uncorrected) for Gannets, large gulls and small gulls. In the distance analysis all birds are assumed to be detected in the distance band closest to the ship, further away detectability decreases with increasing distance from the ship. A set of different detection function models were fitted. Half normal, hazard rate and uniform detection functions were fitted and Cosine adjustment terms were added to the models as well as Hermite polynomials (for Half-normal detection function) and simple polynomial (for the hazard rate detection function). Bird abundance and sea state were available as covariates in the models. Finally the best fitting function was chosen on the basis of the smallest Akaike Information Criterion (AIC) values (Burnham and Anderson 2002).

Detection functions were calculated for the entire dataset (dedicated project surveys) for each species with sufficient number of observations, assuming that detectability of bird species was similar among surveys, as two of four observers were the same during both surveys. Estimated detection functions were used to estimate species-specific effective strip widths (ESW), which represent the width within which the expected number of detected seabirds would be the same as the numbers actually detected within the full width of 300 m (Buckland et al. 2001). Correction factors were then calculated by $1/(ESW/300)$. In line with Leopold et al. (2013), seabird species were pooled into species groups before Distance analysis (Table 3). The abundance of each species in each segment was thereafter corrected using the correction factor. The corrected abundance was merged with the effort data and species-specific densities (birds/km²) was calculated. The data was finally re-segmented (mean density) into approximately 1 km segments, to resemble the historic data resolution. Distance correction of the historic data was done using the corrections factors (and method) reported by Leopold et al. (2013). The historic and dedicated survey data was finally merged and used in species distribution modelling.

Table 3. Grouping of species for distance analysis. Some individuals were only identified to species group level, but could be used in distance analyses for groups: small divers (G stellata/G arctica), ‘commic’ terns (S hirundo/S paradisaea) and large auks (U aalga/A torda).

| Group | Species |
|-------------|---|
| Divers | Red-throated Diver (<i>Gavia stellata</i>) |
| Divers | Black-throated Diver (<i>Gavia arctica</i>) |
| Gannets | Northern Gannet (<i>Morus bassanus</i>) |
| Cormorants | Great Cormorant (<i>Phalacrocorax carbo</i>) |
| Small gulls | Little Gull (<i>Hydrocoloeus minutus</i>) |
| Small gulls | Black-headed Gull (<i>Chroicocephalus ridibundus</i>) |
| Small gulls | Common Gull (<i>Larus canus</i>) |
| Small gulls | Black-legged Kittiwake (<i>Rissa tridactyla</i>) |
| Large gulls | Herring Gull (<i>Larus argentatus</i>) |
| Large gulls | Lesser Black-backed Gull (<i>Larus fuscus</i>) |
| Large gulls | Great Black-backed Gull (<i>Larus marinus</i>) |
| Auks | Common Guillemot (<i>Uria aalge</i>) |
| Auks | Razorbill (<i>Alca torda</i>) |

4.6 Distribution models

For the assessment of potential displacement from LUD and cumulative and in-combination displacement with PAWP and OWEZ, fine-scale distribution models capable of describing the distribution during the LUD post-construction period were developed in line with the baseline models (Skov et al. 2015). In this study a cumulative effect is defined as a displacement from one windfarm affecting the occurrence of the displaced species at another windfarm. The in-combination effect is defined as the combined detection of displacement, i.e. is a bird species displaced from all windfarms or only one or two? For the purpose of this LUD-T2 report the distribution models were mainly developed with the aim to assess the “power” of detecting a significant displacement of seabirds (see chapter 4.7). To enhance the power of detecting a displacement in a highly variable environment it is important to include the factors causing the large variability and account for any unexplained spatial autocorrelation (Perez-Lapena 2010). In one survey seabirds might be in a specific location due to suitable oceanographic conditions which enhance the availability of prey fish. In another survey the condition might be unsuitable and the seabirds therefore absent. If this location happens to be the windfarm it can be difficult to assess a displacement effect if the important factors driving the distribution are not included. In order to assess the impact of LUD (in terms of statistically significant displacement) and map the survey-specific distribution of seabirds during the LUD-T2 winter of 2016-2017, prediction models were therefore applied taking both static (depth) and dynamic habitat conditions (salinity, current speed, eddy potential, current gradient and water depth) as well as pressures (location of the windfarms and shipping intensity AIS) into account. AIS counts of ships were analysed by MARIN www.marin.nl by aggregating the number of ships entering a grid cell of 1000 by 1000 meter over the course of each of the 23 survey periods (see Table 1). A factor variable with each survey as a level was also included as a fixed factor, enabling survey specific predictions and simulations.

The hydrodynamic variables (fixed factors) salinity, current speed, eddy potential (vorticity) and current gradient were extracted to the survey data as mean values during each survey period (whole days), together with water depth and windfarm footprints and 2 km buffer around the windfarms as factor levels (for each windfarm compared to the area outside, i.e. 7 levels in total). In the baseline and T1 report a distance to windfarms truncated at 4 km was used however as there is a potential problem with collinearity with separate distance variables for each windfarm we changed the response variable to a factor variable in the analyses for the T2 report. The environmental variables are mapped in Figure 4.4 for the four surveys during LUD-T2. Data from 2007 until 2017 were included and the two surveys conducted during construction (October 2014 and December 2014) were excluded from the species-specific models, so in total 23 surveys were included. Surveys with no-records (or only 1-2 records) of the model species were also dropped, if any. Generalized additive mixed models (GAMMs) were used as these are capable of fitting different family distributions and nonlinear responses (Hastie & Tibshirani 1990), which are expected between seabirds and habitat variables. The mixed models can also account for potential temporal and spatial autocorrelation in model residuals. To account for zero inflation a two-step model (hurdle model) was fitted consisting of a presence-absence model and a positive model part (densities) where all zeroes were excluded.

The autocorrelation was accounted for by adding a correlation structure (corAR1 or corARMA), grouped by survey hour (in accordance with Leopold et al. 2013), to account for the temporal and spatial autocorrelation. The “`gamm`” function in “`mgcv`” R package was used for fitting the models. The species-specific models were fitted in a stepwise manner, an initial full model was first fitted including all environmental variables and further simplified by dropping uninfluential variables in a stepwise manner. Variables displaying ecologically unrealistic shapes (for example if divers would show a preference of high shipping intensity, or grebes would prefer very deep water response that we know from experience is wrong) were also dropped. The windfarm factor variable were always retained in the model, being significant or not. The model residuals were checked for autocorrelation using a correlogram. The models were evaluated for predictive accuracy by fitting the model on 70% or 80% of the data (randomly selected) and predicted on the 30%/20% withheld data. However, many of the models do not converge on smaller sample sizes and for these models no evaluation results are shown. The presence-absence model part was tested using AUC and the combined density predictions using Spearman’s correlation coefficient.

The species-specific models were finally used for predicting the distribution of mean densities in the whole study area during a range of different surveys. The mean density of the post construction (LUD) surveys were calculated and mapped together with corresponding number of pre-construction surveys (i.e. if eight

post construction surveys were analysed, the mean of eight pre-construction model predictions was also calculated. The change in density between these two periods was also mapped to illustrate potential predicted displacement or attraction.

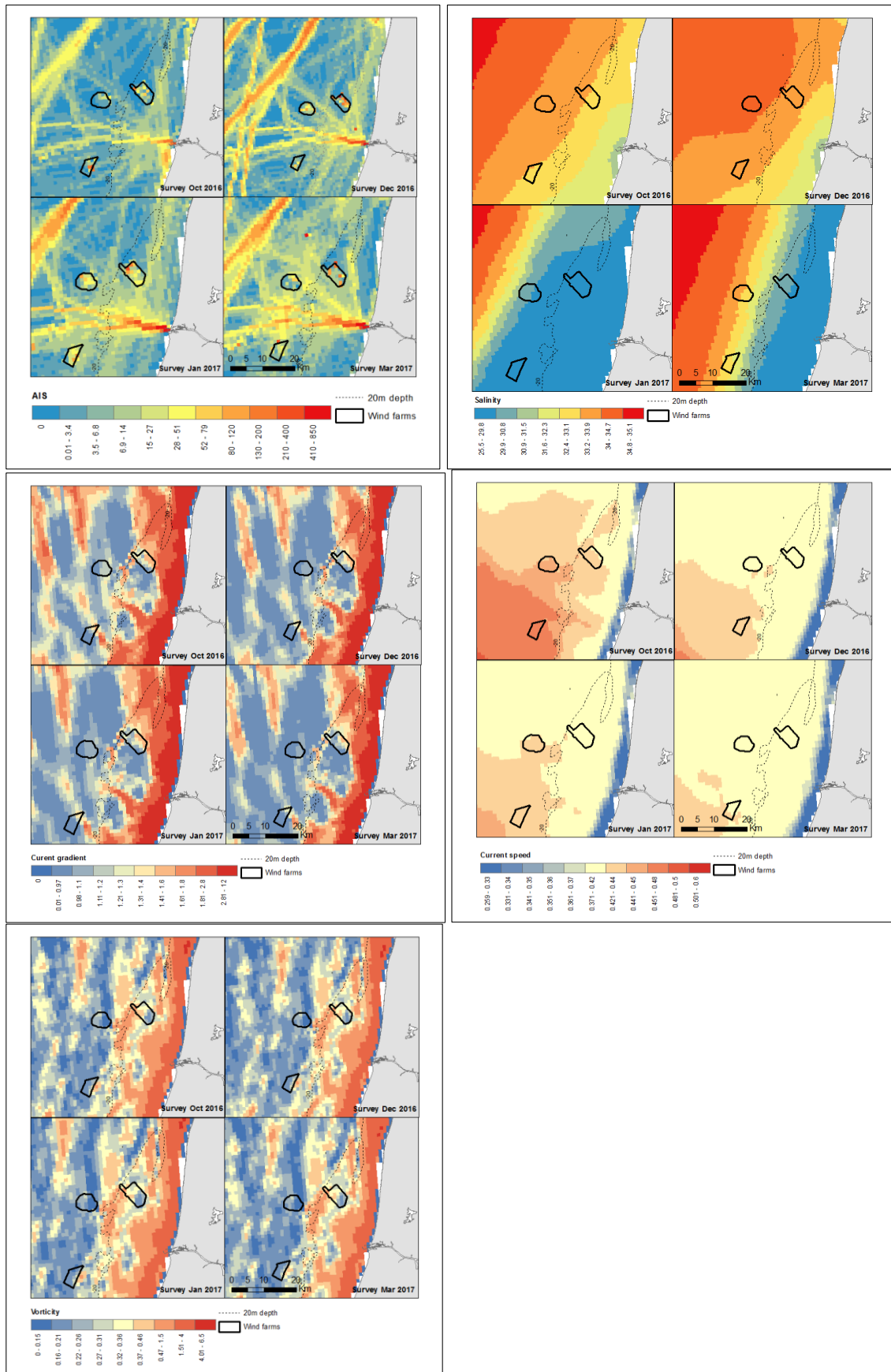


Figure 4.4. Environmental variables (mean values) for the four LUD-T2 surveys.

4.7 Analysis of displacement and number of included surveys

This report includes the results from the second year post-construction of LUD Seabird Monitoring Program of the analyses of displacement of seabirds at LUD and updated results for PAWP and OWEZ. The analyses are reported in two ways, an assessment of significance of the three “distance to windfarm variables” (indicating a statistically significant displacement) and the difference in predicted densities pre- and post-construction for LUD. The power (probability of detecting a change) was tested using simulated bird observations on the same environmental conditions as the actual surveys.

The power tests were conducted on the two species identified by Leopold et al. (2013) as displaying a strong displacement at PAWP and OWEZ; Northern Gannet and Common Guillemot, as both species show similar trends at LUD.

We assessed the power of detecting a significant displacement of Northern Gannet and Common Guillemot from LUD by using a simulation approach. We refitted the GAMMs for these two species as Generalized Linear Mixed Models, GLMMs (with survey hour as a random effect using the R package “lme4” and function “glmer”), without the variable distance to LUD included (i.e. ignoring the windfarm effect and by that simulating a distribution as it would be without the LUD windfarm). The reason for refitting the GAMMs as GLMMs is because there is a readily available function for simulating GLMMs in the package lme4 (function called “simulate”), which allowed us to simulate 100 new bird distributions (based on the modelled relationships) on the actual survey conditions (i.e. the conditions extracted to each real survey). In other words, all 23 surveys included in the modelling were artificially re-surveyed 100 times (for each simulation displacement scenario). During each simulated survey bird distribution were simulated in accordance with the model relationships (which could for example be decreasing shipping intensity in deeper more saline water, see the real species-specific model results below). The variability in the “true” environmental conditions and pressures between surveys and years were therefore included in the simulations. We further artificially and randomly reduced (or displaced) the occurrences and bird density (conditional on occurrences) within the windfarm by for example 10%, 25%, 50% and 75%. For each simulation, GAMMs were fitted (same as the “original” final models), and the proportion of models that resulted in a significant effect of LUD was calculated. Therefore, if 80 models of 100 models were significant (<0.01) the proportion and power of the data was 80%. The simulation approach taken in this study, is similar to the approach taken by Perez-Lapena et al. (2010), Maclean et al. 2013 and Vanermen et al. 2015 in the sense that statistical model parameters are used as a basis for simulations and artificial reductions are further made for the purpose of assessing the power of detecting a displacement. We have included hydrodynamic variables to account for the large variability seen in the dynamic marine environment, which influences the distribution of the birds and should enhance the power of detecting a displacement (Perez-Lapena et al. (2010), Maclean et al. 2013). The modelling and simulation approach is schematically presented in Figure 4.5).

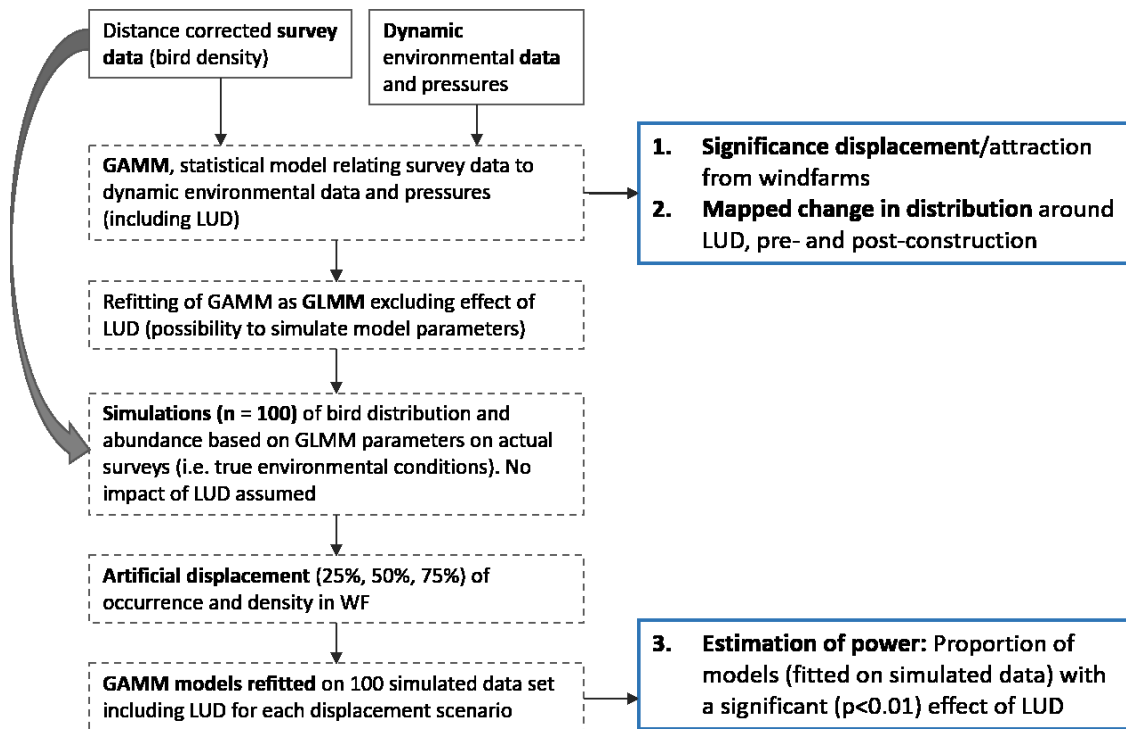


Figure 4.5. Modelling framework for the simulation based power tests. Input data is indicated by boxes with black outlines, analysis steps are indicated by boxes with dashed outlines and results/outputs by boxes with blue outlines.

4.8 Presentation of data

Maps showing observed densities and (modelled and) predicted mean distributions during the LUD-T2 surveys in the winter 2016-2017 have been produced in UTM 32N WGS84 projection. The observed densities are shown for segments (mid points) of approximately 1 km and the mean predicted density is presented for cells with a resolution of 1 km. The mean of model predictions from four LUD pre-construction surveys are also presented together with a map displaying the change between pre and post construction. Note, that the predictions are based on the statistical models and should be interpreted as model results together with model statistical outputs, see Appendix A. The three disturbance areas (LUD, PAWP, OWEZ) and the 20 m depth contour are indicated.

5 Results

5.1 Effort and sample sizes

Four surveys were undertaken during the 2016-2017 winter using the Ivero. The first survey was conducted from 30th of October and 3rd of November 2016, the second from 3rd to 7th of December 2016, the third from 16th to 20th of January 2017 and the fourth from 4th to 10th of March 2017. During the LUD-T2 surveys, the primary transects within PAWP, OWEZ and LUD were completed, and the majority of the secondary transects around LUD were completed. An overview of the survey effort is given in Table 4 and Figure 5.1. Number of recorded seabirds during the T-2 surveys are listed in Table 5. During the T2-02 survey a Black Guillemot was recorded for the first time during the LUD monitoring programme. A flock of Egyptian Geese was recorded during the T2-03 and T2-04 surveys.

Table 4. *Survey effort (km² covered by observation transect) obtained during the four ship-based surveys in the LUD-T1 winter season (2015-2016).*

| Period | Survey | Area covered (km ²) |
|-----------|--------------------|---------------------------------|
| LUD-T2-01 | 30/10-3/11 2016 | 303.22 |
| LUD-T2-02 | 3-7/12 2016 | 312.11 |
| LUD-T2-03 | 16-20/1 2017 | 332.92 |
| LUD-T204 | 6-10/3 2017 | 358.66 |

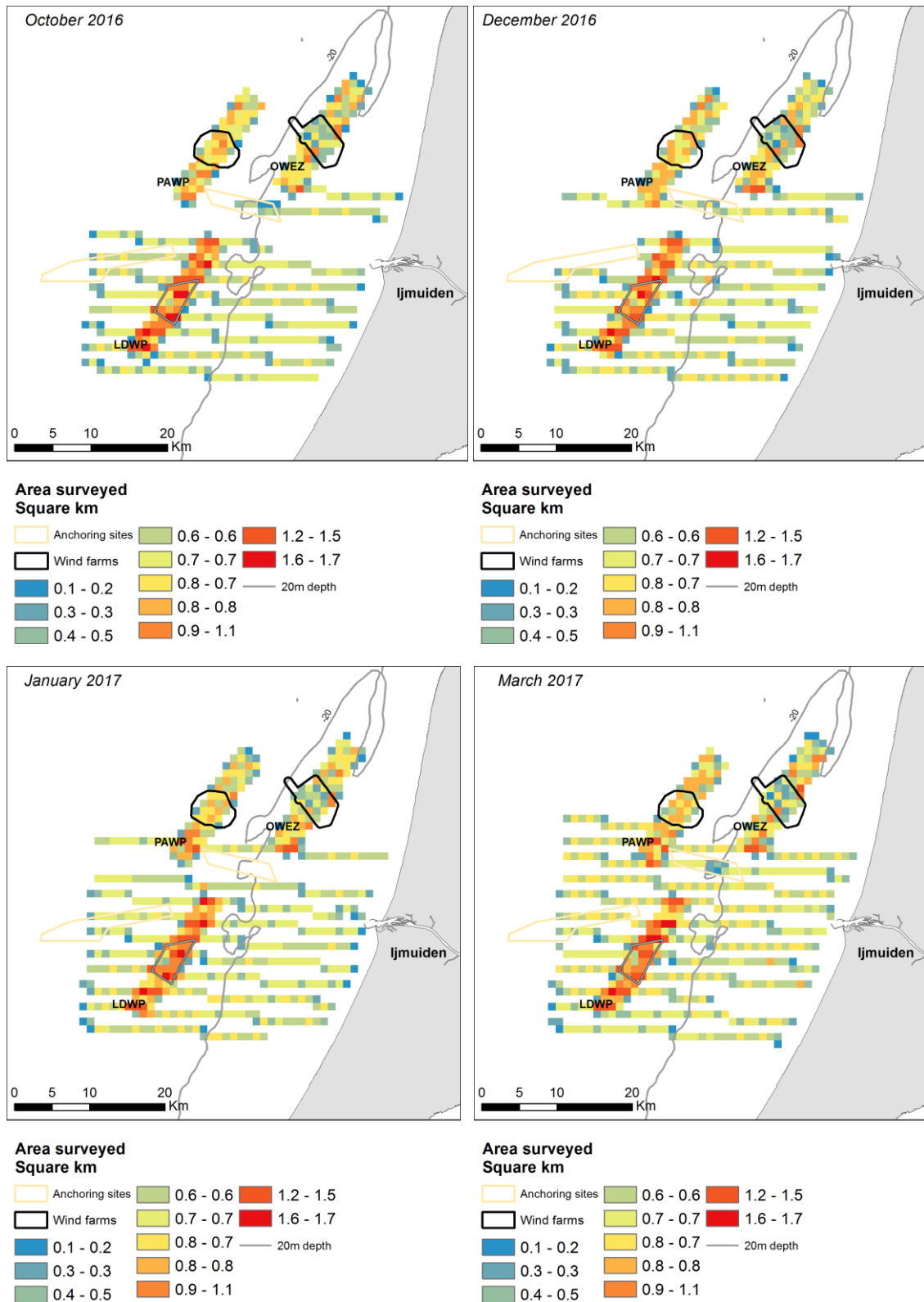


Figure 5.1. The spatial coverage of survey effort (km²) obtained during the four ship-based surveys in the LUD-T2 season (2016-2017).

Table 5. Numbers of seabirds observed during the four LUD-T2 surveys in winter 2015/2016.

| Species | Total Oct 2016 | Total Dec 2016 | Total Jan 2017 | Total Mar 2017 |
|----------------------------|-------------------|-------------------|-------------------|-------------------|
| Red-throated Diver | 12 | 93 | 47 | 11 |
| Black-throated Diver | 0 | 1 | 0 | 0 |
| Red-Black-throated Diver | 2 | 1 | 1 | 2 |
| Great Crested Grebe | 2 | 43 | 400 | 17 |
| Northern Fulmar | 0 | 0 | 1 | 0 |
| Northern Gannet | 78 | 74 | 55 | 531 |
| Great Cormorant | 341 | 425 | 232 | 146 |
| Egyptean Goose | 0 | 0 | 5 | 3 |
| White-fronted Goose | 0 | 0 | 9 | 0 |
| Pink-footed Goose | 0 | 0 | 0 | 350 |
| Barnacle Goose | 0 | 0 | 5 | 409 |
| Greylag Goose | 0 | 6 | 55 | 0 |
| Unid. Goose sp. | 0 | 0 | 1 | 0 |
| Mallards | 0 | 0 | 2 | 0 |
| Teal | 0 | 0 | 0 | 2 |
| Common Pochard | 0 | 0 | 1 | 0 |
| Wigeon | 0 | 0 | 5 | 42 |
| Gadwall | 0 | 6 | 0 | 0 |
| Common Eider | 0 | 0 | 0 | 1 |
| Common Scoter | 398 | 4,859 | 71 | 45 |
| Velvet Scoter | 0 | 610 | 4 | 0 |
| Great Skua | 0 | 1 | 0 | 1 |
| Little Gull | 6 | 2 | 14 | 287 |
| Black-headed Gull | 36 | 28 | 39 | 11 |
| Common Gull | 100 | 548 | 385 | 110 |
| Lesser Black-backed Gull | 189 | 10 | 4 | 5,455 |
| Herring Gull | 59 | 46 | 19 | 181 |
| Great Black-backed Gull | 77 | 71 | 30 | 63 |
| Black-legged Kittiwake | 88 | 0 | 169 | 27 |
| Unid. Gull sp. | 1,111 | 1 | 27 | 3,359 |
| Common Guillemot | 843 | 1,380 | 1,396 | 119 |
| Razorbill | 135 | 135 | 419 | 44 |
| Black Guillemot | 0 | 1 | 0 | 0 |
| Unidentified <i>Alcids</i> | 66 | 20 | 81 | 0 |
| Total | 3,531 | 8,361 | 3,477 | 11,216 |

5.2 Distance analysis

Table 6 gives an overview of the selected models used for estimating detection of sitting birds with distance for the different species groups.

Table 6. Distance statistics for sitting birds in each species group.

| Species group | Sample size | Key function* | Adjustment term | Effective strip width (ESW) | % CV ESW |
|---------------|-------------|---------------|-----------------|-----------------------------|----------|
| Divers | 74 | HR | - | 121 | 41.2 |
| Grebes | 167 | HN | Cosine (2) | 153 | 10.8 |
| Gannets | 165 | HN | Cosine (2) | 203 | 13.7 |
| Cormorants | 271 | HN | Cosine (2) | 243 | 12.0 |
| Small gulls | 770 | Uniform | Cosine (1,2,3) | 152 | 6.9 |
| Large gulls | 934 | Uniform | Cosine (1,2,3) | 154 | 6.4 |
| Auks | 6416 | HR | Cosine (2) | 135 | 1.9 |

* HN=Half normal, HR= Hazard rate

5.3 Species accounts

In this chapter an account of the results of the analyses and modelling of the LUD-T2 data (together with T0, T1 and the “historic” PAWP and OWEZ data) is given. For each species the description of the LUD-T2 status starts with a general introduction in which the results of the LUD-T2 surveys during the 2016-2017 winter are summarised. The results of the species-specific distribution models are given in a separate subsection called ‘model results’, based on all surveys.

5.3.1 Divers: Red-throated *Gavia stellata* and Black-throated Divers *Gavia arctica*

The LUD-T2 surveys showed similar distribution patterns to LUD baseline and T1 surveys with most of the overall few sightings done in the coastal zone, and only two observations offshore south of PAWP and OWEZ recorded during the March survey (Figure 5.2). There is a large variability in mean density between surveys as indicated by Figure 5.3.

Model results

Survey 18, 21, 23, 25 and 28 were not included as there were no diver sightings or very few (sitting on water) during those surveys. The model did not “behave” properly when LUD and PAWP footprints were included in the model as factor levels and the reason is because these two areas are outside the general distribution range of the divers in the area. Therefore, only OWEZ was included as a factor level in the model, while the 2 km buffers for all three windfarms were included. The windfarms had no effect in the positive model part and were therefore dropped altogether. Probability of presence was significantly lower inside OWEZ and also within the 2 km buffer of OWEZ and PAWP. The results indicate that divers are displaced from the windfarms and in this region do not occur in the area around LUD. An increasing probability of presence of divers was also explained by water depths lower than 20 m, where the water is less saline and the mean current speed lower and shipping intensity is low. Increasing density (when present) was further explained by decreasing current speed (Appendix A). All responses indicating a preference for coastal waters, which is also apparent from the predictions (Figure 5.5). The model had a good predictive ability with an AUC value of 0.87, indicating the model is good at distinguishing between presence and

absence. The Spearman's correlation between observed and predicted was also fair with a value of 0.47 (Appendix A). The predicted distributions indicate a general reduction in the density when the mean of (LUD) pre-construction surveys were compared against the mean of (LUD) post-construction surveys (Figure 5.5).

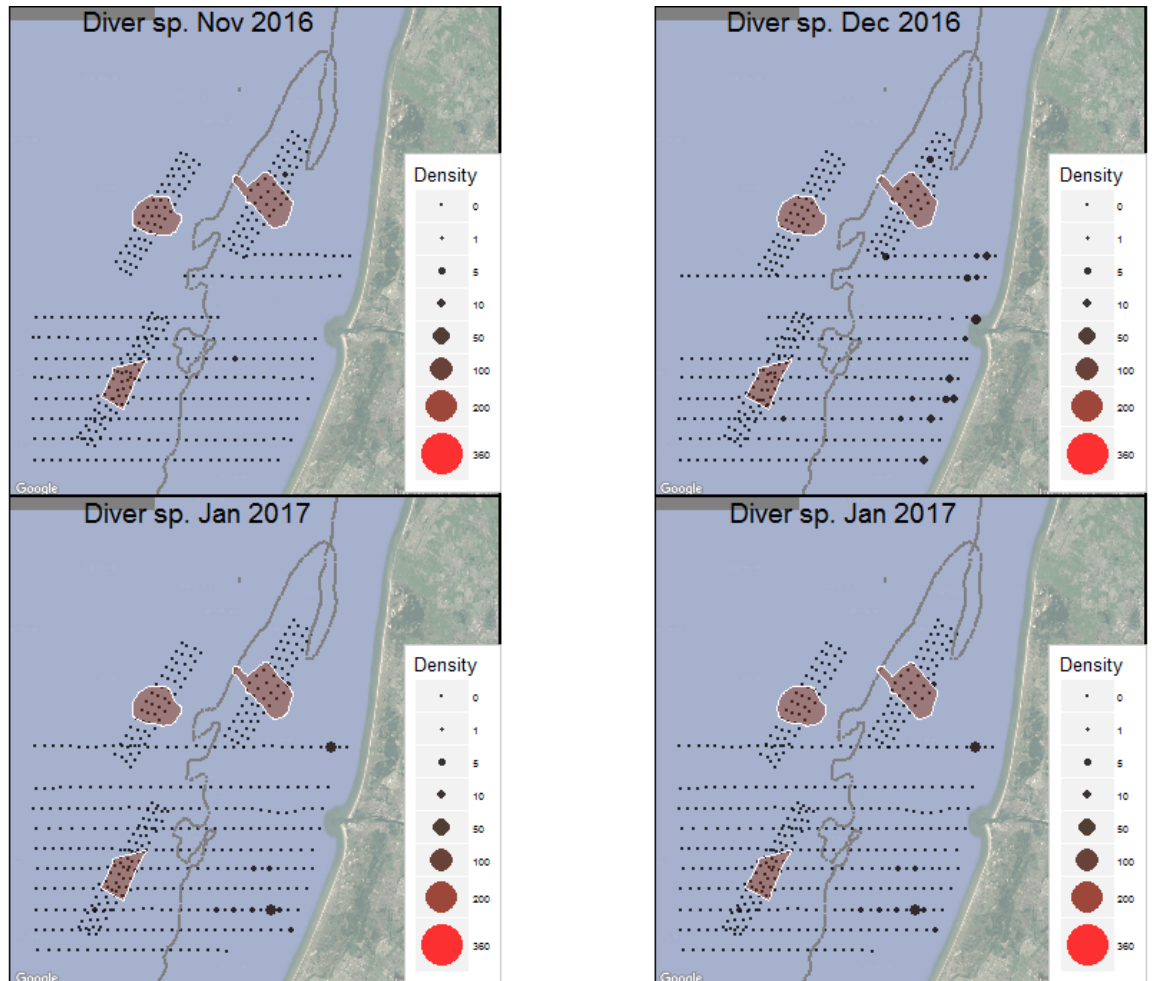


Figure 5.2. Observed density (birds/km²) of Diver sp. during LUD-T2 surveys 2016-2017. Densities have been corrected for distance bias.

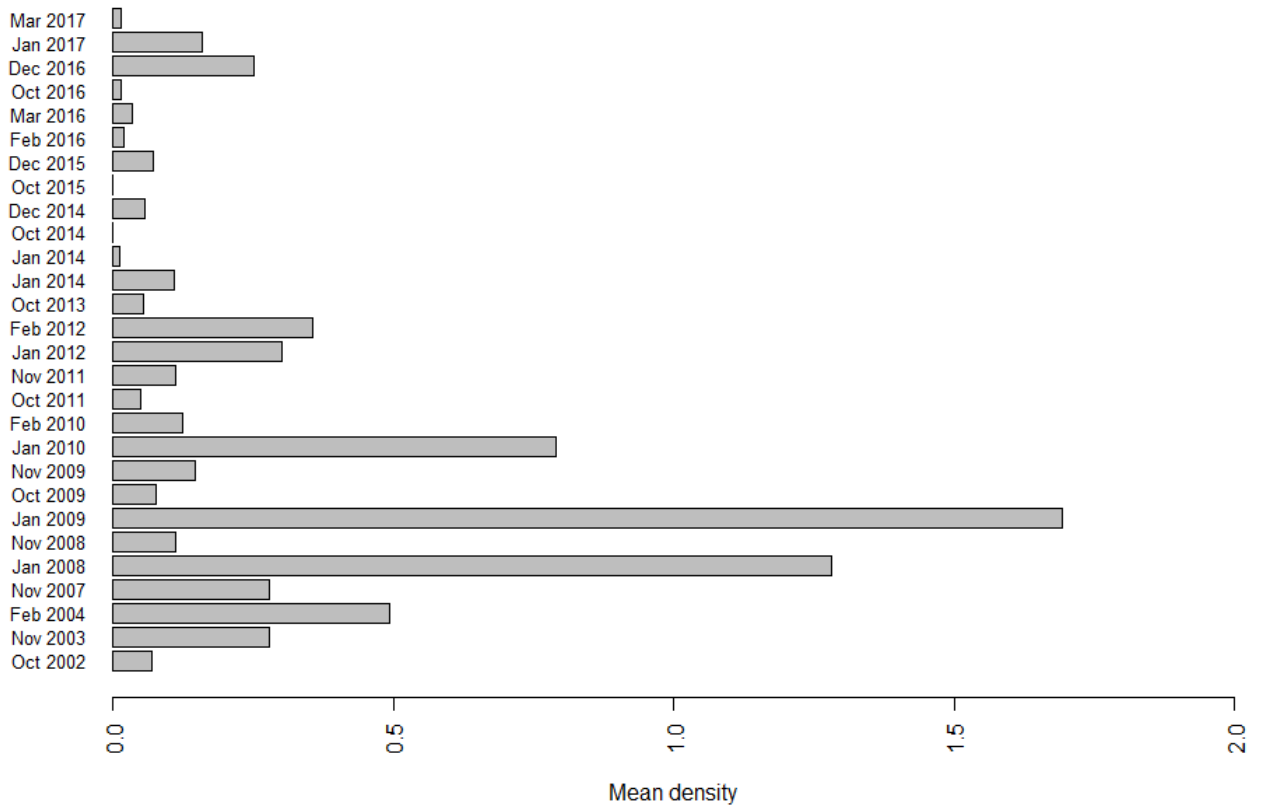


Figure 5.3. Mean observed density (birds/km²) of Diver sp. in the entire surveyed area during LUD pre- and post-construction surveys. Densities have been corrected for distance bias.

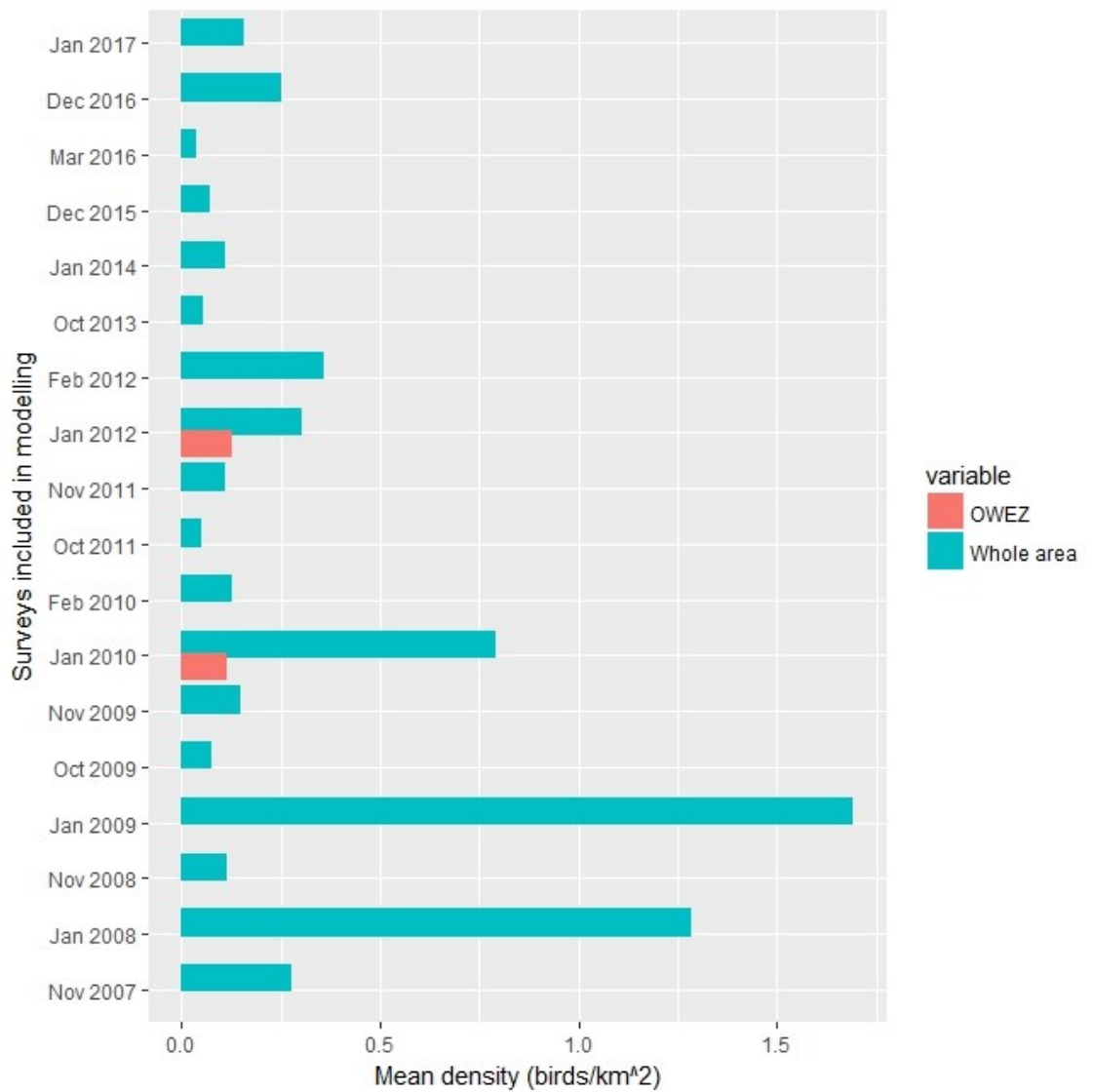


Figure 5.4 Mean density of Diver species during surveys included in the modelling. The mean density within the OWEZ footprint is shown as well as the mean in the whole surveyed area (including windfarms).

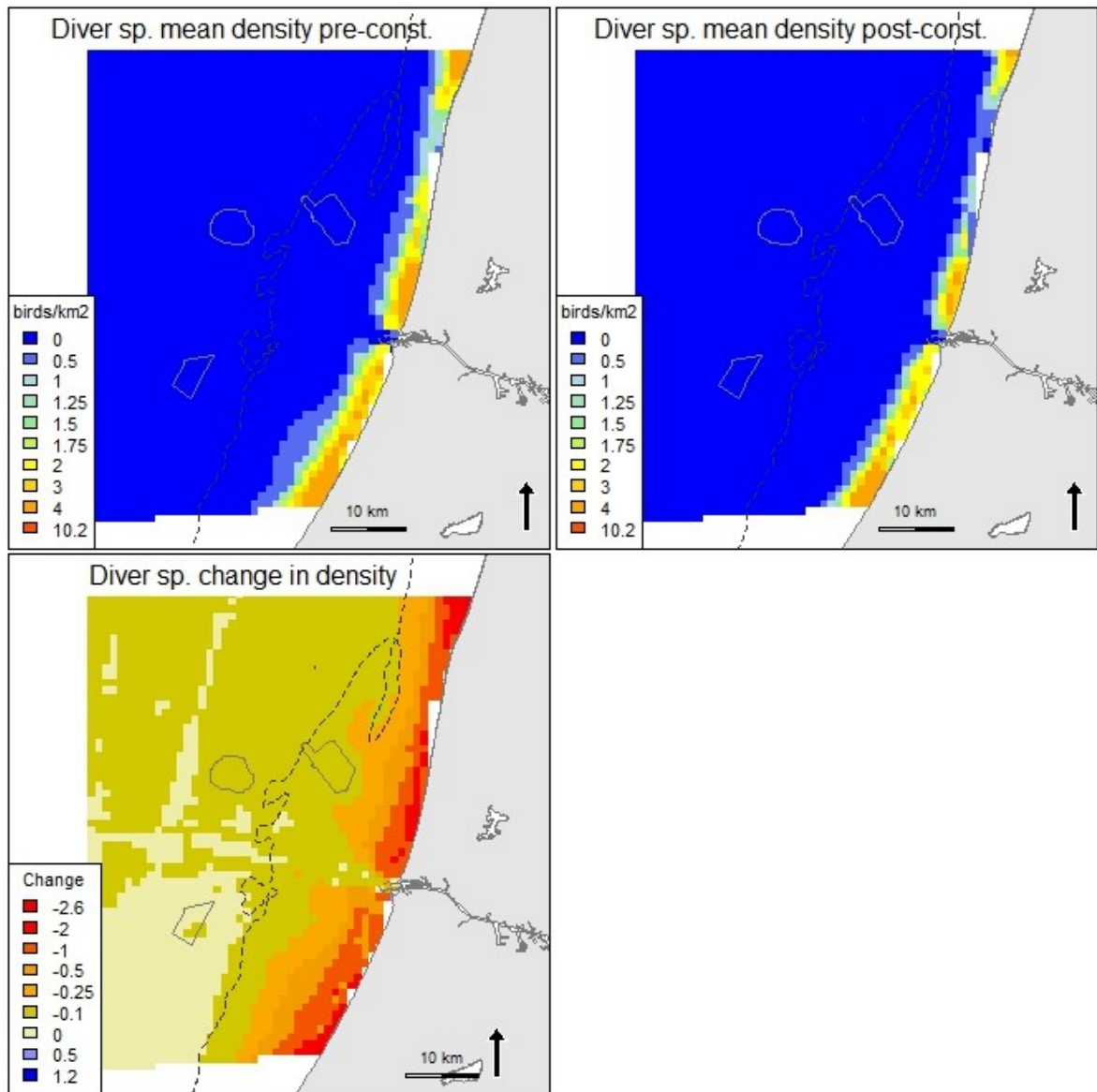


Figure 5.5. Predicted mean density (birds/km²) and distribution of wintering Diver sp. during four LUD pre- and four LUD post-construction surveys, and the relative change in predicted density between the two periods. Note that all included surveys are OWEZ and PAWP post-construction surveys.

5.3.2 Great Crested Grebe *Podiceps cristatus*

During the T-2 surveys Great Crested were exclusively recorded in the coastal zone (Figure 5.6) only during the two midwinter surveys (Figure 5.6, Figure 5.7).

Model results

Survey 4, 6, 8, 12, 16, 21, 23, 24, 25 and 28 were excluded from the analyses as there were no or very few records of grebes in the model data set. As for divers only OWEZ footprint was included in the model together. PAWP and LUD was not included because they were outside the distribution range of the species in the region. The probability of presence was significantly lower in the OWEZ footprint ($p < 0.05$) indicating a displacement although also the OWEZ windfarm is outside the range of the general grebe distribution in the area (Figure 5.7). Further decreasing depth, salinity, mean current speed and shipping intensity was included in the presence-absence model part and decreasing water depth and salinity in the positive part (Appendix A). The responses describes the preference of Great Crested to coastal waters (Figure 5.7). The

split-sample evaluation model did not converge, however the explanation degree of the presence absence model was fair while very low for the positive part (Appendix A). The predicted distributions indicate a general reduction in Great Crested Grebe density when the mean of post-(LUD)-construction surveys were compared against the mean pre-(LUD)-construction surveys (Figure 5.9), which is accordance with the mean densities shown in Figure 5.7.

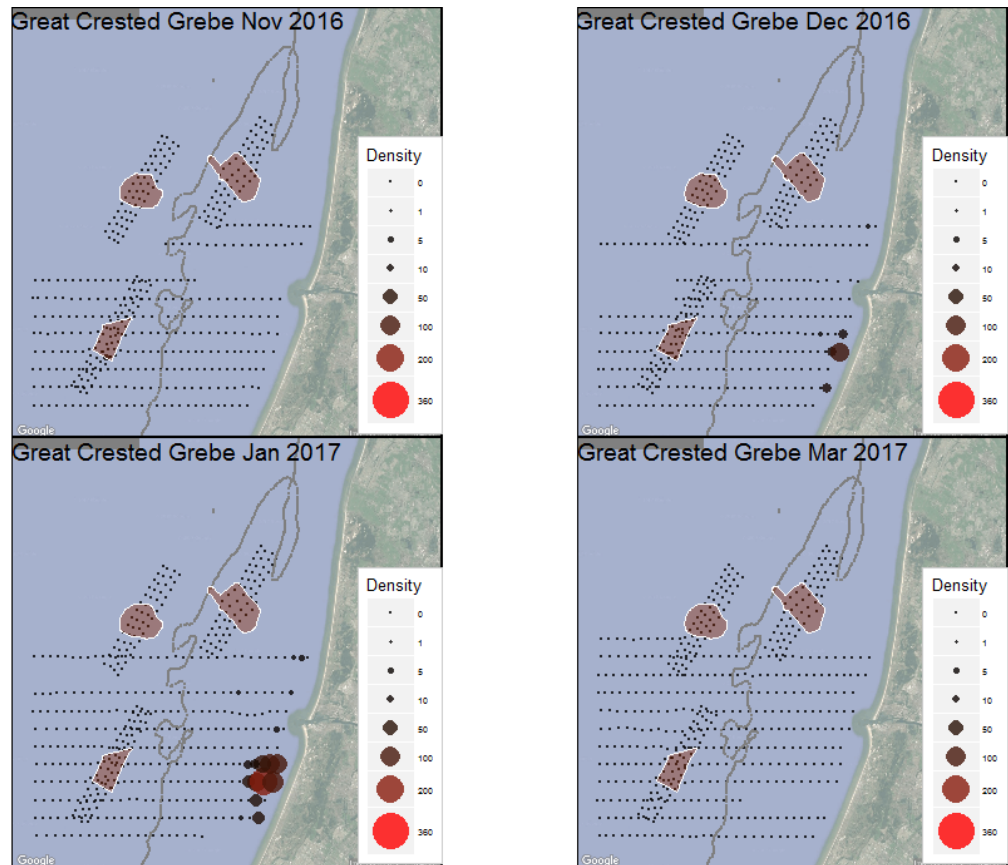


Figure 5.6. Observed density (birds/km²) of Great Crested Grebe during LUD-T2 surveys 2016-2017. Densities have been corrected for distance bias.

Great Crested Grebe, 2002-2017

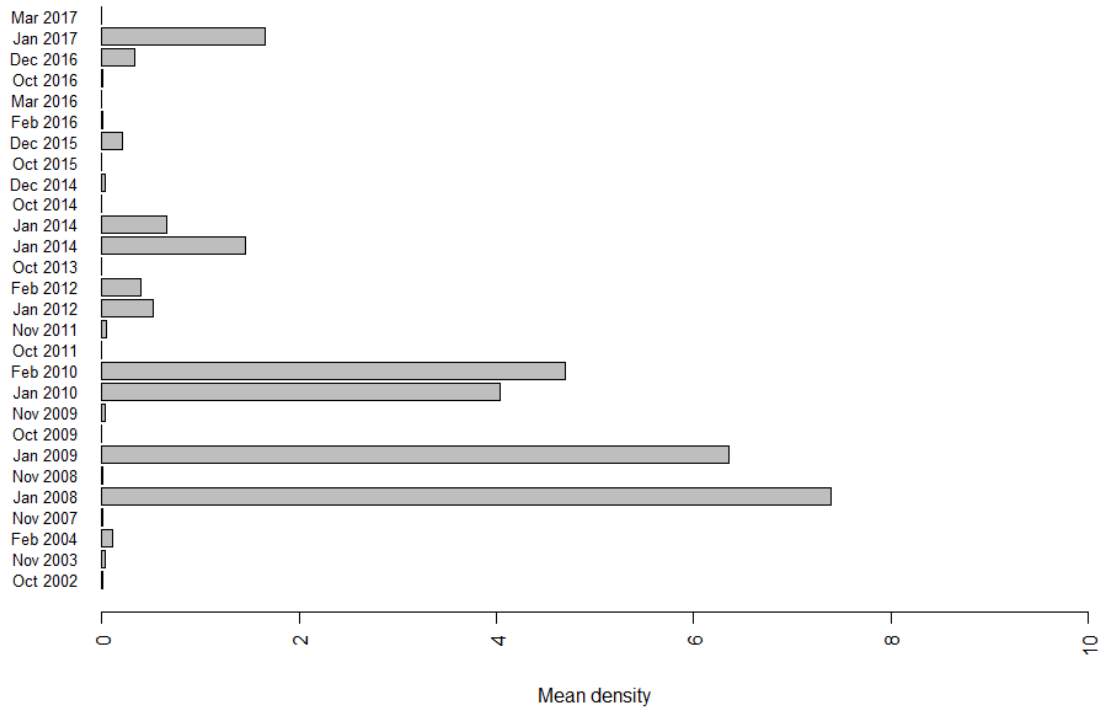


Figure 5.7. Mean observed density (birds/km²) of Great Crested Grebe in the entire surveyed area during LUD pre- and post-construction surveys. Densities have been corrected for distance bias.

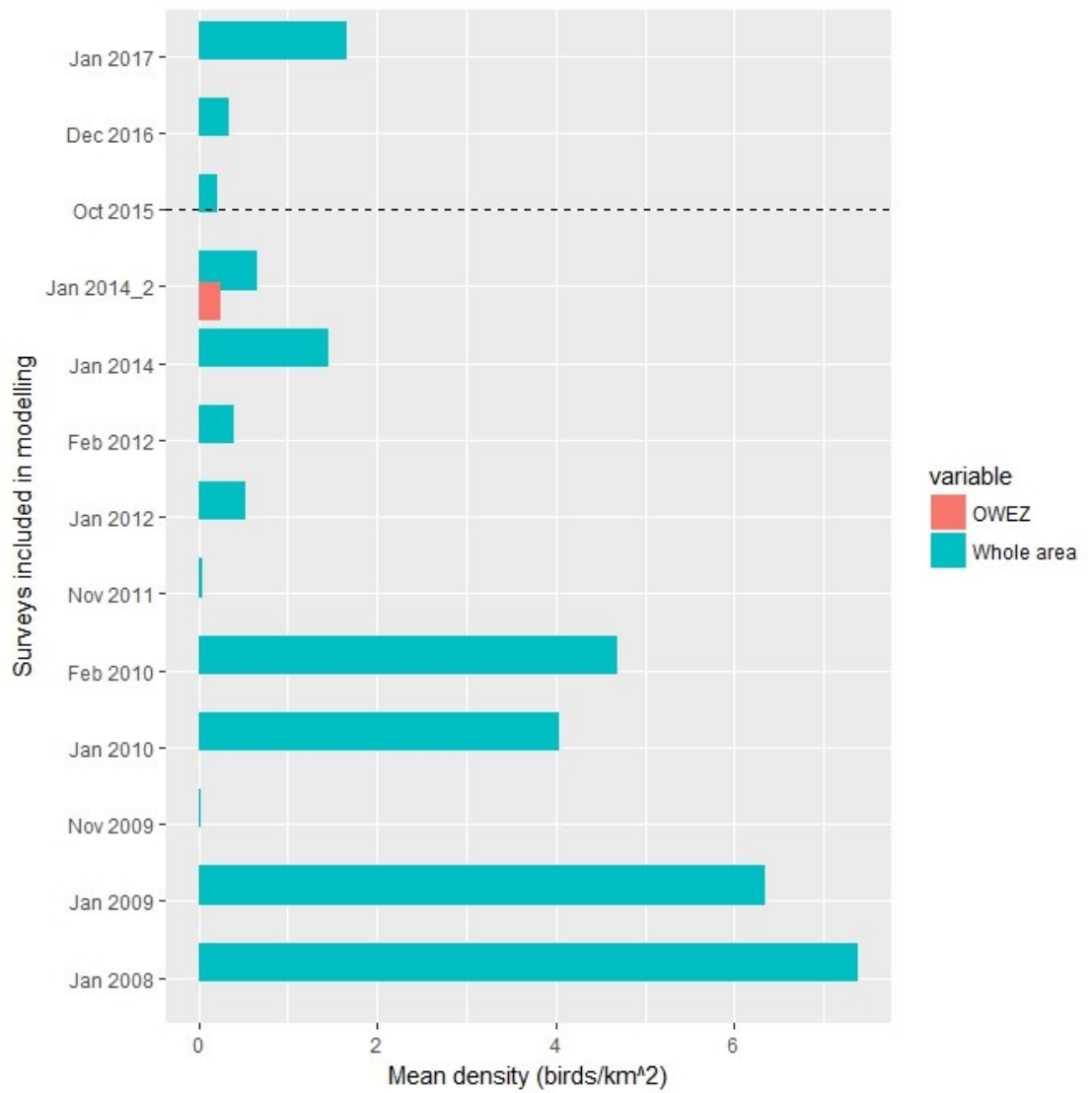


Figure 5.8. Mean density of Great Crested Grebe species during surveys included in the modelling. The mean density within the OWEZ footprint is shown as well as the mean in the whole surveyed area (including windfarms).

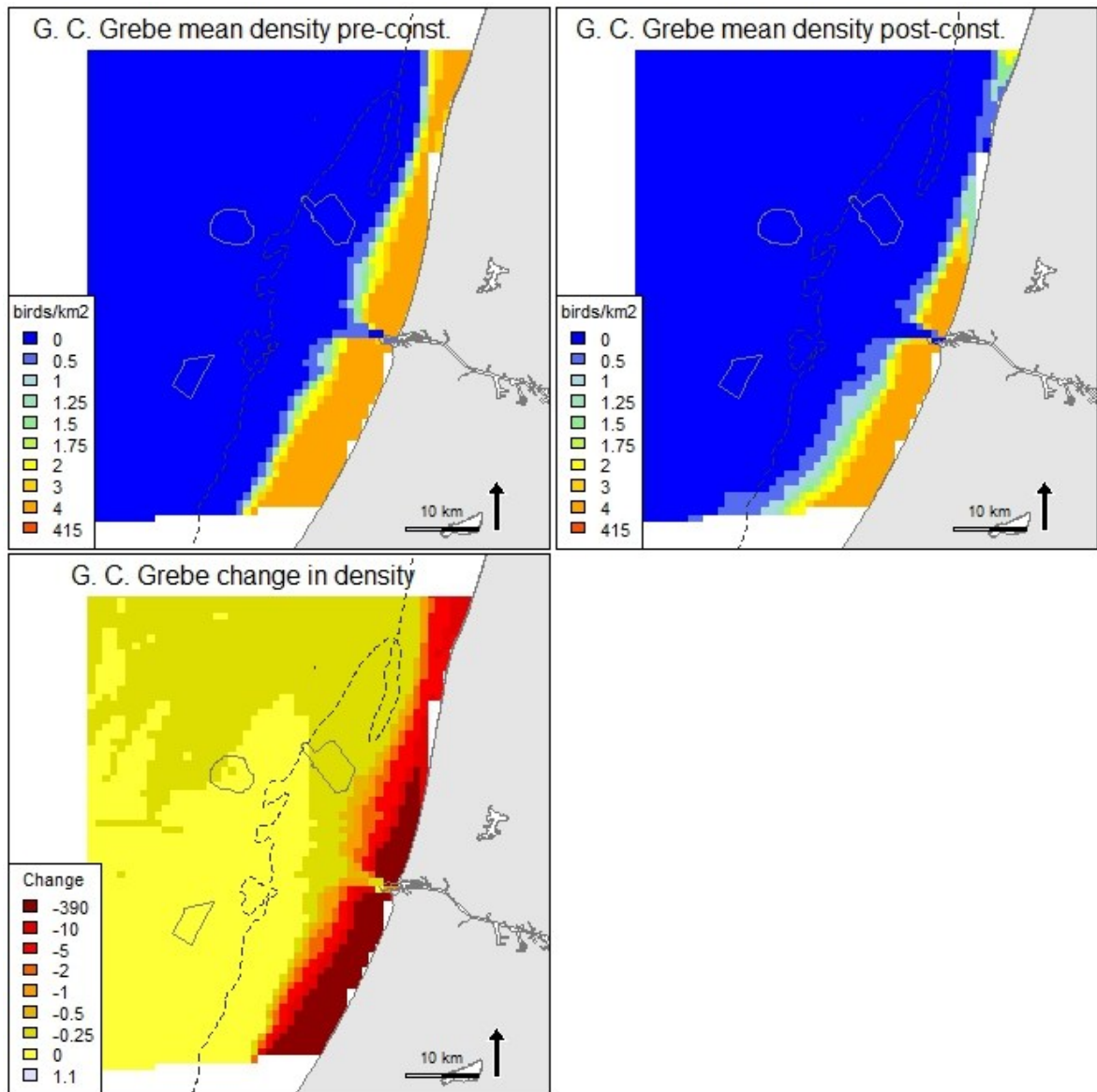


Figure 5.9. Predicted mean density (birds/km²) and distribution of wintering Great Crested Grebe during three LUD pre- and three LUD post-construction surveys, and the relative change in predicted density between the two periods. Note that all included surveys are OWEZ and PAWP post-construction surveys.

5.3.3 Northern Gannet *Morus bassanus*

During the LUD-T2 surveys the highest numbers of Gannets were recorded in March in the offshore area between LUD and PAWP. Most Gannets were observed outside the windfarms, and only a few records inside the windfarms indicating a potential displacement (Figure 5.10). A marked variation is apparent in the recorded densities of Gannet between the 27 surveys conducted (Figure 5.9) of which 23 were included in the distribution modelling (Figure 5.12). There is also a large variation in observed mean densities inside the wind farm footprints, however in most surveys the mean density is clearly lower than the average in the whole area or no Gannets were recorded at all inside the footprints (Figure 5.12). According to the results in the T1 one report (Skov et al 2016) the Gannet did not seem to prefer the LUD footprint even before construction when comparing mean density within the windfarms with three buffers outside the windfarm.

Model results

The modelling results indicated that the Northern Gannets preferred deeper and saline North Sea water masses with lower mean current speeds. The Northern Gannet avoided all three windfarm footprints ($p < 0.01$) and the probability of presence was also significantly lower in a 2 km buffer around OWEZ windfarm (Appendix A). The explanation degree of the distribution model for the Northern Gannet was poor for the positive part, whereas the explanation degree was fair for the presence-part of the model (Appendix A). The AUC indicated that the presence-absence model part had a quite good predictive ability (i.e. the model is good at discriminating between presence and absence) while the Spearman's correlation coefficient indicated that the model is rather poor at explaining and predicting accurate density patterns (Appendix A).

The predicted patterns described a general increasing density in the North Sea water mass while there seem to be lower densities in the coastal water mass from 8 pre-construction to 8 post construction surveys. The significant displacement from LUD is clear from the predicted densities when comparing LUD pre-construction vs. post-construction (Figure 5.13). When evaluating predictions, by predicting on model input data with and without the response of the wind farm the results indicate that there is in average a 55% decrease in probability of detecting a Gannet inside the wind farm, in comparison to a case without a wind farm. When both model parts are combined there is a 73% decrease in density within the windfarm when comparing model predictions including the windfarm response (factor variable) with model predictions excluding the wind farm response (Figure 5.14). This can be regarded as an indication of level of displacement, however it is important to consider the model errors as well as potential unknown uncertainties around the estimates (Figure 5.14).

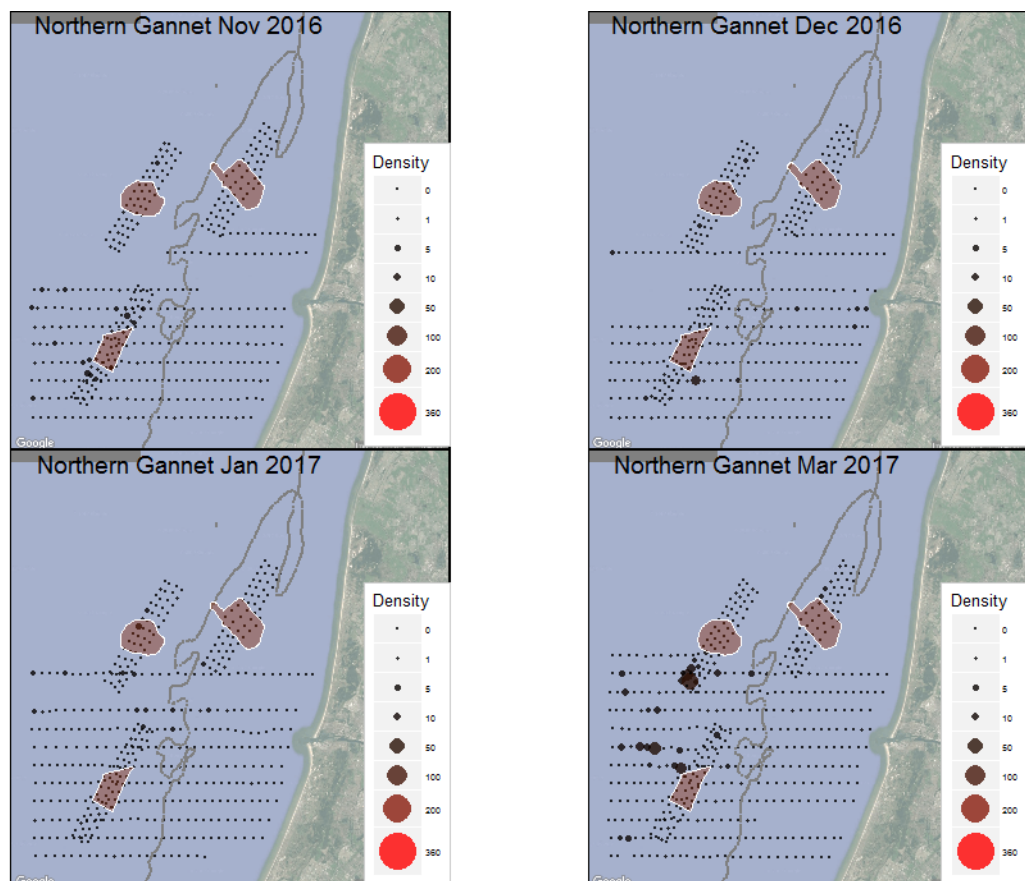


Figure 5.10 Observed density (birds/km²) of Northern Gannet during LUD-T2 surveys 2016-2017. Densities have been corrected for distance bias.

Northern Gannet, 2002-2017

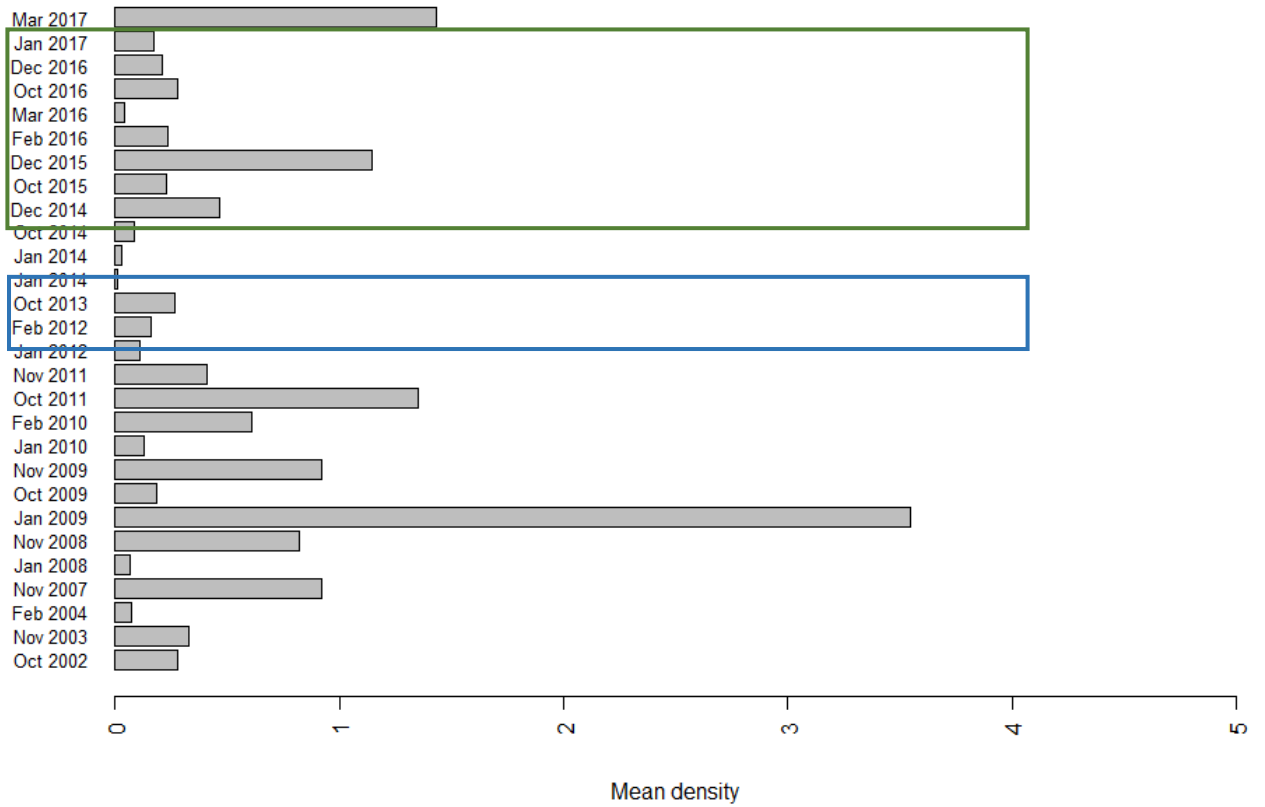


Figure 5.11. Mean observed density (birds/km²) of Northern Gannet in the entire surveyed area during LUD pre-construction (marked with a blue rectangle) and post-construction surveys (green rectangle). Densities have been corrected for distance bias.

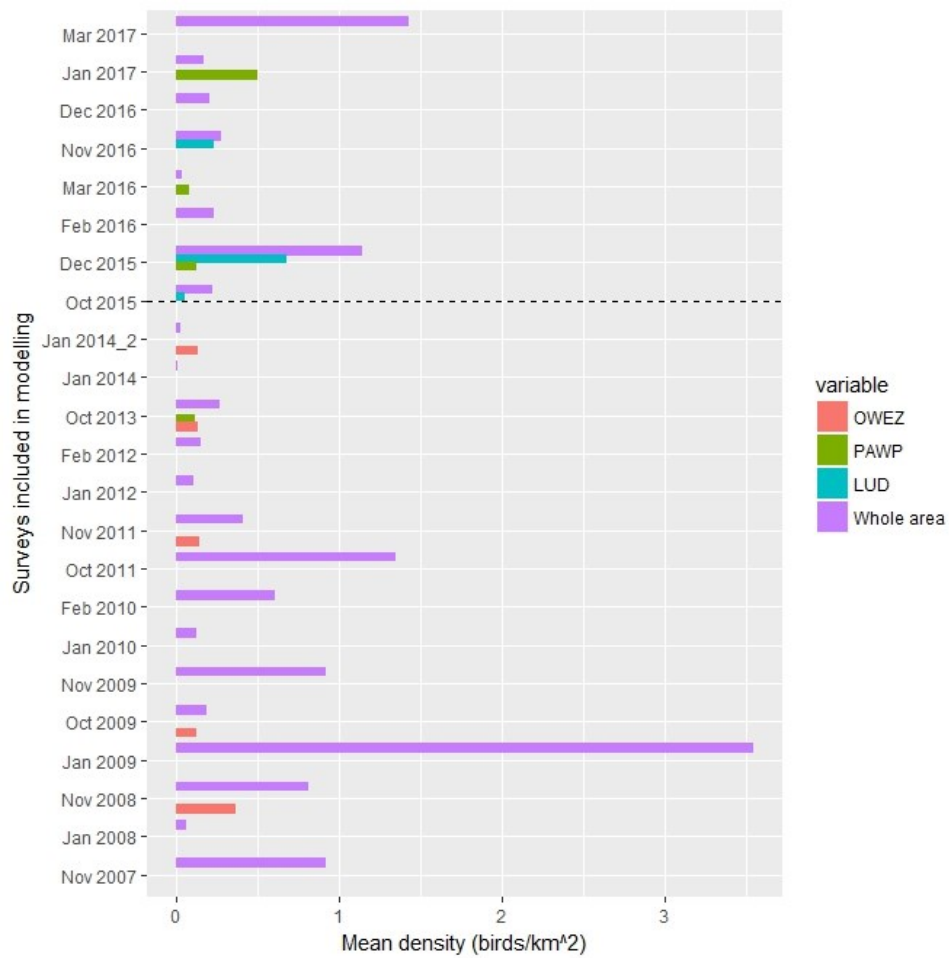


Figure 5.12. Mean density of Northern Gannet during surveys included in the modelling. The mean density within each of the three wind farm footprints (OWEZ, PAWP and LUD) is shown as well as the mean in the whole surveyed area (including windfarms).

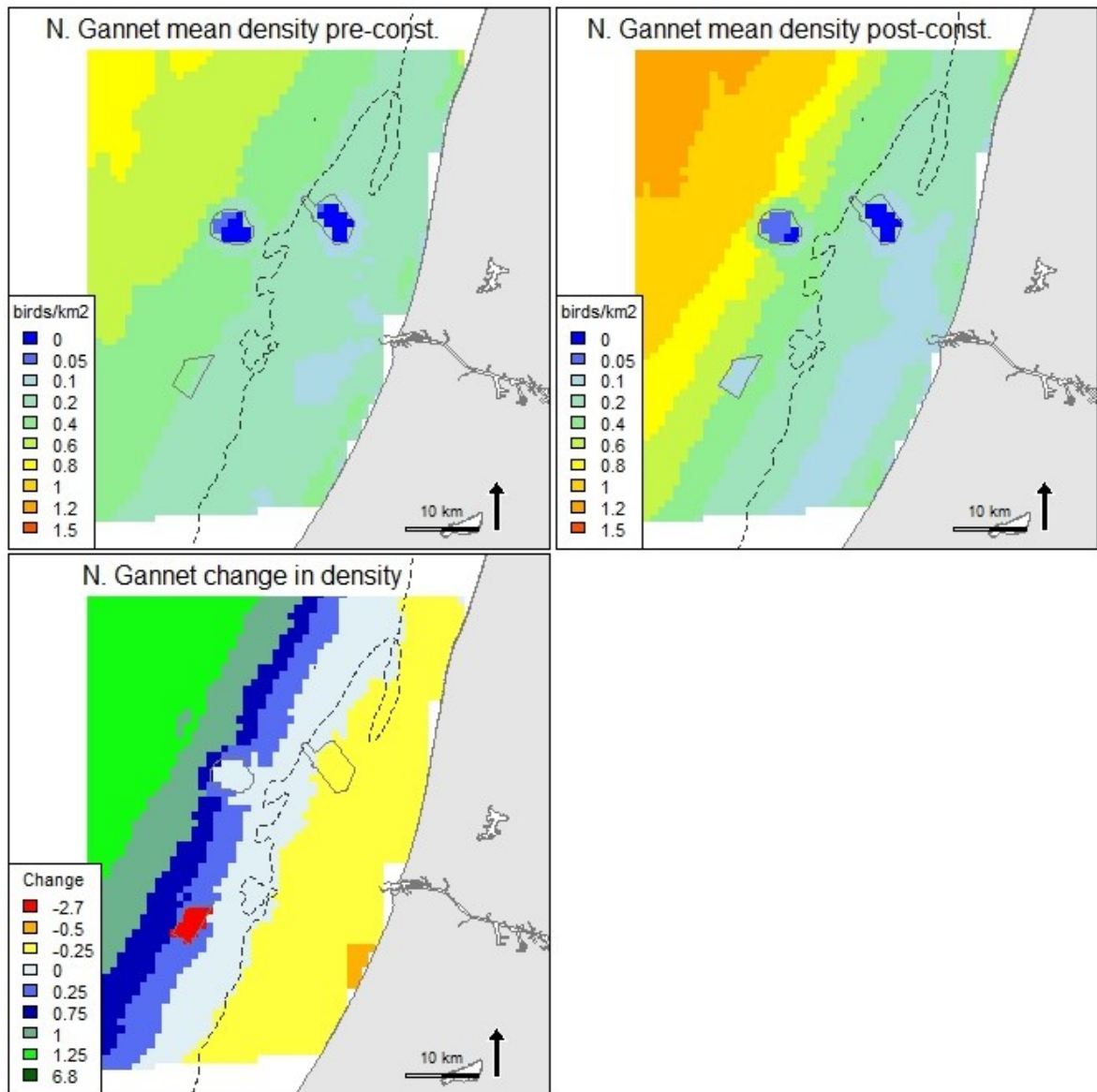


Figure 5.13. Predicted mean density (birds/km²) and distribution of wintering Northern Gannet during eight LUD pre- and eight LUD post-construction surveys, and the relative change in predicted density between the two periods. Note that all included surveys are OWEZ and PAWP post-construction surveys

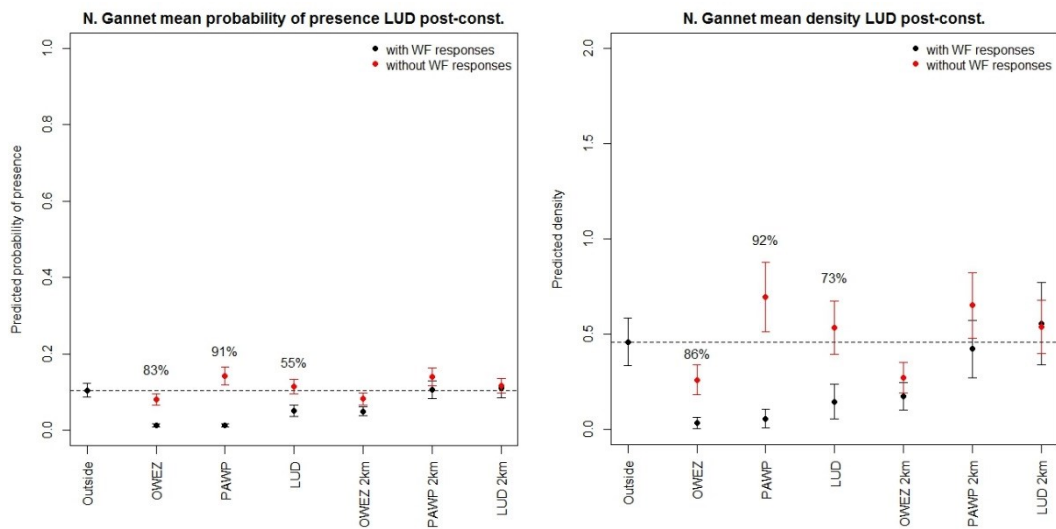


Figure 5.14. Model predictions (on model data) for Northern Gannet during the eight LUD post-construction surveys, with (fitted values) and without the response of the wind farm, when taking into account the dynamic environmental conditions. The difference indicate a mean displacement in probability of presence (to the left) or the density (to the right) if the wind farm(s) would not be present compared to a WF present. The mean displacement in % is indicated above the estimates for the footprints (GAMM model errors, SE, are indicated as error bars).

Simulation “power” analysis

Simulations based on the relationships modelled using GAMM reported above were refitted and simulated on the existing eight post-construction survey conditions using GLMM (excluding the response from LUD). The power of detecting a decline of 25-75% in LUD was assessed using 100 simulations (of which generally around 90% converged, Table 8, Table 9). The power test was conducted aiming at assessing what the power of using 8 survey is and what the power would be if four surveys are added. In T3 3 additional surveys will be carried out resulting in a total of 11 survey. The power of 11 survey is a good indication of the power of 12 surveys¹

A high power (>80%) was achieved when 75% of both presence and density of Northern Gannets was reduced within windfarm (Table 8). A 50% reduction within the LUD resulted in a power of 65% (Table 8). To further assess whether 12 surveys would be sufficient for detecting a 25% and a 50% reduction with a high power, we used the 2 pre-construction survey and the 2 construction survey as fictional post-construction surveys and thus simulated 100 times 12 post-construction surveys with a 25%/50% displacement within the LUD windfarm. The results indicated that the power of detecting a 25% displacement following 12 post-construction surveys was similar to the results obtained by 8 post-construction surveys (Table 9). Also a detection of a 50% displacement based on 12 post construction survey but was similar to the power based on 8 surveys (Table 9). The power did not increase by adding for surveys because the observed densities in the 4 added surveys were low, particularly the 2 surveys conducted in January 2014 (see Figure 5.11). The power would most likely increase markedly if a survey with a high density would be added.

Table 8. The power of a presence/absence (PA) model part and positive density model part (POS, conditional on PA) including eight post-construction surveys, with an artificial displacement of 50%, 75% and 90% from within the windfarm perimeter. Power larger than 80% is indicated with green.

| Displacement from WF | PA | POS | N sim. |
|----------------------|----|-----|--------|
|----------------------|----|-----|--------|

¹ (number of surveys according to original monitoring scheme was 12, but was reduced to 11).

| | | | |
|-----|-------|-------|----|
| 25% | 0.135 | 0.056 | 89 |
| 50% | 0.646 | 0.313 | 96 |
| 75% | 0.989 | 0.528 | 89 |

Table 9. The power of a presence/absence (PA) model part and positive density model part (POS, conditional on PA) including 12 post-construction surveys, with an artificial displacement of 25%.

| Displacement from WF | PA | POS | N sim. |
|----------------------|-------|-------|--------|
| 25% | 0.079 | 0.101 | 89 |
| 50% | 0.681 | 0.415 | 94 |

5.3.4 Great Cormorant *Phalacrocorax carbo*

The LUD-T2 surveys corroborated the findings of the LUD baseline and T1 surveys that the distribution of Cormorants offshore is exclusively associated with PAWP and OWEZ, and now also with LUD (Figure 5.15).

Model results

The modelling results stressed the importance of PAWP, OWEZ and LUD for the presence of Cormorants, as all windfarm footprints were significant ($p < 0.01$) as well as the 2 km buffer around each windfarm (Appendix A). The large degree of variation seen in the overall abundance of recorded Cormorants during the 27 surveys is displayed in Figure 5.16. The predicted patterns of change in density between pre-(LUD) and post-(LUD)-construction periods further underlined the attraction effect of the windfarms on the Cormorants (Figure 5.18). The explanatory degree of the distribution model for the Great Cormorant was poor for both the presence-absence and the density model parts (Appendix A). The model is nevertheless useful for describing a significant attraction effect.

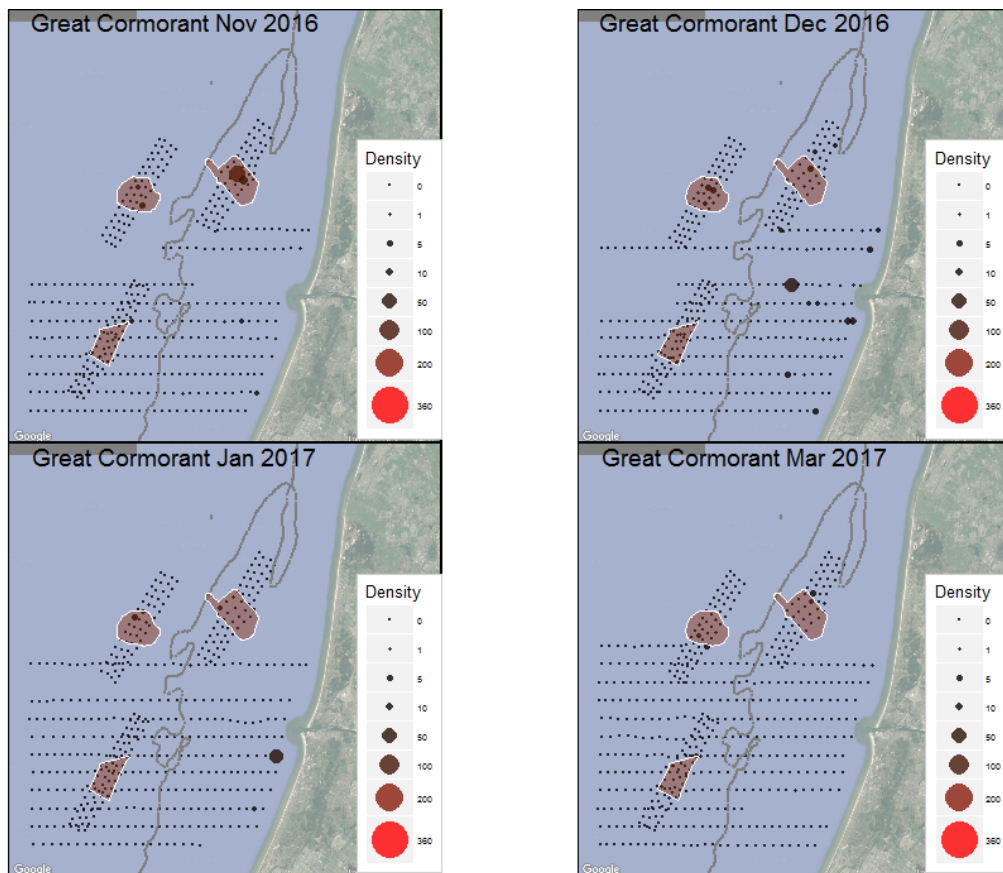


Figure 5.15. Observed density (birds/km²) of Great Cormorant in the entire surveyed area during LUD-T2 surveys 2016-2017. Densities have been corrected for distance bias.

Great Cormorant, 2002-2017

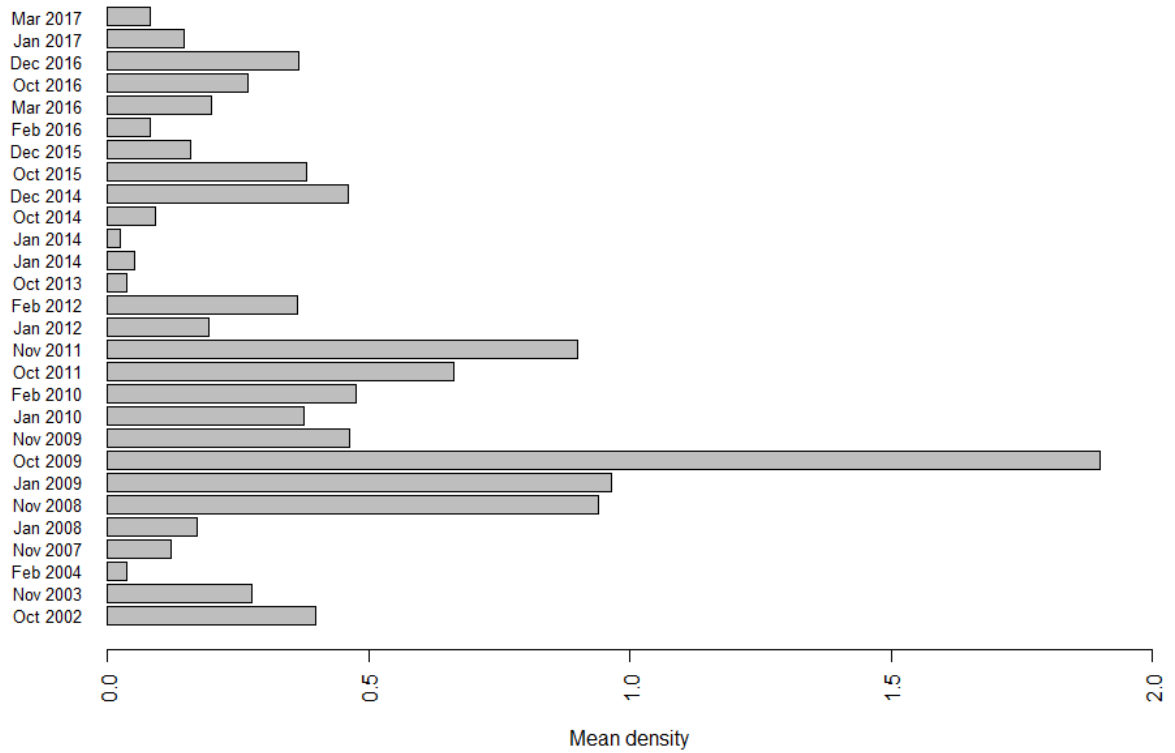


Figure 5.16. Mean observed density (birds/km²) of Great Cormorant during LUD pre- and post-construction surveys. Densities have been corrected for distance bias.

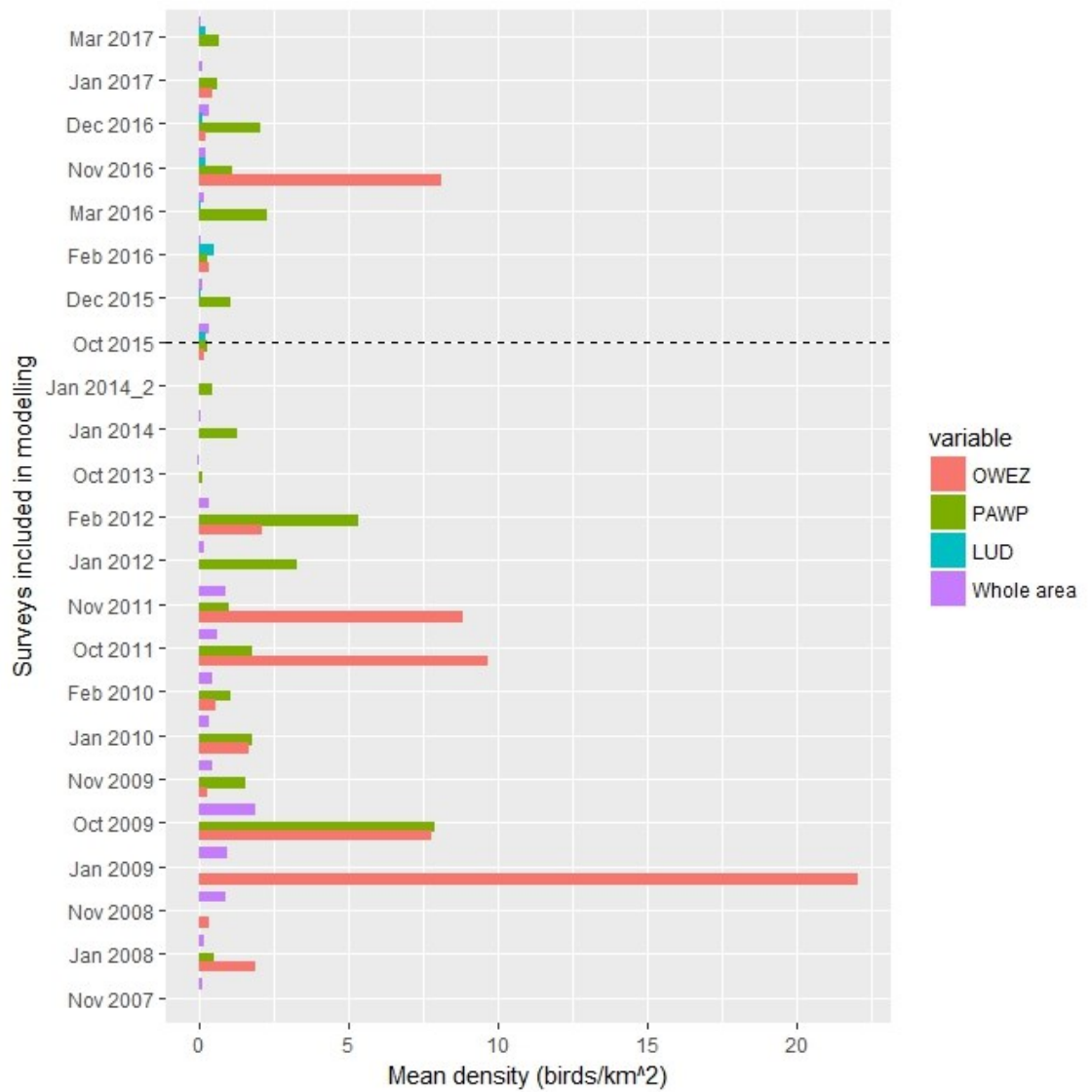


Figure 5.17. Mean density of Great Cormorant during surveys included in the modelling. The mean density within each of the three wind farm footprints (OWEZ, PAWP and LUD) is shown as well as the mean in the whole surveyed area (including windfarms).

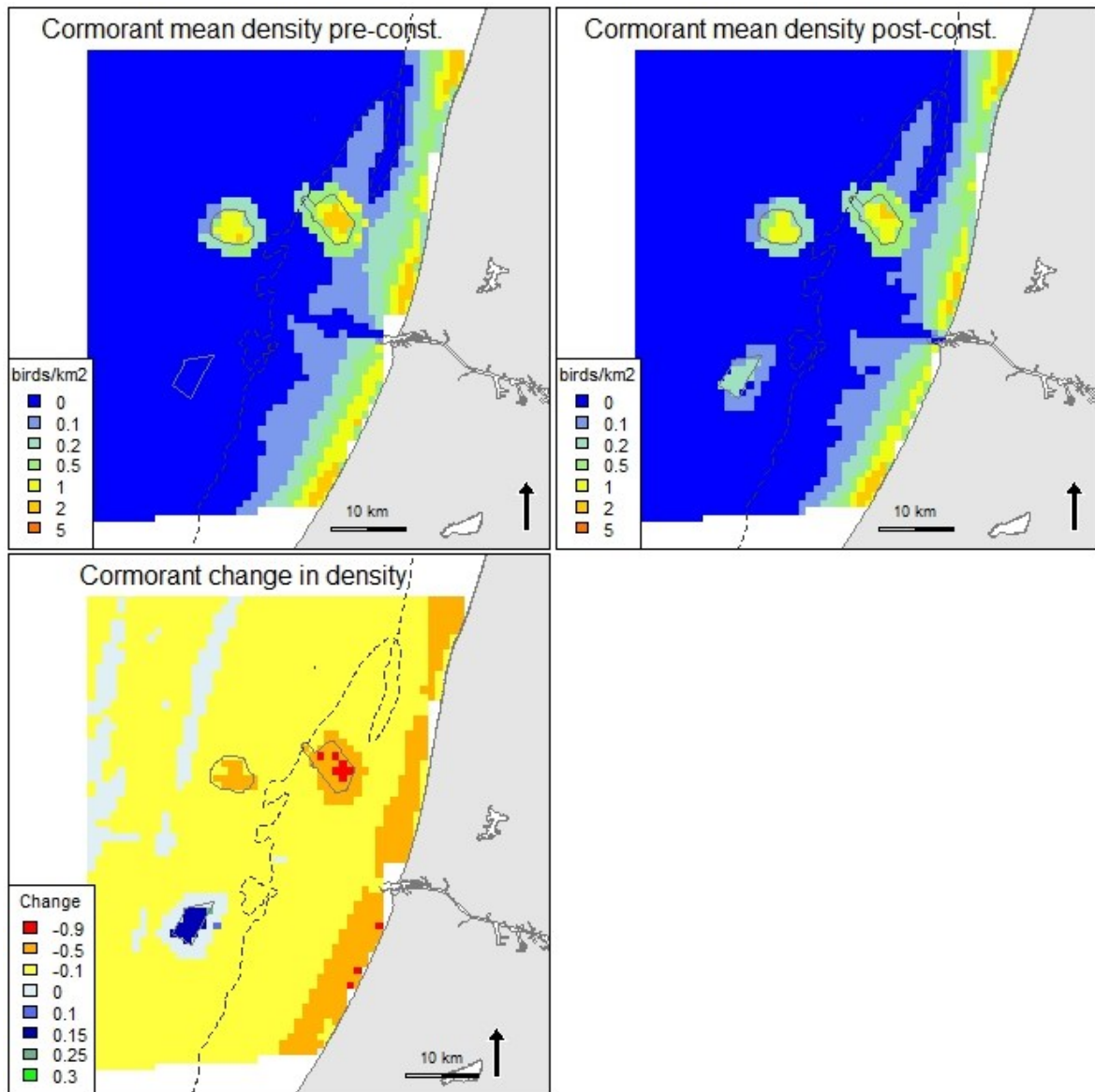


Figure 5.18. Predicted mean density (birds/km²) and distribution of wintering Great Cormorant during eight LUD pre- and eight LUD post-construction surveys, and the relative change in predicted density between the two periods. Note that all included surveys are OWEZ and PAWP post-construction surveys.

5.3.5 *Little Gull Hydrocoloeus minutus*

During the three first LUD-T2 surveys scattered observations of Little Gull were made over the surveyed area. During the March 2017 survey, an apparent influx (spring migration) of birds was recorded in the southern part of the area (Figure 5.19, Figure 5.20). The same temporal pattern was observed in the LUD-T1 surveys.

Model results

Survey 15 and 26 were dropped from the analysis as there were no or very few Little Gulls observed during those surveys. Inclusion of LUD and PAWP footprints as factor levels in the model resulted in strange results, and these were therefore dropped. The presence-absence model indicated a significant lower probability in the OWEZ footprint ($p < 0.01$) and buffer ($p < 0.05$). The probability of presence also increased with decreasing, water depth and shipping intensity, increasing salinity and current speed as well as an

intermediate current gradient (Appendix A). The only smooth term included in the positive model part was current speed (Appendix A). The model was poor and strong conclusions should not be drawn based on the model results. There seemed to be a concentration of Little Gulls just outside LUD based on both the mapped observations and model predictions (Figure 5.19, Figure 5.22).

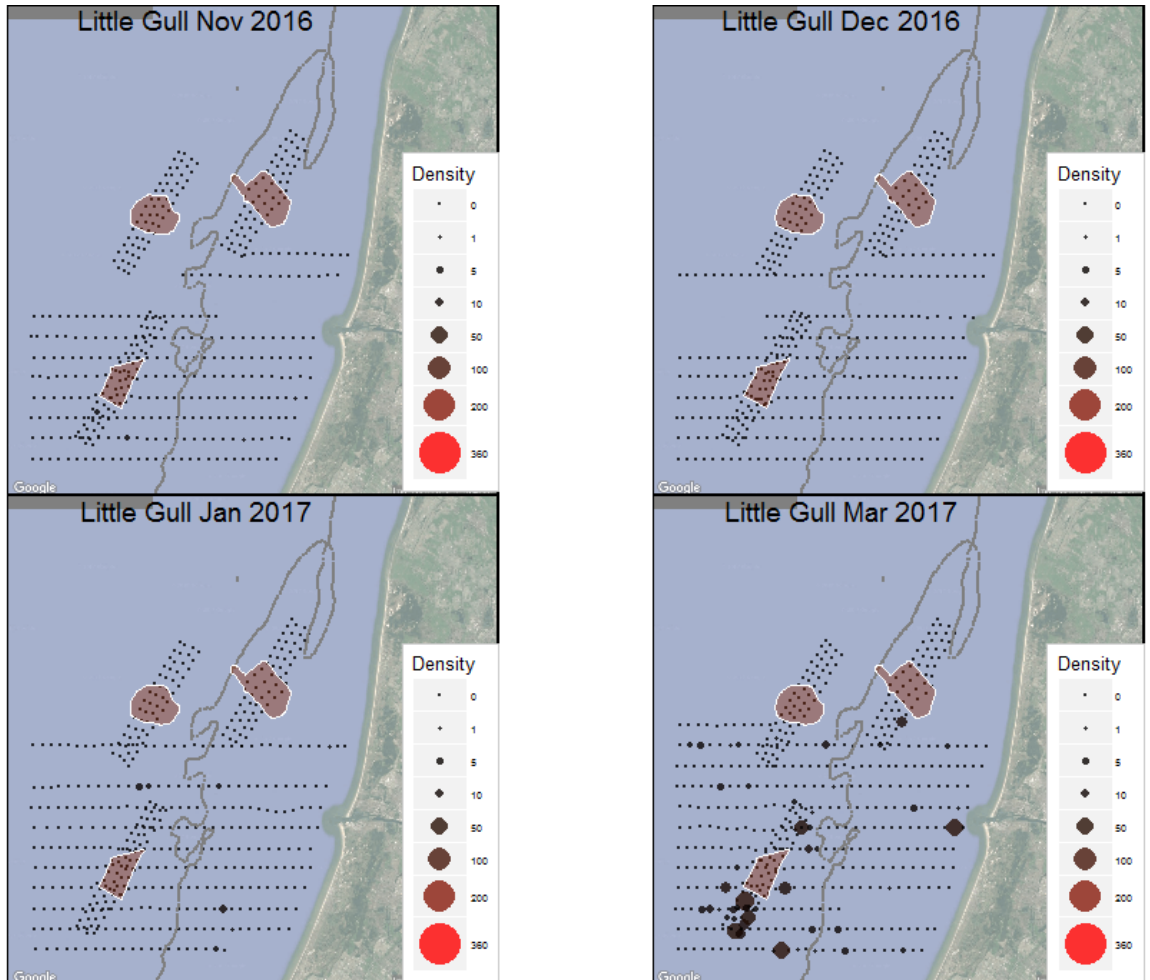


Figure 5.19. Observed density (birds/km²) of Little Gull during LUD-T2 surveys 2016-2017. Densities have been corrected for distance bias.

Little Gull, 2002-2017

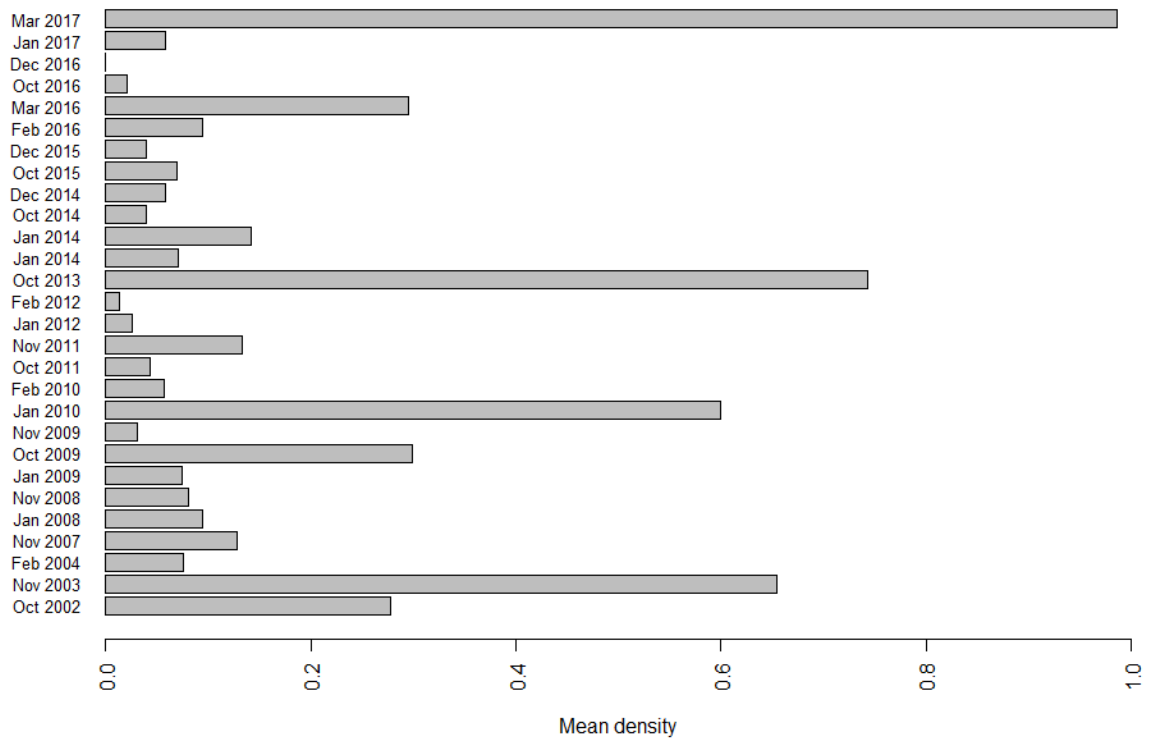


Figure 5.20. Mean observed density (birds/km²) of Little Gull in the entire surveyed area during LUD pre- and post-construction surveys. Densities have been corrected for distance bias.

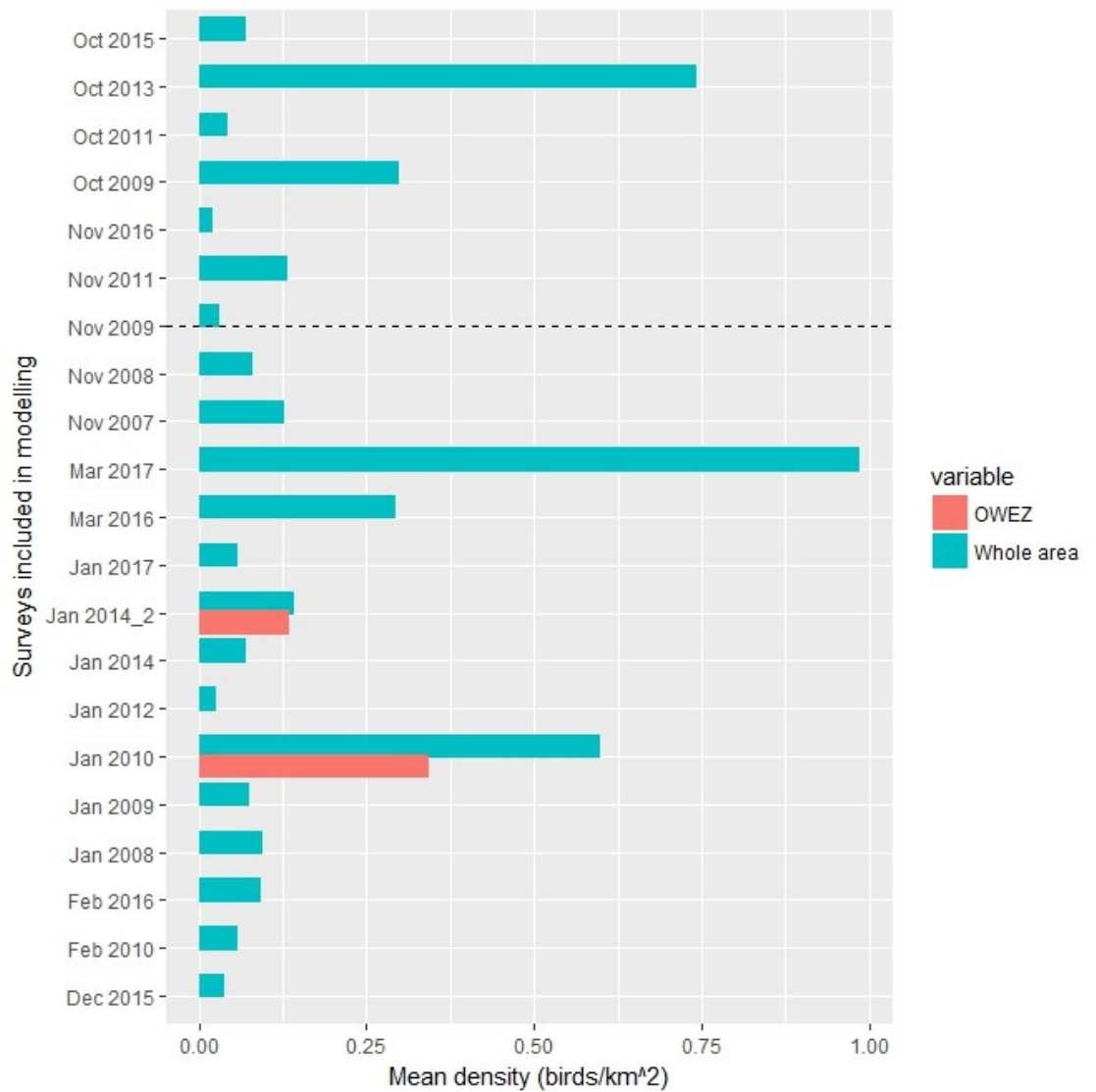


Figure 5.21. Mean density of Little Gull during surveys included in the modelling. The mean density within OWEZ wind farm footprint is shown as well as the mean in the whole surveyed area (including windfarms).

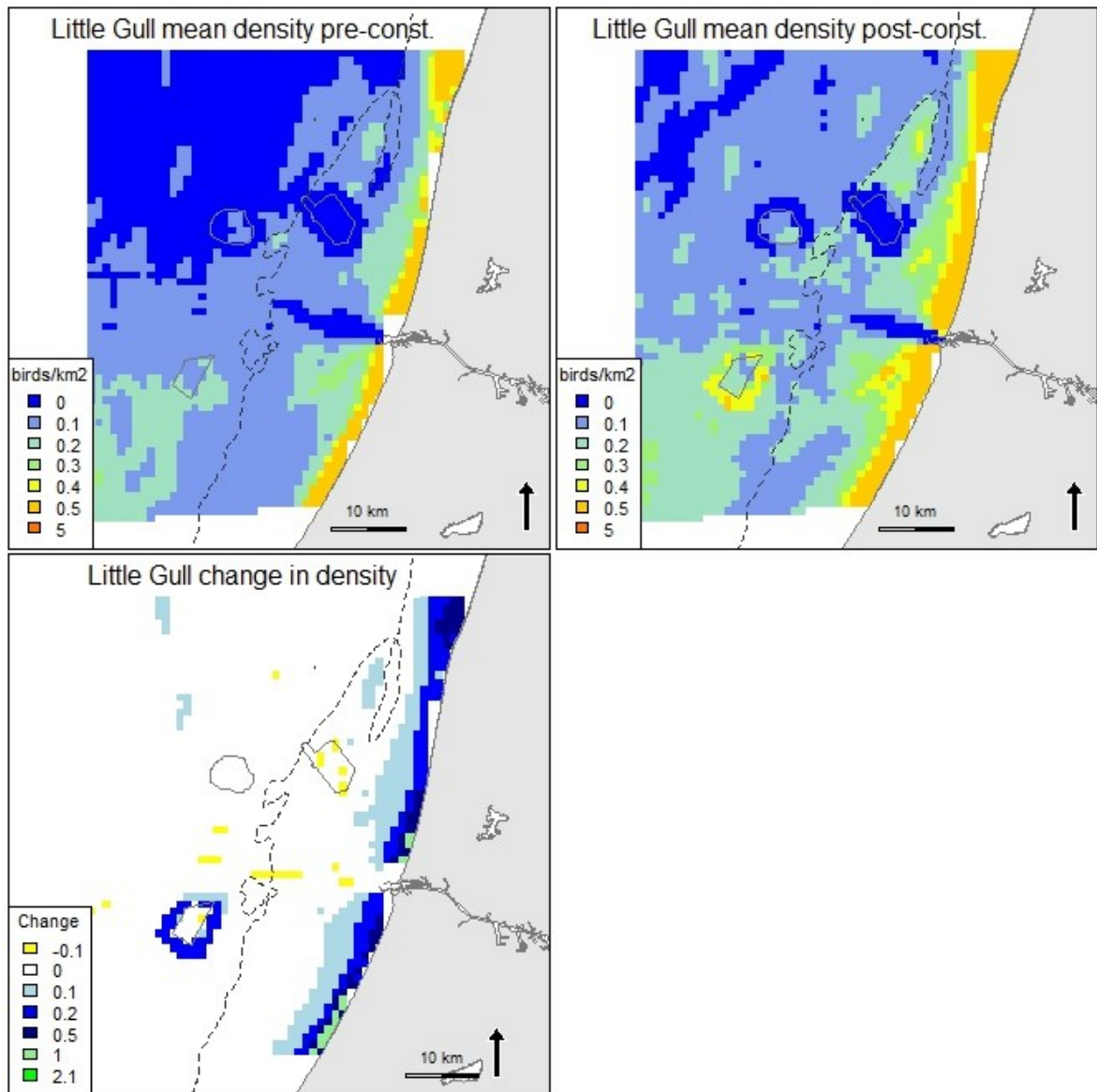


Figure 5.22. Predicted mean density (birds/km²) and distribution of wintering Little Gull during eight LUD pre- and eight LUD post-construction surveys, and the relative change in predicted density between the two periods. Note that all included surveys are OWEZ and PAWP post-construction surveys.

5.3.6 Black-headed Gull *Chroicocephalus ridibundus*

During the LUD-T2 surveys low densities of Black-headed Gulls were recorded in the study area (Figure 5.23, Figure 5.24). No Black headed gull was recorded in LUD.

Model results

According to the model the probability of presence was significantly lower in LUD and in the 2 km buffer around LUD. Other included variables in the presence-absence model part were decreasing depth, salinity and current speed as well as increasing CG gradient. In the positive model part Depth and current speed was influential. Generally the model was rather poor although, the explanation degree of the presence-absence part was fair 24% (Appendix A). The predictions indicate a preference to the coastal water mass (Figure 5.26).

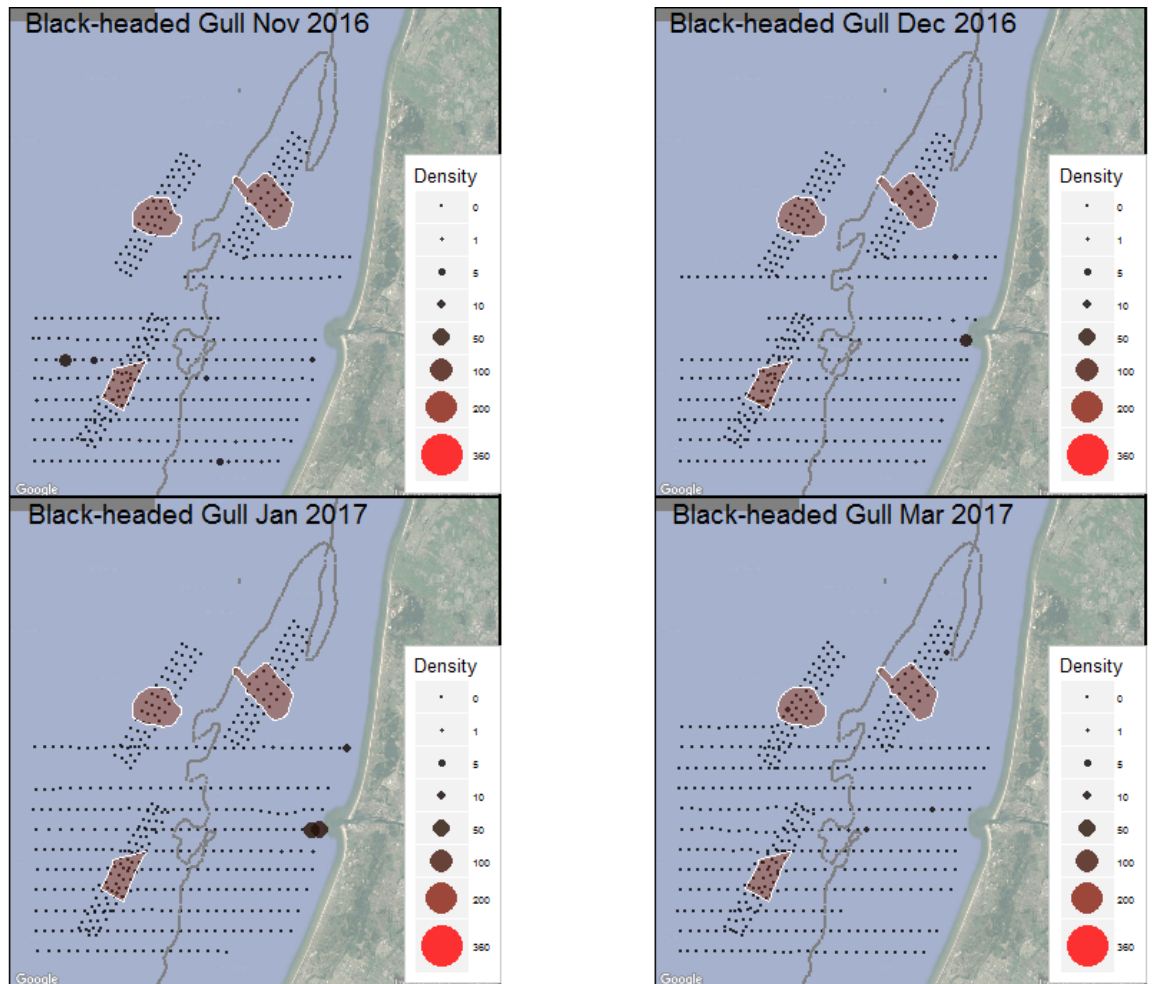


Figure 5.23. Observed density (birds/km²) of Black-headed Gull during LUD-T2 surveys 2016-2017. Densities have been corrected for distance bias.

Black-headed Gull, 2002-2017

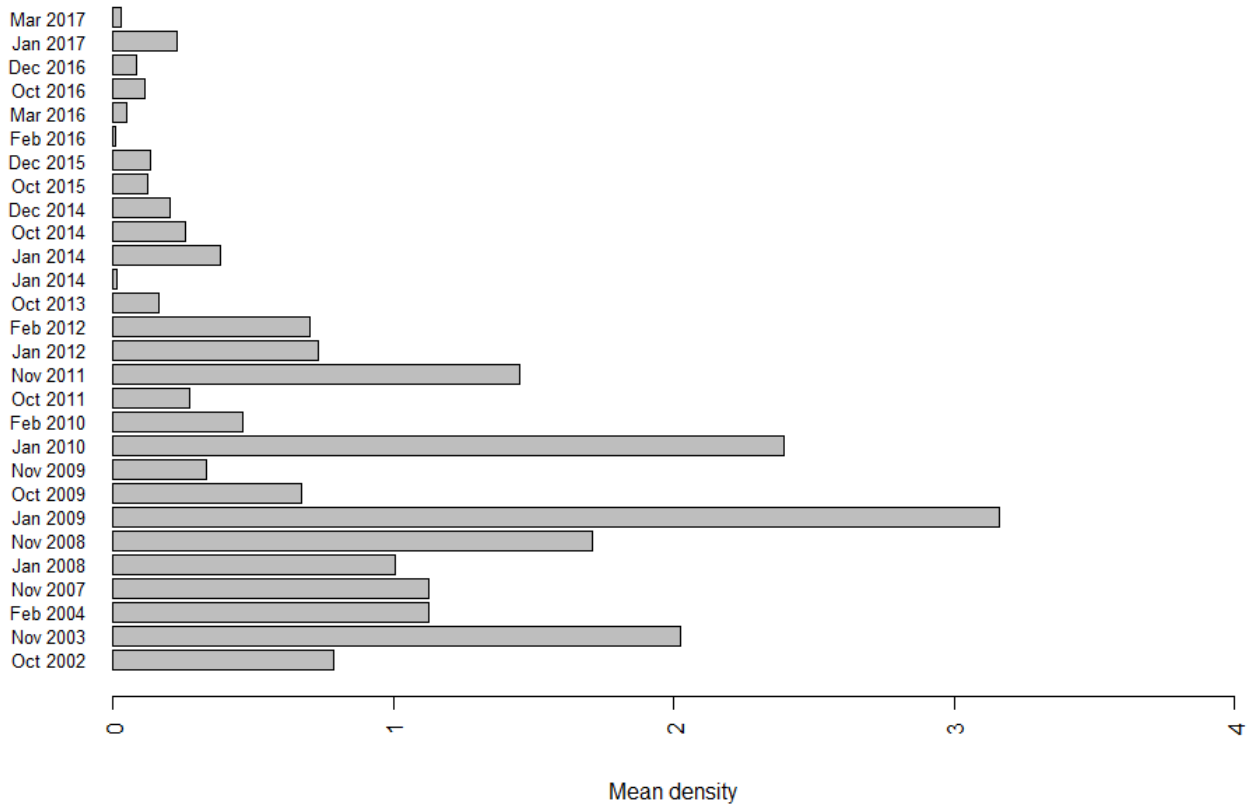


Figure 5.24. Mean observed density (birds/km²) of Black-headed Gull in the entire surveyed area during LUD pre- and post-construction surveys. Densities have been corrected for distance bias.

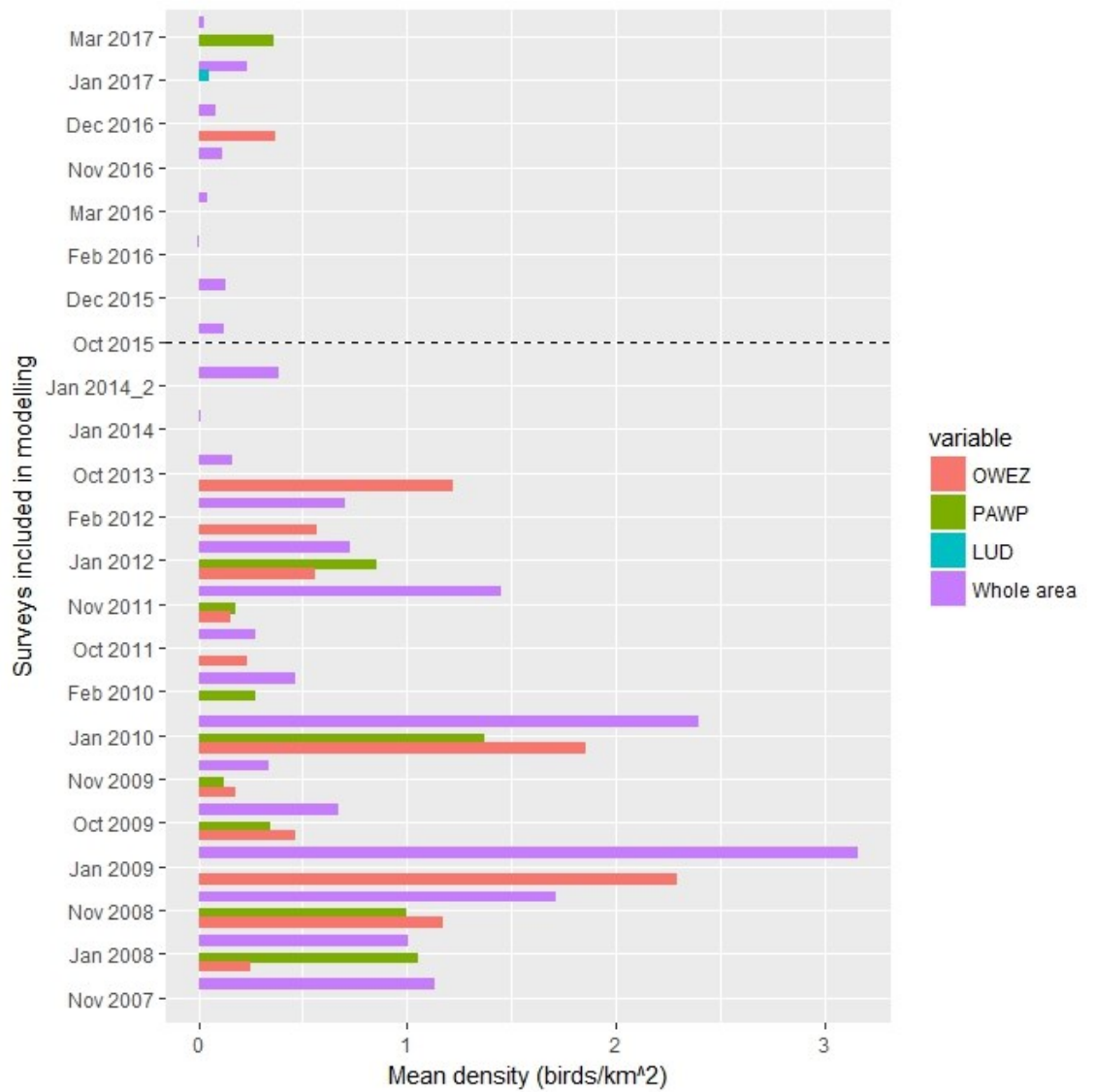


Figure 5.25. Mean density of Black-headed Gull during surveys included in the modelling. The mean density within each of the three wind farm footprints (OWEZ, PAWP and LUD) is shown as well as the mean in the whole surveyed area (including windfarms).

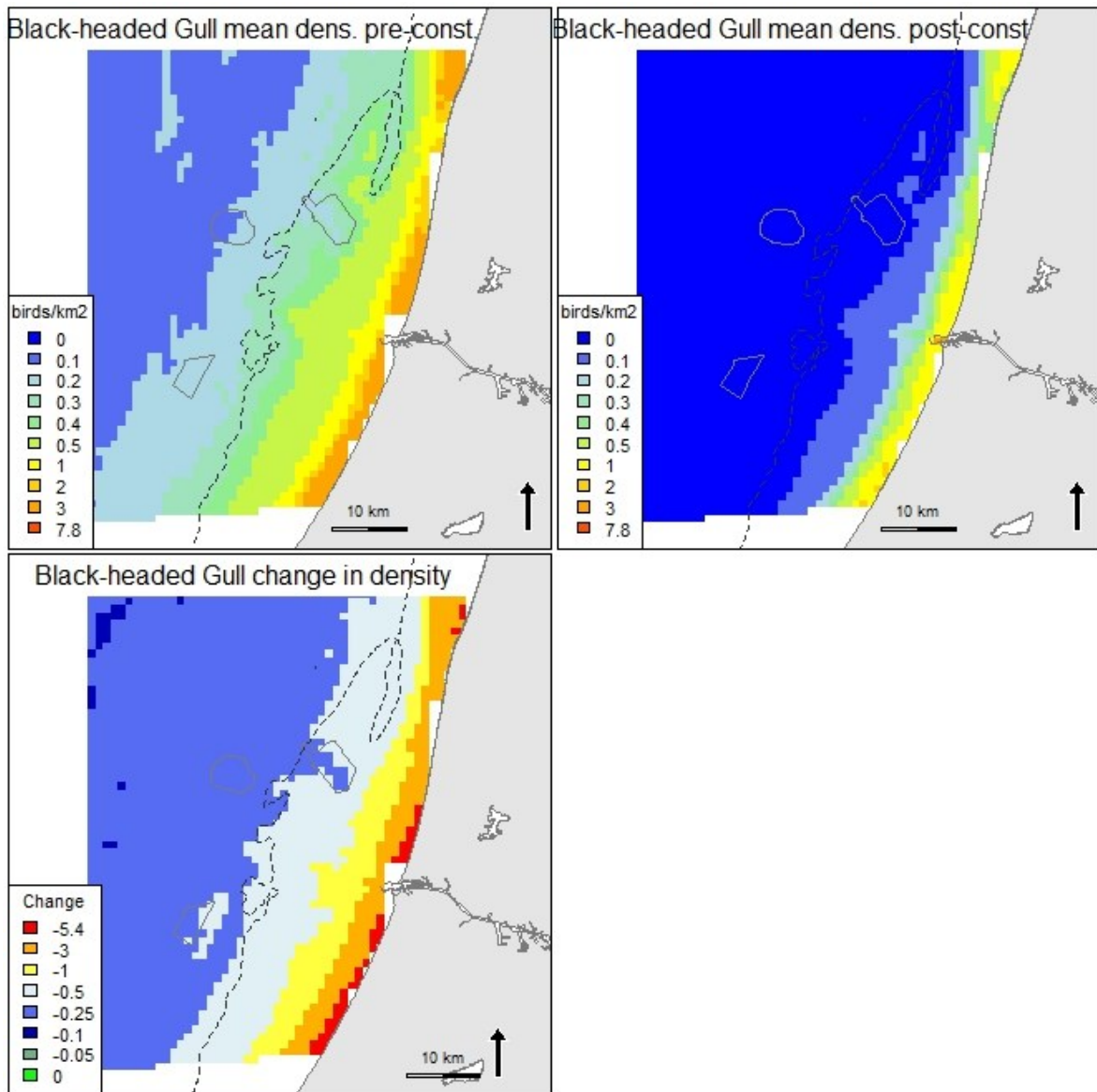


Figure 5.26. Predicted mean density (birds/km²) and distribution of wintering Black-headed Gull during eight LUD pre- and eight LUD post-construction surveys, and the relative change in predicted density between the two periods. Note that all included surveys are OWEZ and PAWP post-construction surveys.

5.3.7 Common Gull *Larus canus*

During the LUD-T2 surveys highest densities were observed in December and January with observations scattered around the study area (Figure 5.27, Figure 5.28). Birds were recorded inside all three windfarm footprints (Figure 5.27).

Model results

The model indicated that the probability of presence is highest in water depths around 15 m where mean current speed is low. Increasing density, when present, was further explained by increasing salinity and current gradient (Appendix A). The windfarm footprints were not significant in the model, however the model predictions indicate a potential small increase in the vicinity of the LUD windfarm (Figure 5.30).

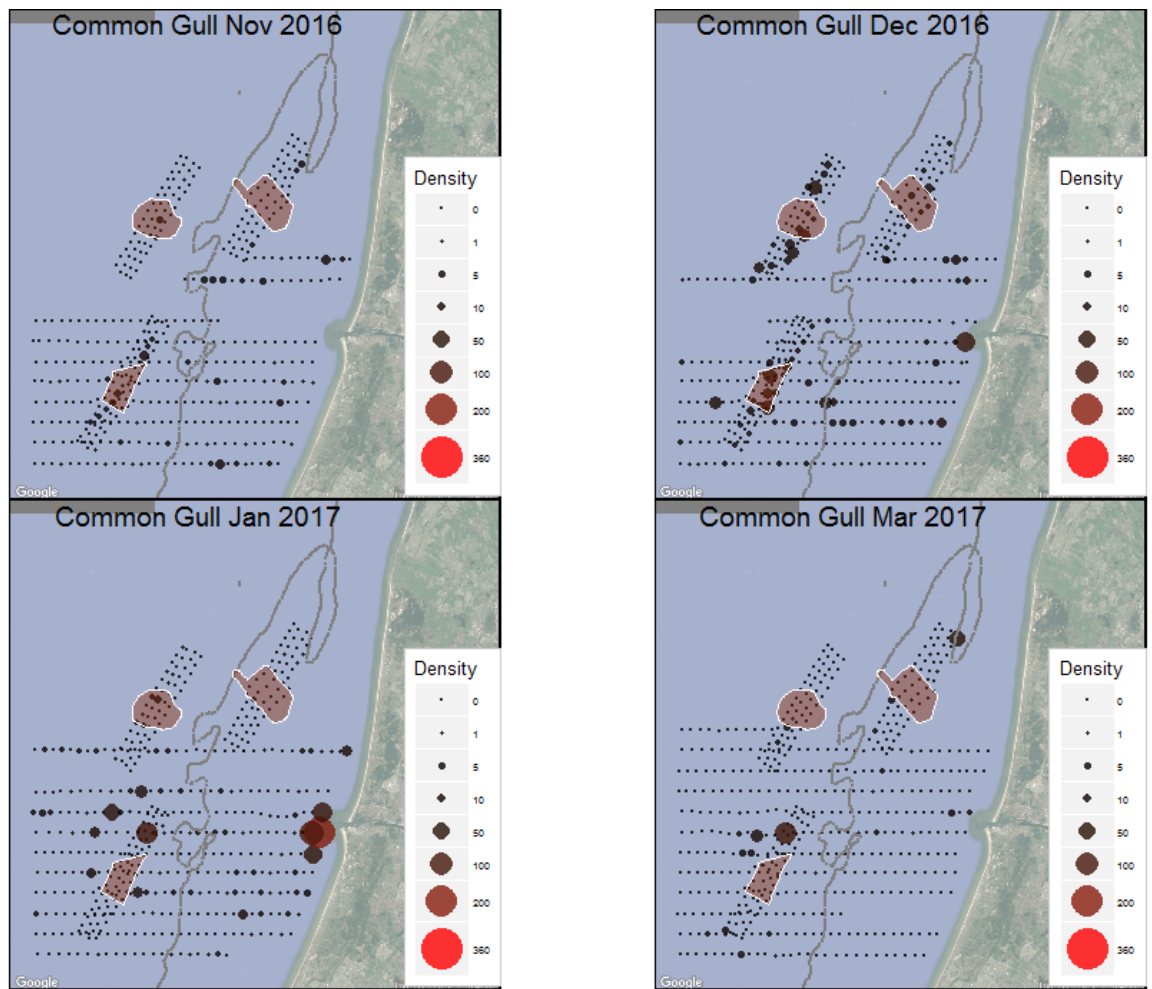


Figure 5.27. Observed density (birds/km²) of Common Gull during LUD-T2 surveys 2016-2017. Densities have been corrected for distance bias.

Common Gull, 2002-2017

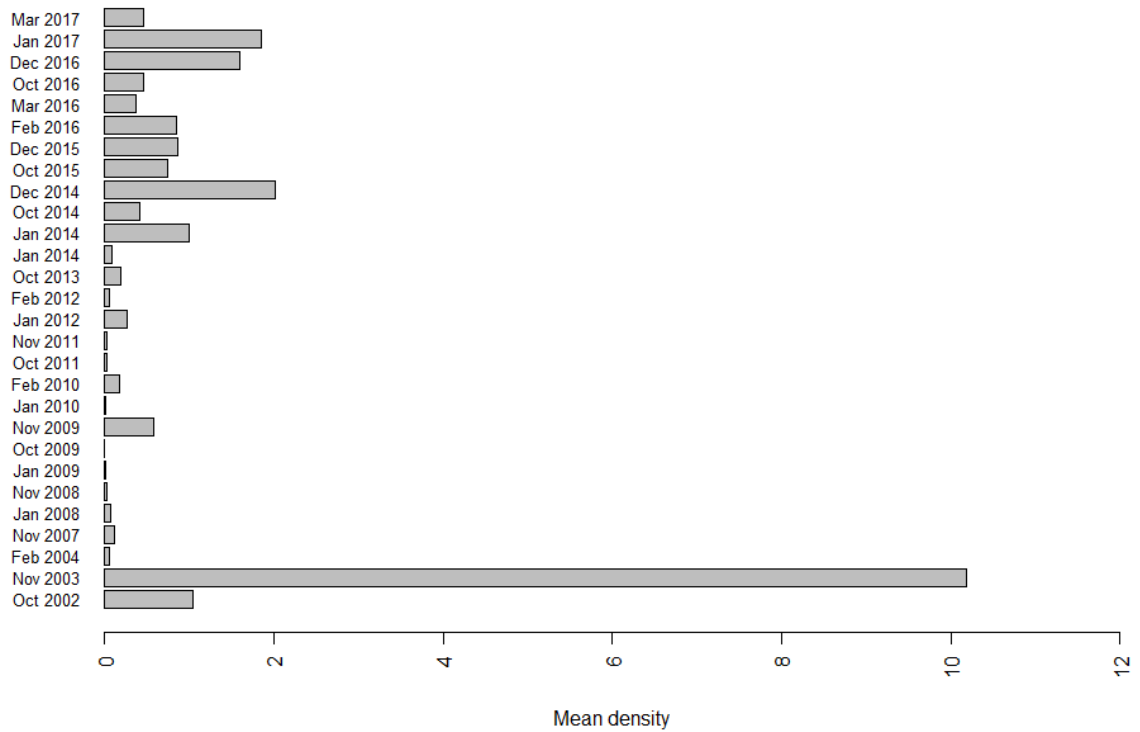


Figure 5.28. Mean observed density (birds/km²) of Common Gull in the entire surveyed area during LUD pre- and post-construction surveys. Densities have been corrected for distance bias.

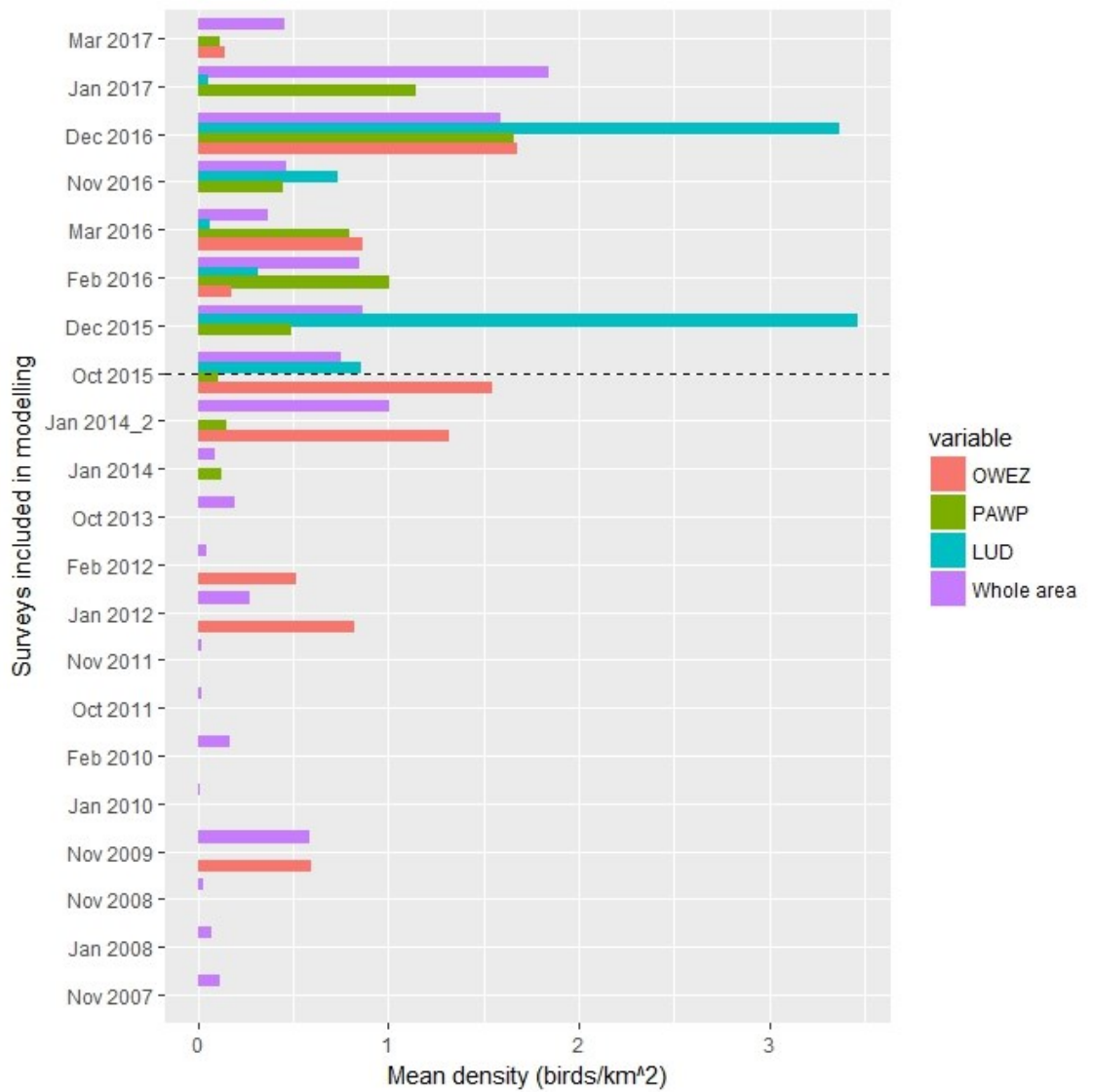


Figure 5.29. Mean density of Common Gull during surveys included in the modelling. The mean density within each of the three wind farm footprints (OWEZ, PAWP and LUD) is shown as well as the mean in the whole surveyed area (including windfarms).

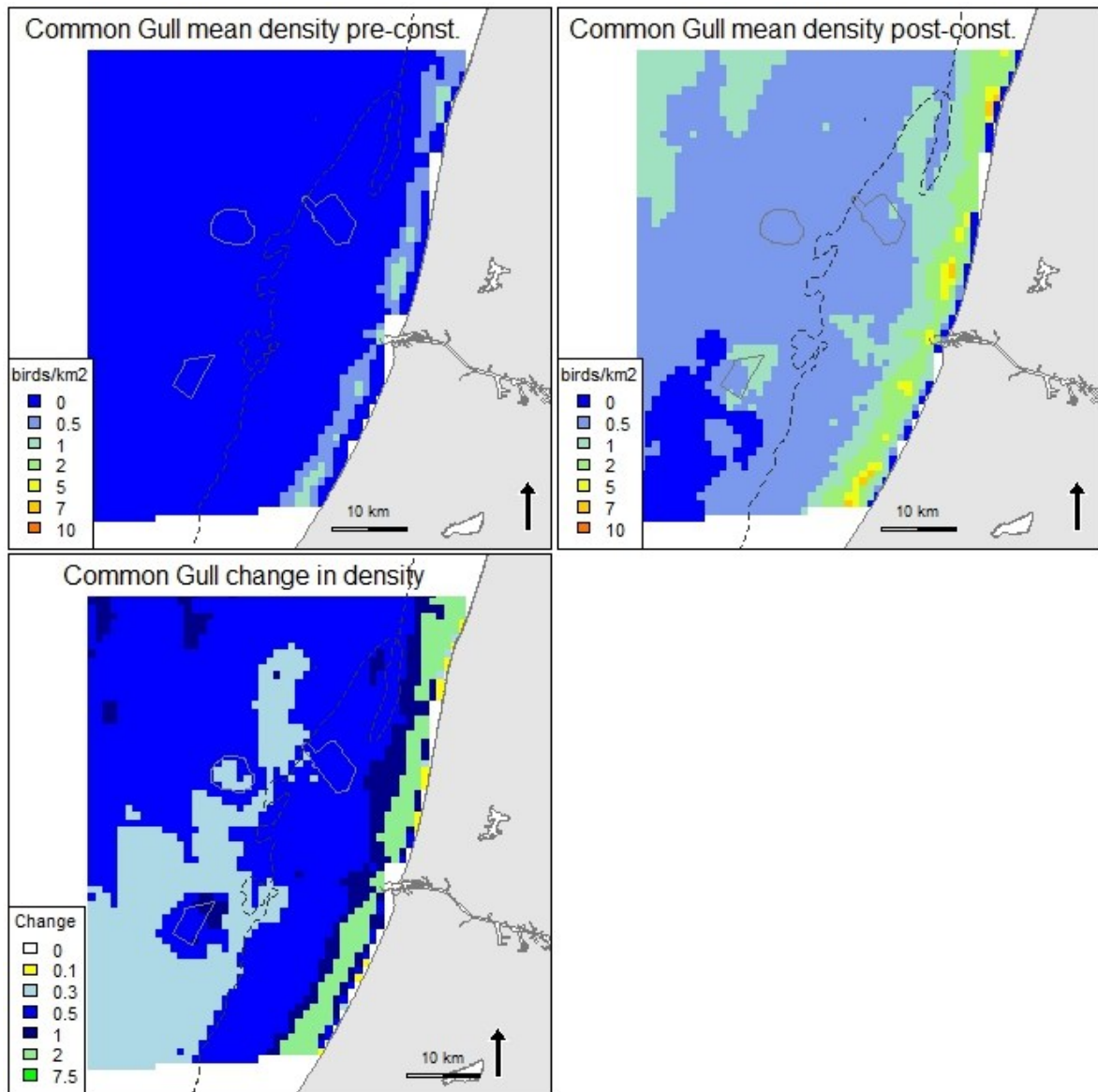


Figure 5.30. Predicted mean density (birds/km²) and distribution of wintering Common Gull during eight LUD pre- and eight LUD post-construction surveys, and the relative change in predicted density between the two periods. Note that all included surveys are OWEZ and PAWP post-construction surveys.

5.3.8 Lesser Black-backed Gull *Larus fuscus*

During the LUD-T2 surveys the distribution of Lesser Black-backed gulls appears to be “bi-modal” with birds either closer to the coast or farther offshore (Figure 5.31), similar to the distribution pattern observed during the T1 surveys. Very high mean densities were observed in March in comparison to other surveys, which most likely is an influx of migrating birds (Figure 5.31, Figure 5.32).

Model results

According to the model the probability of presence was significantly lower within the LUD footprint ($p < 0.01$). Otherwise the same variables were influential in both model parts, decreasing water depth and increasing salinity and current gradient (Appendix A). The explanation degree of the model was low, indicating a rather poor model. The predictions indicate that the densities are highest closest to the coast and farther offshore (Figure 5.34).

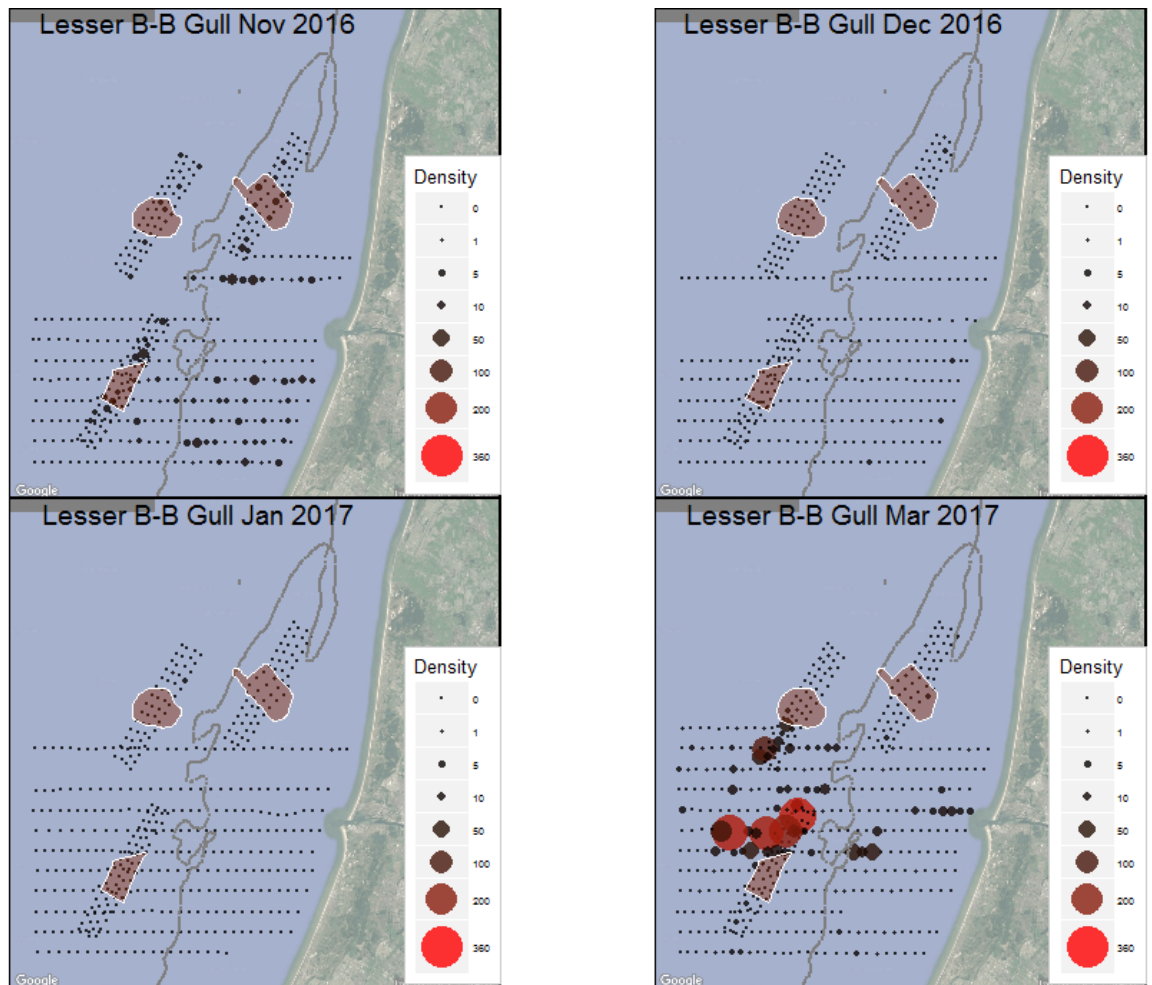


Figure 5.31. Observed density (birds/km²) of Lesser Black-backed Gull during LUD-T2 surveys 2016-2017. Densities have been corrected for distance bias.

Lesser Black-backed Gull, 2002-2017

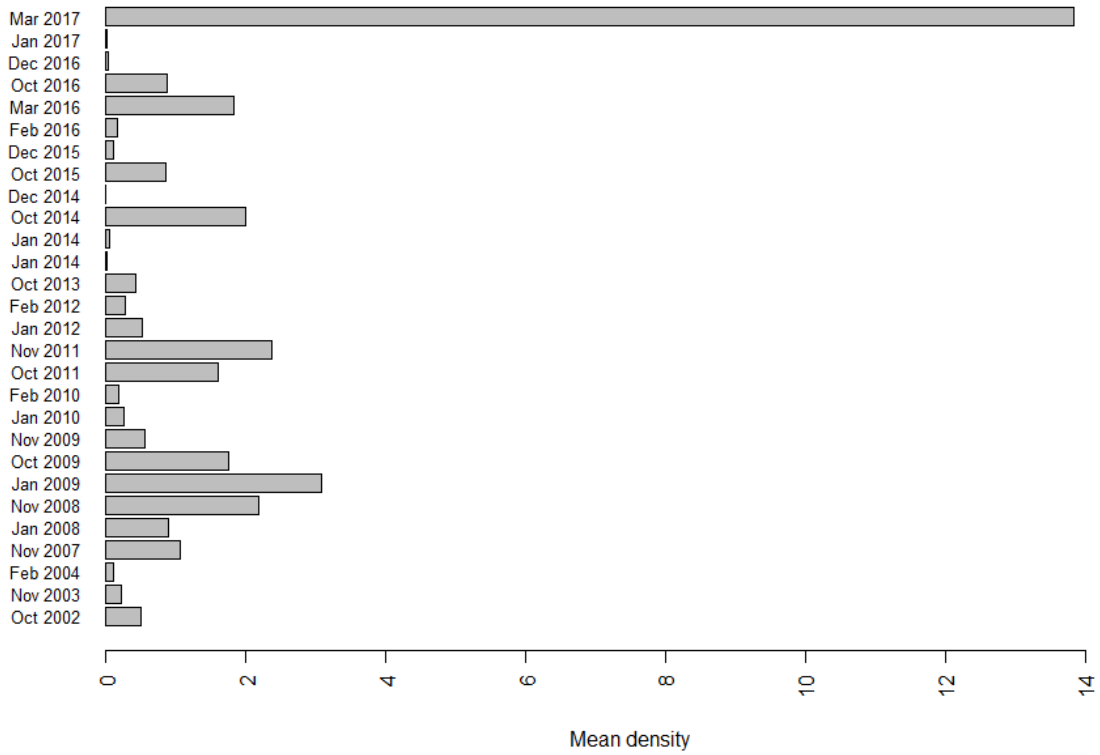


Figure 5.32. Mean observed density (birds/km²) of Lesser Black-backed Gull in the entire surveyed area during LUD pre- and post-construction surveys. Densities have been corrected for distance bias.

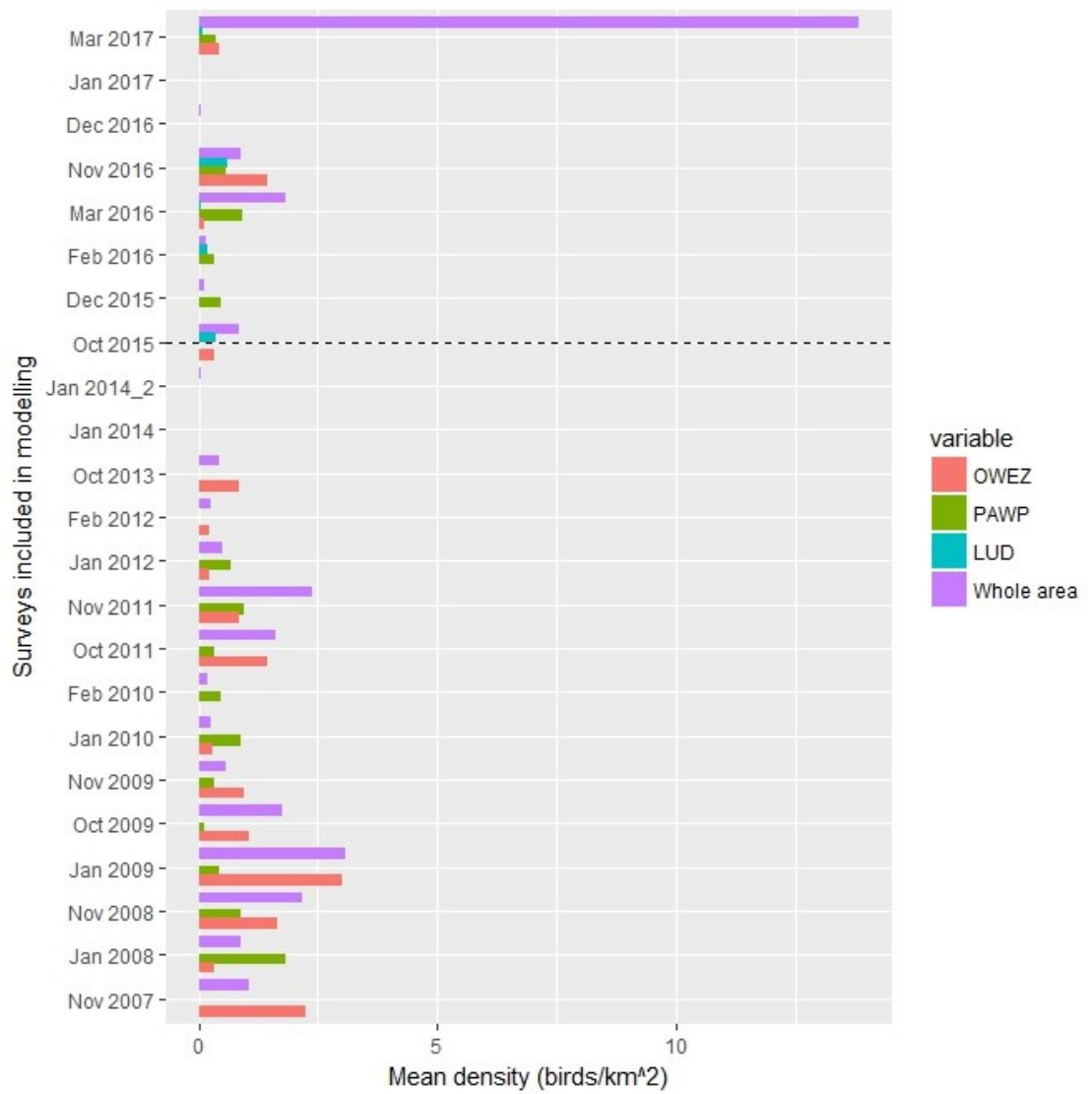


Figure 5.33. Mean density of Lesser Black-backed Gull during surveys included in the modelling. The mean density within each of the three wind farm footprints (OWEZ, PAWP and LUD) is shown as well as the mean in the whole surveyed area (including windfarms).

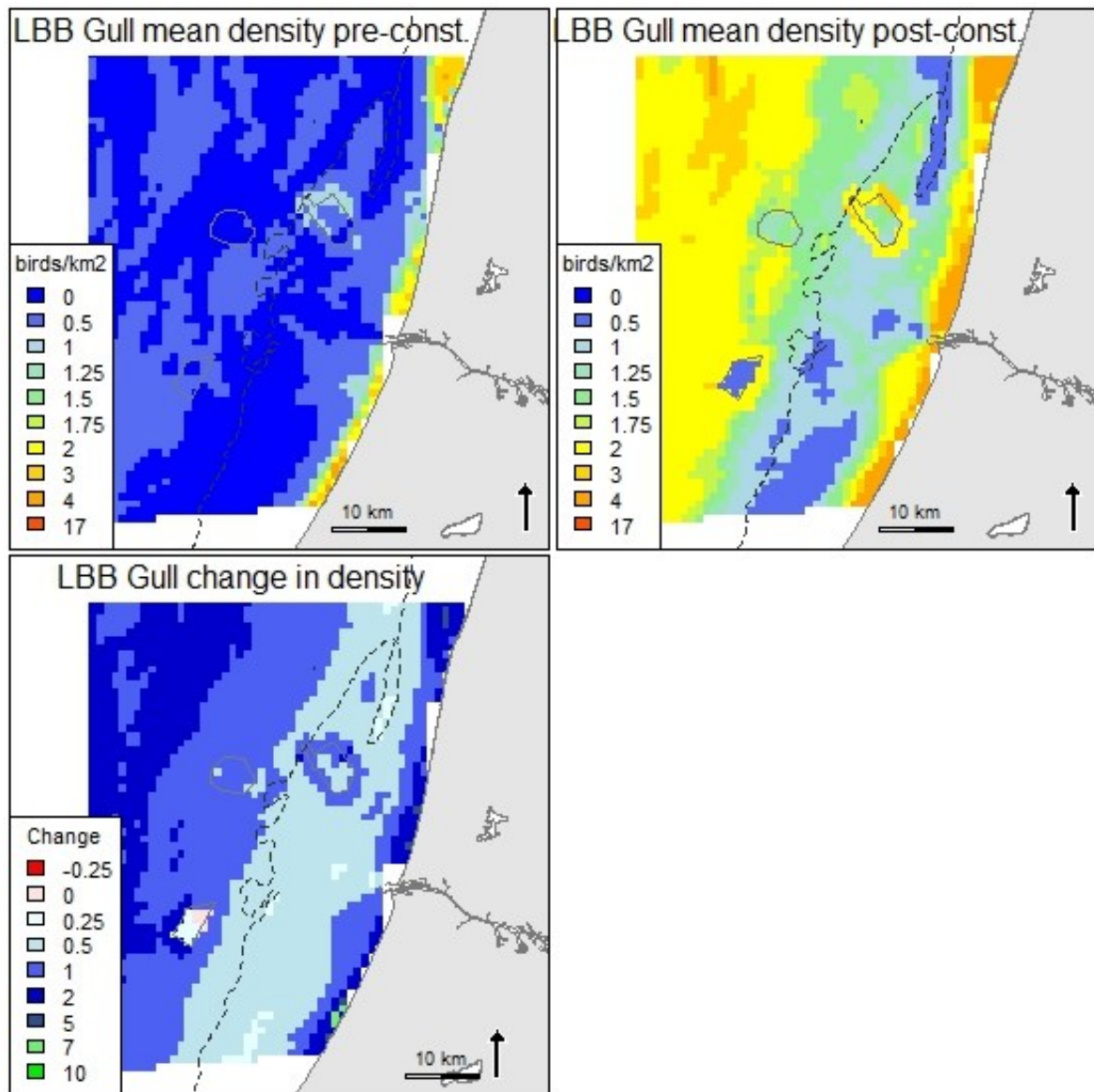


Figure 5.34. Predicted mean density (birds/km²) and distribution of wintering Lesser Black-backed Gull during eight LUD pre- and eight LUD post-construction surveys, and the relative change in predicted density between the two periods. Note that all included surveys are OWEZ and PAWP post-construction surveys.

5.3.9 Herring Gull *Larus argentatus*

During the LUD-T2 surveys low densities of Herring Gulls were observed without a clear spatial pattern (Figure 5.35, Figure 5.36). Highest mean density was observed during the survey in March 2017 (Figure 5.36). Herring Gulls were observed in all three windfarms (Figure 5.35).

Model results

According to the model the probability of presence was significantly higher in the PAWP footprint indicating an attraction the PAWP. The probability of presence also significantly increased with decreasing current speed (Appendix A). If present, an increase in density was explained by increasing salinity and current gradient (Appendix A). Overall, the model was poor with low explanation degree and predictive power (Appendix A). The mapped predictions indicate that the coastal waters are preferred by the Herring

Gull (Figure 5.38), however as already indicated the model is poor and the birds were observed scattered around the whole study area (Figure 5.35).

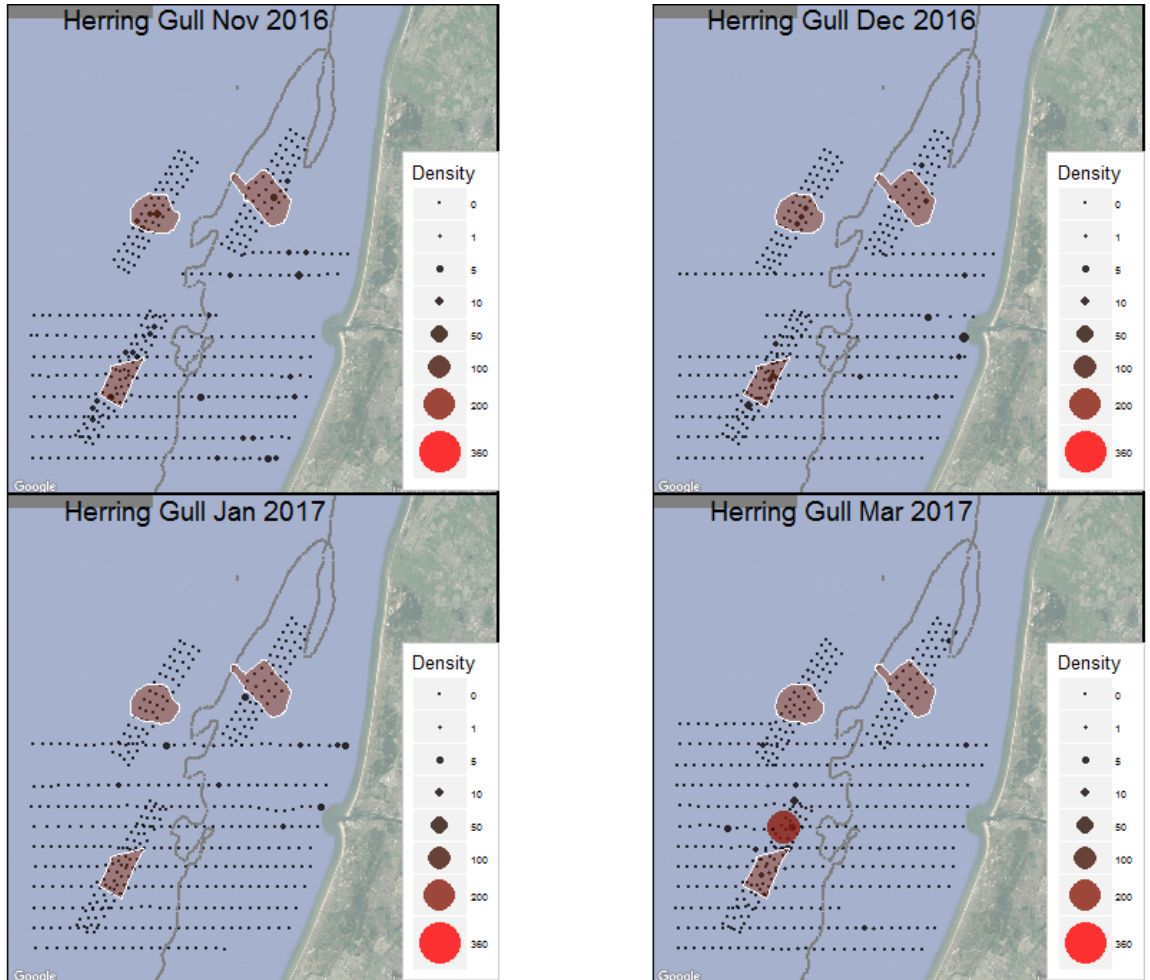


Figure 5.35. Observed density (birds/km²) of Herring Gull during LUD-T2 surveys 2016-2017. Densities have been corrected for distance bias.

Herring Gull, 2002-2017

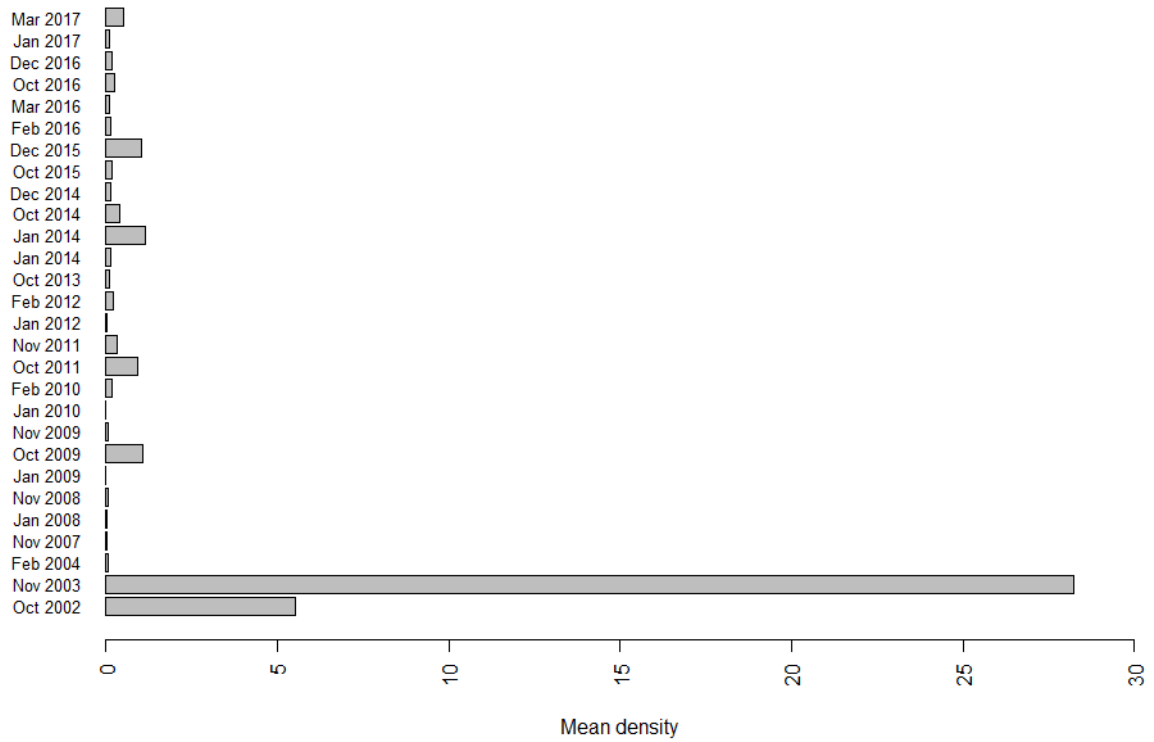


Figure 5.36. Mean observed density (birds/km²) of Herring Gull in the entire surveyed area during LUD pre- and post-construction surveys. Densities have been corrected for distance bias.

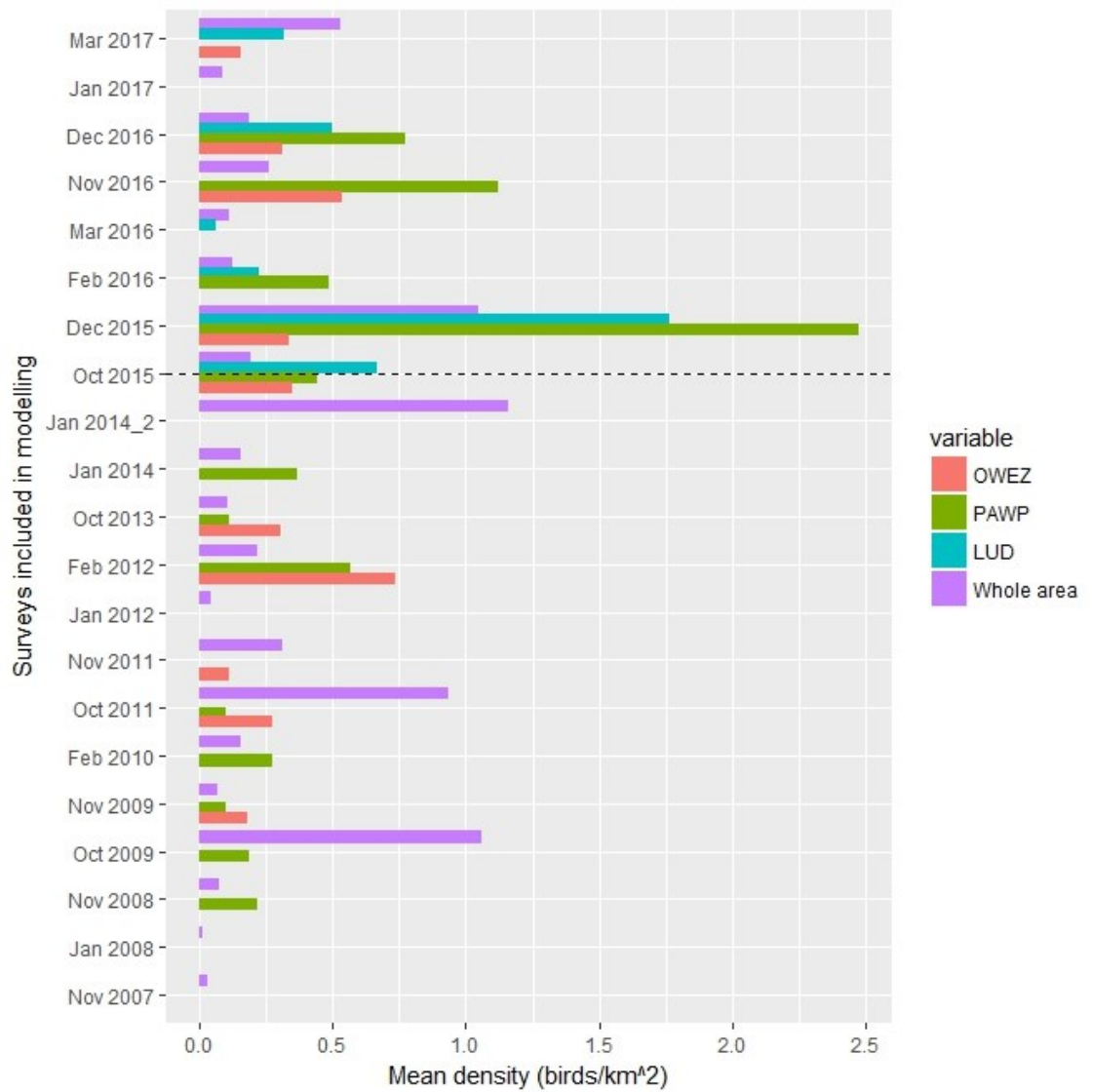


Figure 5.37. Mean density of Herring Gull during surveys included in the modelling. The mean density within each of the three wind farm footprints (OWEZ, PAWP and LUD) is shown as well as the mean in the whole surveyed area (including windfarms).

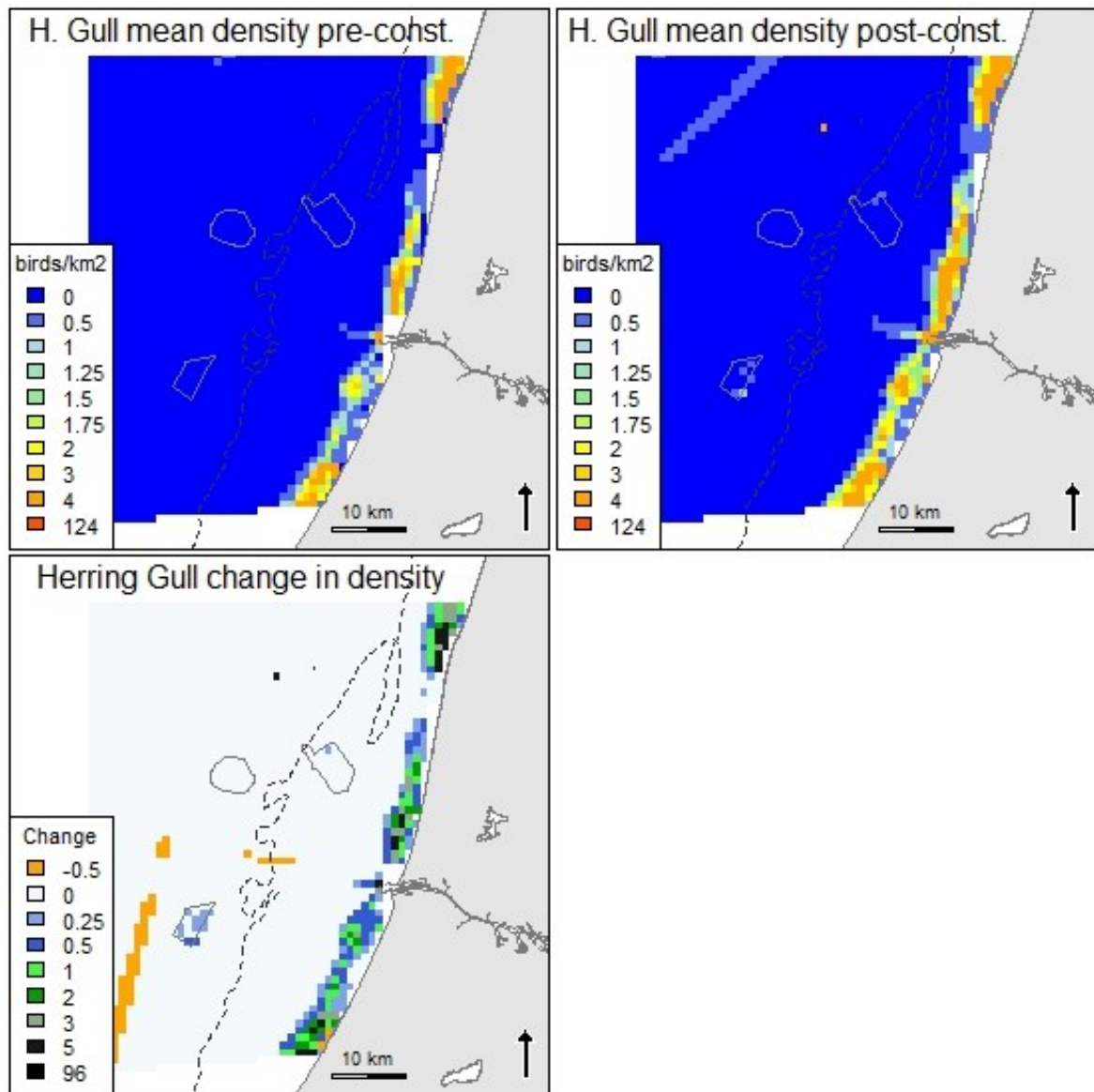


Figure 5.38. Predicted mean density (birds/km²) and distribution of wintering Herring Gull during eight LUD pre- and eight LUD post-construction surveys, and the relative change in predicted density between the two periods. Note that all included surveys are OWEZ and PAWP post-construction surveys.

5.3.10 Great Black-backed Gull *Larus marinus*

Low densities of Great Black-backed Gulls were observed during all four LUD-T2 surveys (Figure 5.39, Figure 5.40). It is difficult to identify any clear distribution patterns but many observations were made in the vicinity of LUD in March and several within PAWP during the October-November survey (Figure 5.39).

Model results

In accordance with the observations the model indicated an attraction to PAWP with a significantly higher probability within the PAWP footprint ($p < 0.01$) and 2 km buffer ($p < 0.05$). Of the continuous variables only current gradient (increasing response) was included in both model parts. The predictions indicate a potential small attraction to all windfarms, however in low densities (Figure 5.42). Highest densities were predicted close to the coast (Figure 5.42).

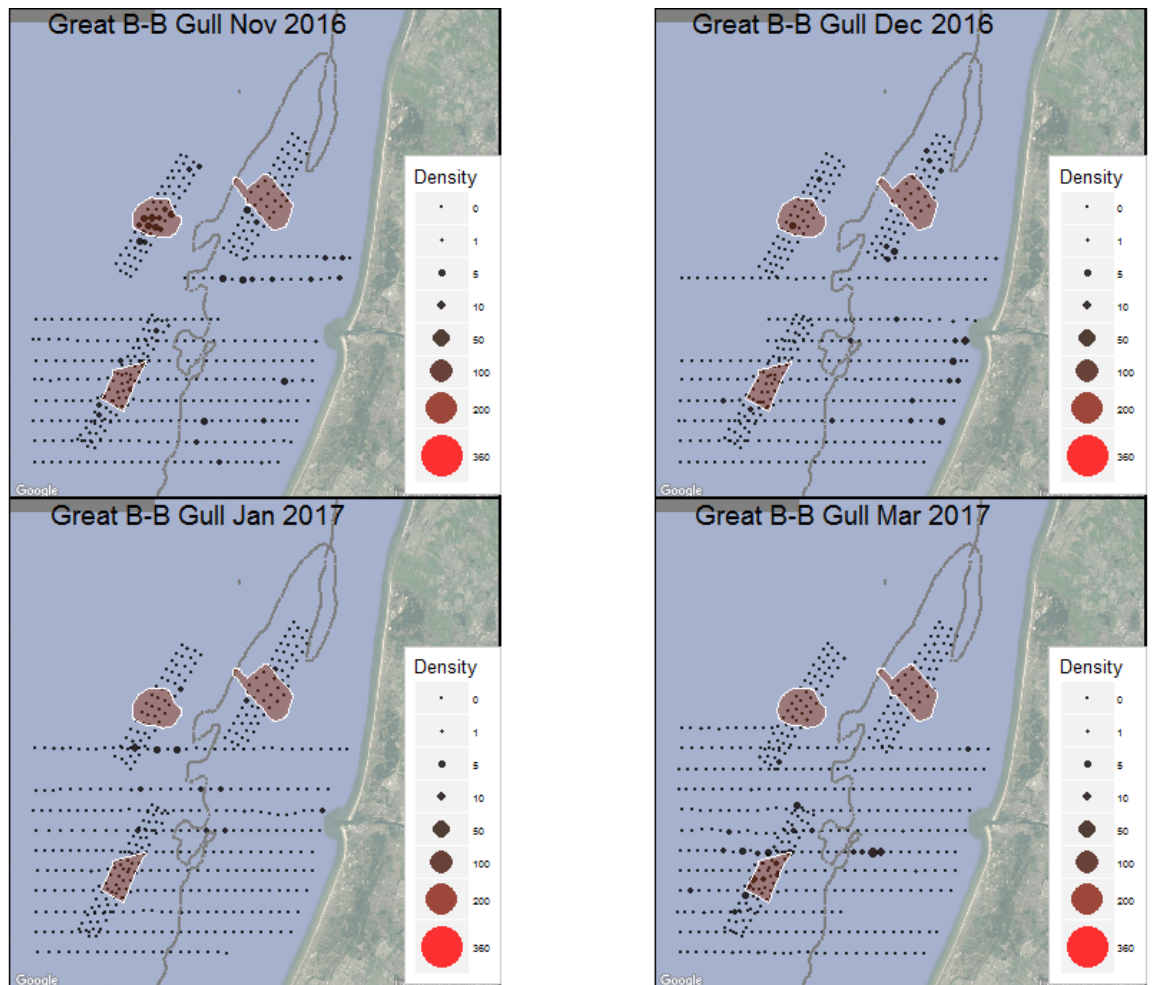


Figure 5.39. Observed density (birds/km²) of Great Black-backed Gull during LUD-T2 surveys 2016-2017. Densities have been corrected for distance bias.

Great Black-backed Gull, 2002-2017

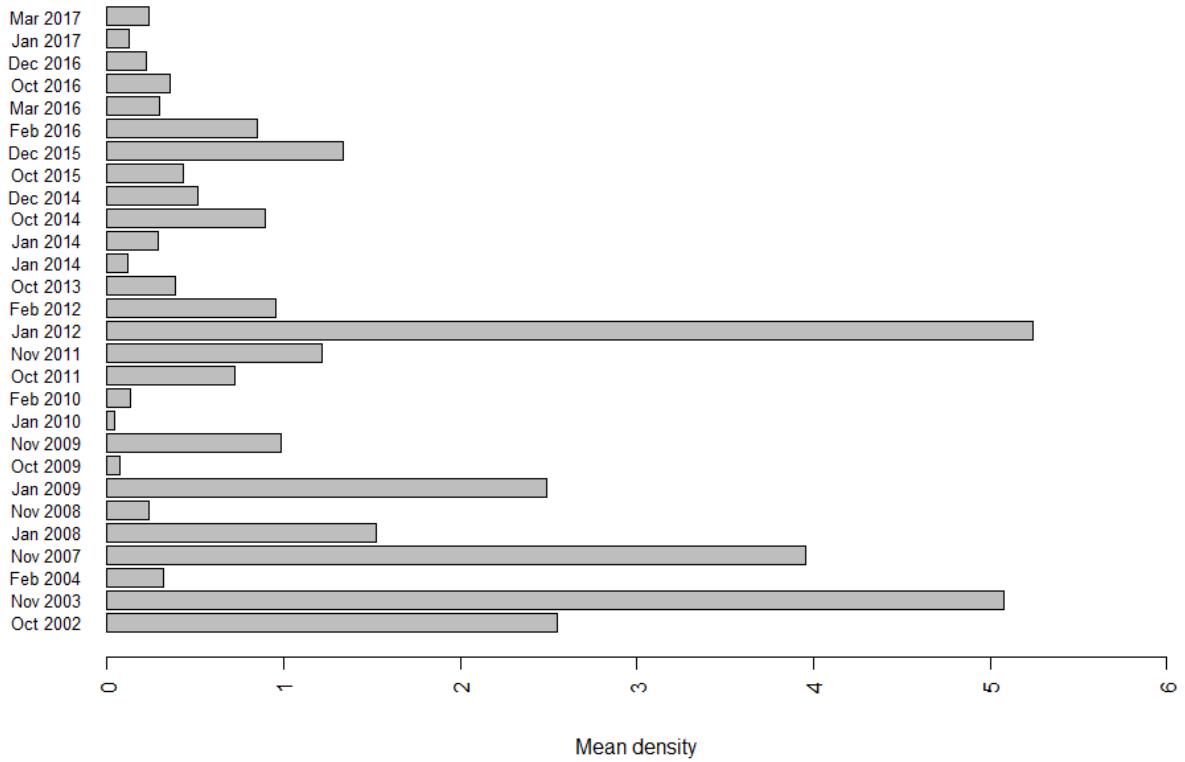


Figure 5.40. Mean observed density (birds/km²) of Great Black-backed Gull in the entire surveyed area during LUD pre- and post-construction surveys. Densities have been corrected for distance bias.

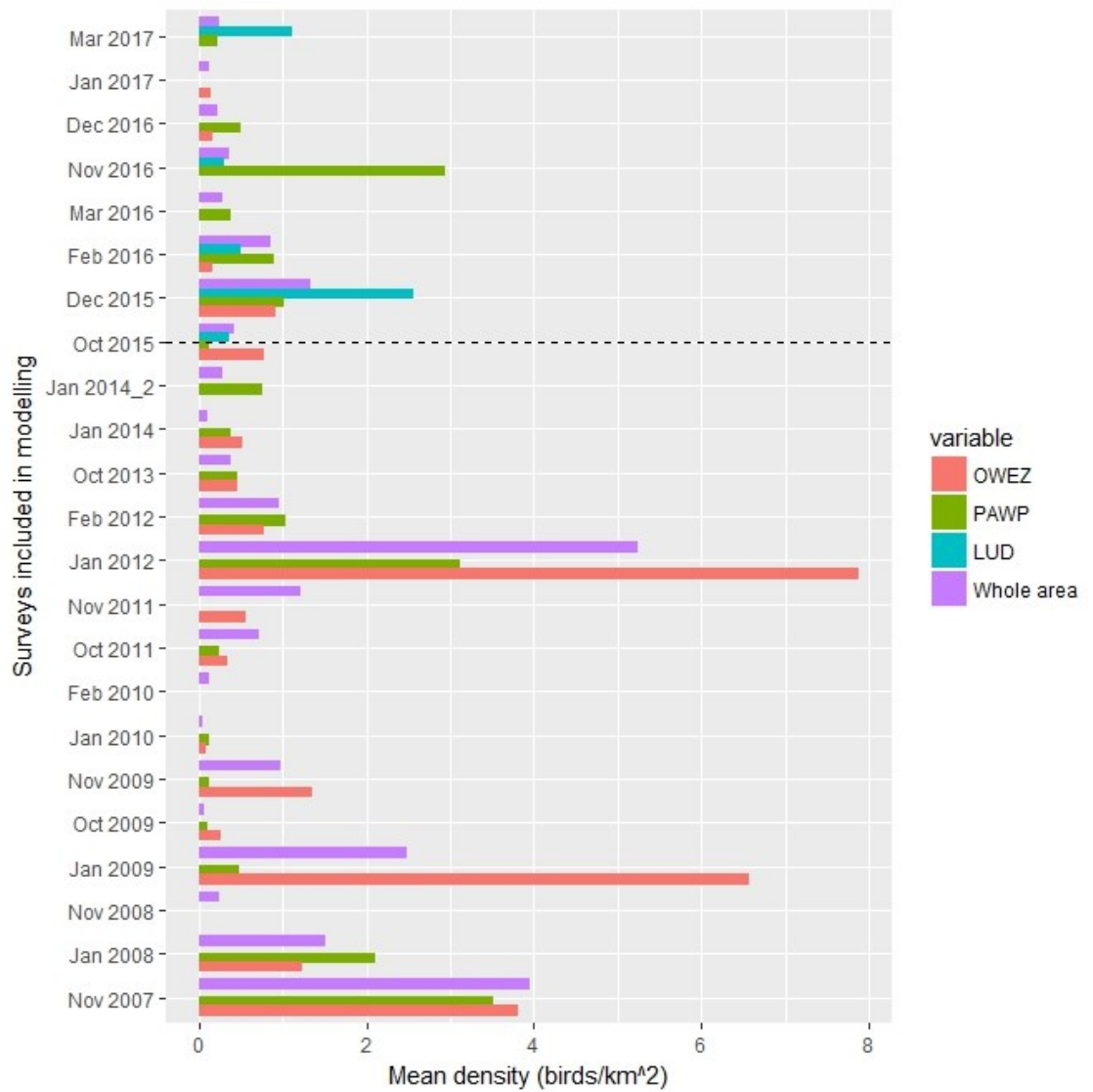


Figure 5.41. Mean density of Great Black-backed Gull during surveys included in the modelling. The mean density within each of the three wind farm footprints (OWEZ, PAWP and LUD) is shown as well as the mean in the whole surveyed area (including windfarms).

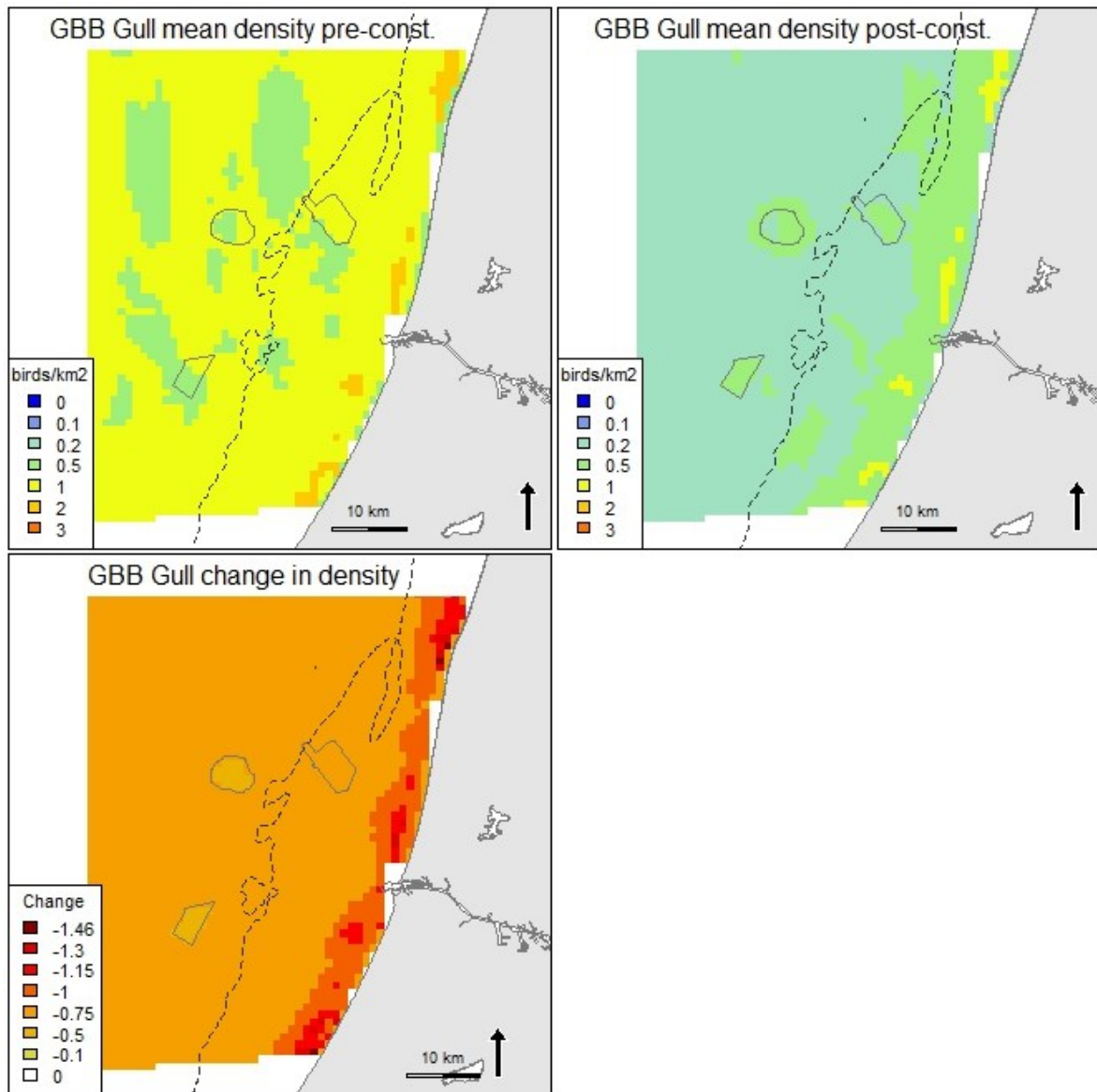


Figure 5.42. Predicted mean density (birds/km²) and distribution of wintering Great Black-backed Gull during eight LUD pre- and eight LUD post-construction surveys, and the relative change in predicted density between the two periods. Note that all included surveys are OWEZ and PAWP post-construction

5.3.11 Black-legged Kittiwake *Rissa tridactyla*

Medium densities of Black-legged Kittiwakes were recorded during the December and January surveys, and low densities during the other two LUD-T2 surveys (Figure 5.43, Figure 5.44). During the December survey several birds were recorded inside LUD. Lower densities were observed close to the coast.

Model results

According to the model higher probability of presence was related to increasing water depth and salinity as well as lower current speeds, - characteristics typical for the North Sea waters of the study area (Appendix A). The PAWP windfarm had a slight negative effect on the density of kittiwakes as did intensity of shipping (Figure 5.46).

In the positive model, higher salinities and lower current speeds were the most influential factors (Appendix A). It can be concluded that based on the surveys the distribution of Black-legged Kittiwake is strongly

governed by the occurrence of North Sea water masses, and only a modest displacement effect can be determined at PAWP. The explanatory degree of the distribution model for the Black-legged Kittiwake was fair for the presence-absence part, but low for the positive part of the model (Appendix A).

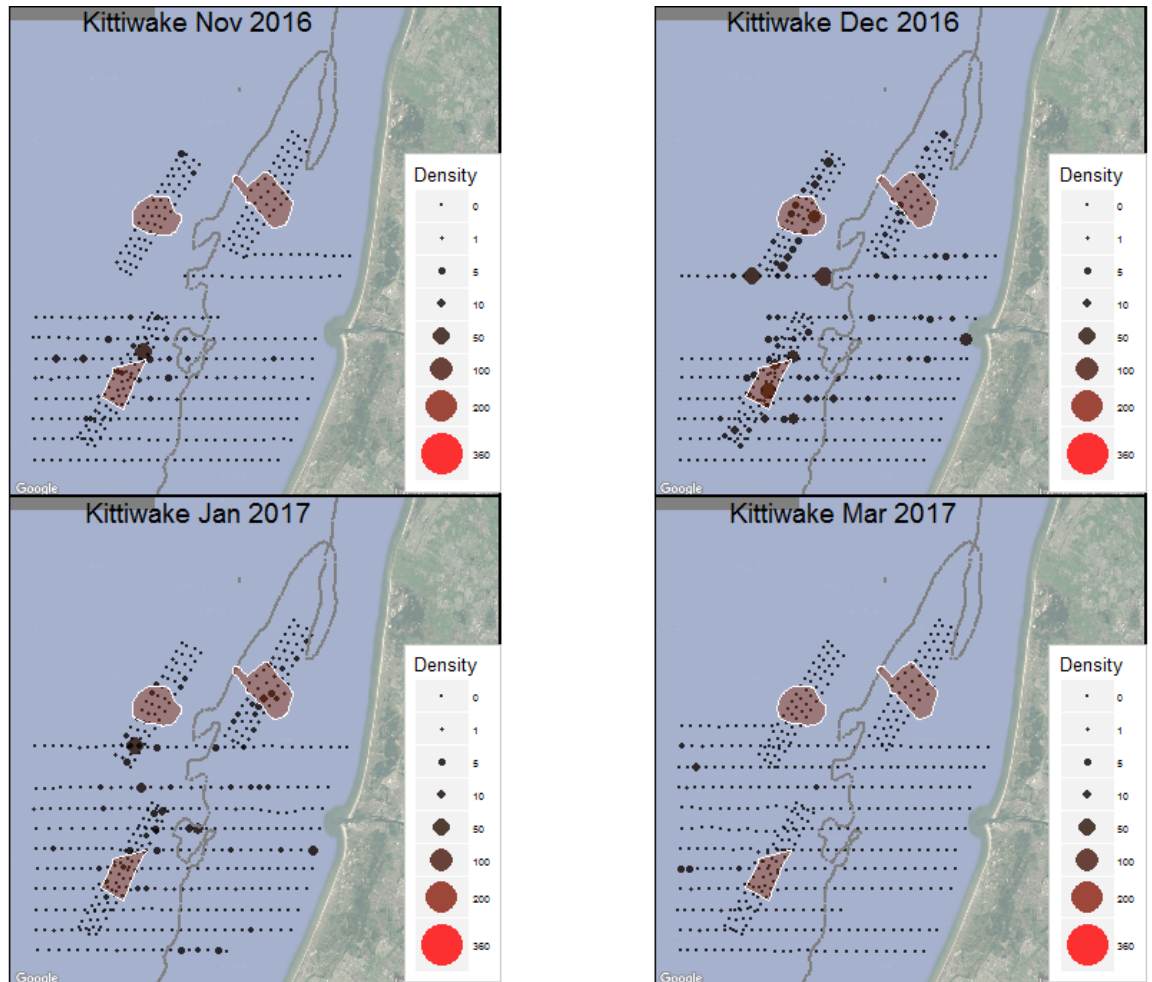


Figure 5.43. Observed density (birds/km²) of Black-legged Kittiwake during LUD-T2 surveys 2016-2017. Densities have been corrected for distance bias.

Kittiwake, 2002-2017

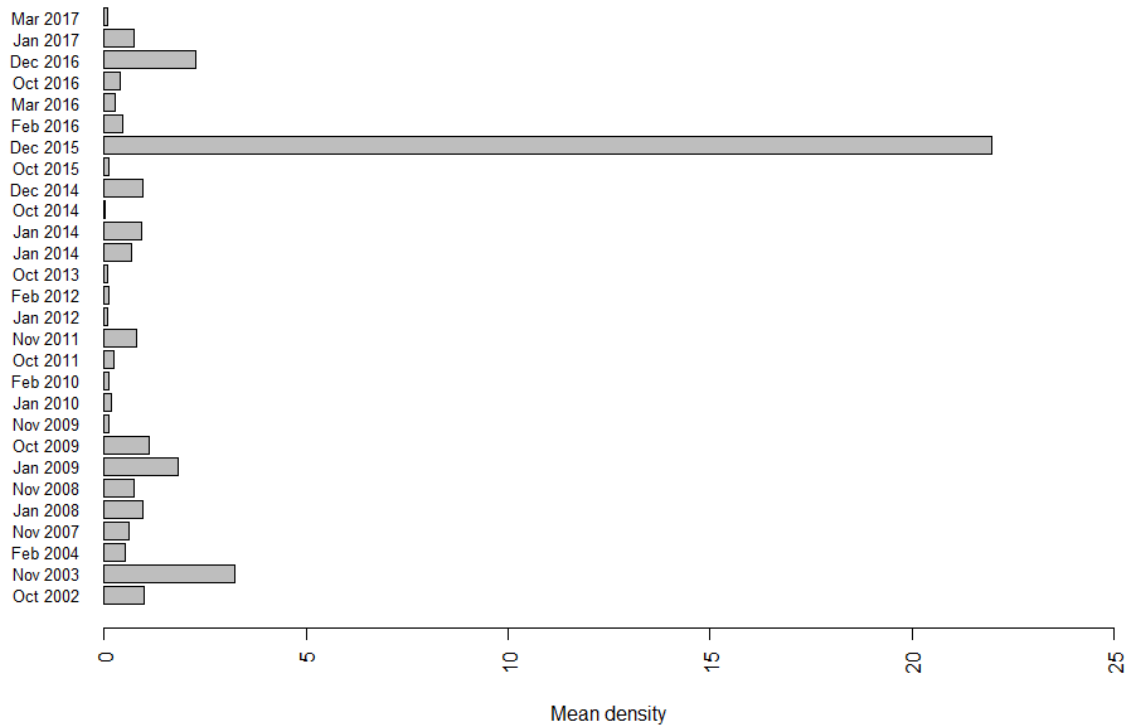


Figure 5.44. Mean observed density (birds/km²) of Black-legged Kittiwake in the entire surveyed area during LUD pre- and post-construction surveys. Densities have been corrected for distance bias.

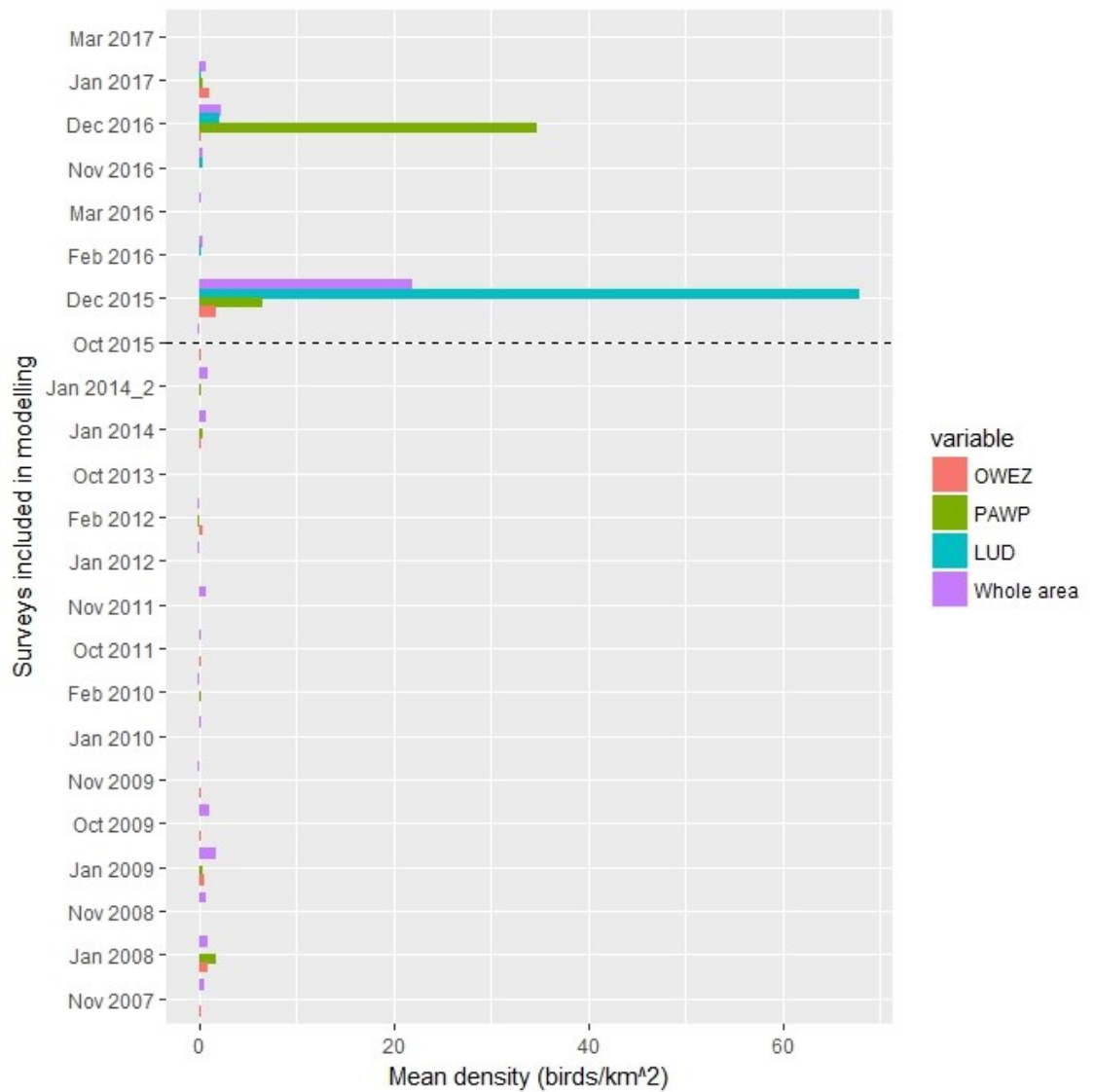


Figure 5.45. Mean density of Black-legged Kittiwake during surveys included in the modelling. The mean density within each of the three wind farm footprints (OWEZ, PAWP and LUD) is shown as well as the mean in the whole surveyed area (including windfarms).

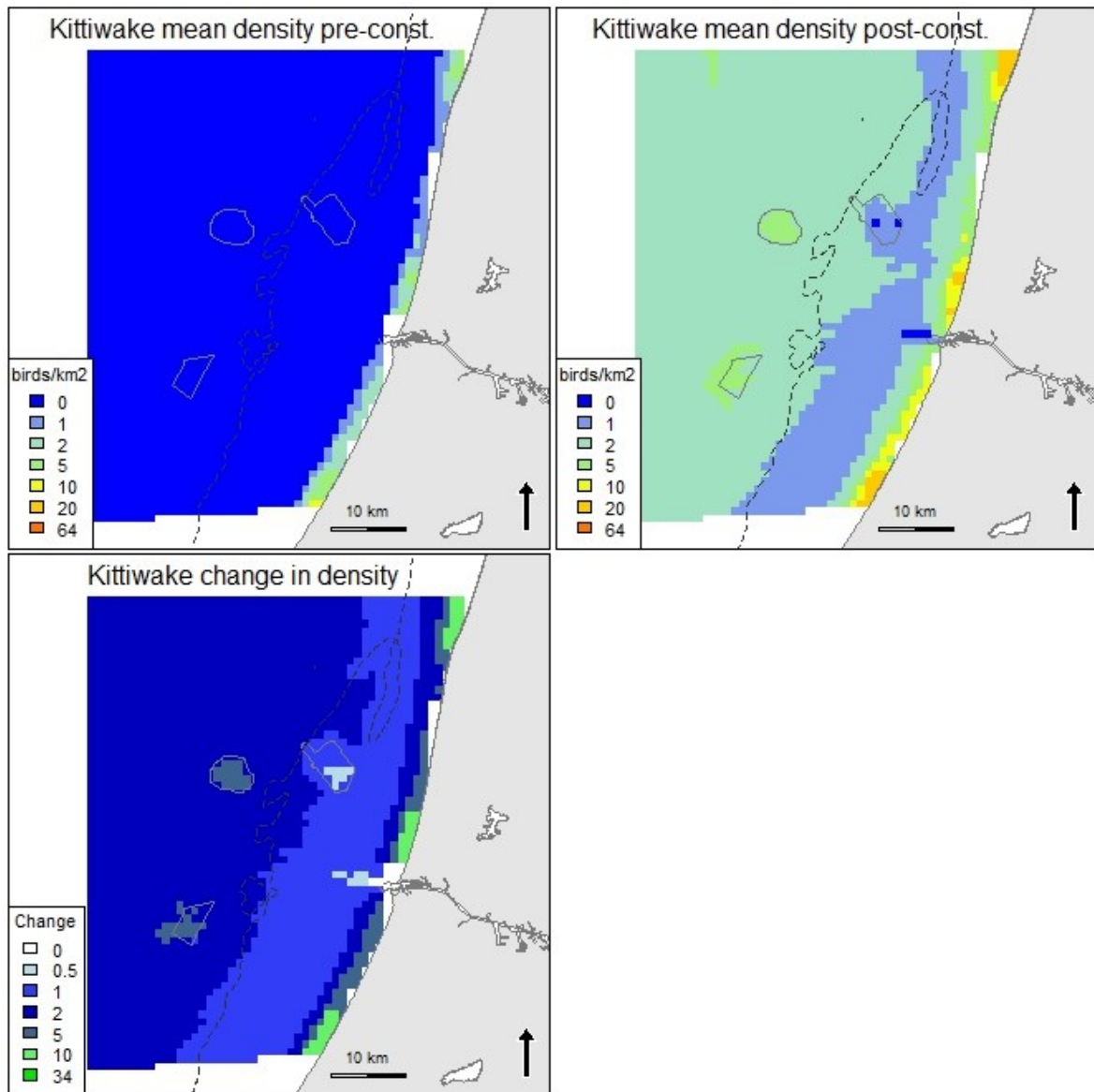


Figure 5.46. Predicted mean density (birds/km²) and distribution of wintering Black-legged Kittiwake during eight LUD pre- and eight LUD post-construction surveys, and the relative change in predicted density between the two periods. Note that all included surveys are OWEZ and PAWP post-construction surveys.

5.3.12 Common Guillemot *Uria aalge*

During the LUD-T2 surveys the highest densities of Common Guillemot were recorded in December and January (Figure 5.47 and Figure 5.48), and birds were seen in all three windfarms but clearly in lower numbers than outside. In the October-November survey in 2016, the density inside LUD footprint was clearly higher than the mean density in the whole area. In most other surveys the mean density in the wind farm footprints are, however, lower than the mean density in the whole surveyed area (Figure 5.49). The overall distribution reflected higher mean densities in the offshore parts of the study area, but with some high densities also close to the coast and lowest densities in between (Figure 5.47). A marked variation is apparent in the recorded densities of Common Guillemots between the 28 surveys of which 23 were included in the distribution analyses (Figure 5.48 Figure 5.49).

Model results

According to the model the probability of presence increased with increasing salinity and current speeds and low shipping intensity in water depths around 20 m. Probability of presence was significantly ($p < 0.01$) lower in all windfarm footprints and within the 2km buffer around PAWP ($p < 0.01$). Hence, the model indicated an avoidance from all three windfarms (Figure 5.50). Higher density was further explained by increasing water depth, both low and high current speeds and an increasing current gradient. Significantly lower densities (when present) were predicted inside PAWP ($p < 0.01$) and LUD ($p < 0.05$) (Appendix A). The explanatory degree of the distribution model for the Common Guillemot was fair for both the presence-absence (27 %) and the positive part (15 %) of the model (Appendix A). The predictive accuracy was good according to the evaluation statistics with an AUC of 0.80 and a Spearman's correlation between observed and predicted abundance of 0.50 when evaluated on 30% withheld data (Appendix A). When evaluating predictions, by predicting on model input data with and without the response of the wind farm the results indicate that there is on average a 31% decrease in probability of detecting a Common Guillemot inside the wind farm, in comparison to a case without a wind farm (Figure 5.51). When both model parts are combined there is on average a 46% decrease in density within the wind farm when comparing model predictions including the windfarm response (factor variable) with model predictions excluding the windfarm response (Figure 5.51). This can be regarded as an indication of level of displacement, however it is important to consider the model errors as well as potential unknown uncertainties around the estimates (Figure 5.51).

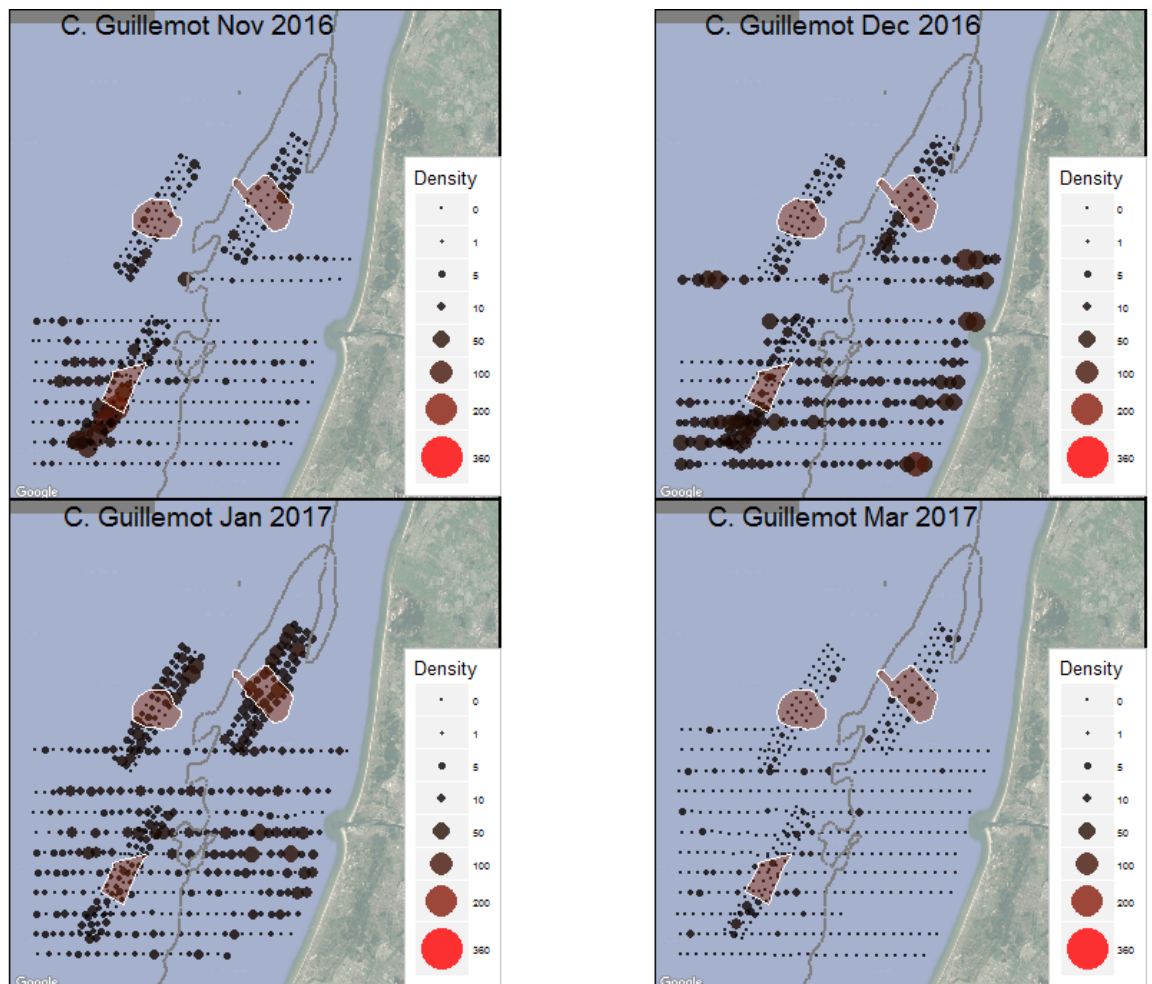


Figure 5.47. Observed density (birds/km²) of Common Guillemot during LUD-T2 surveys 2016-2017. Densities have been corrected for distance bias.

Common Guillemot, 2002-2017

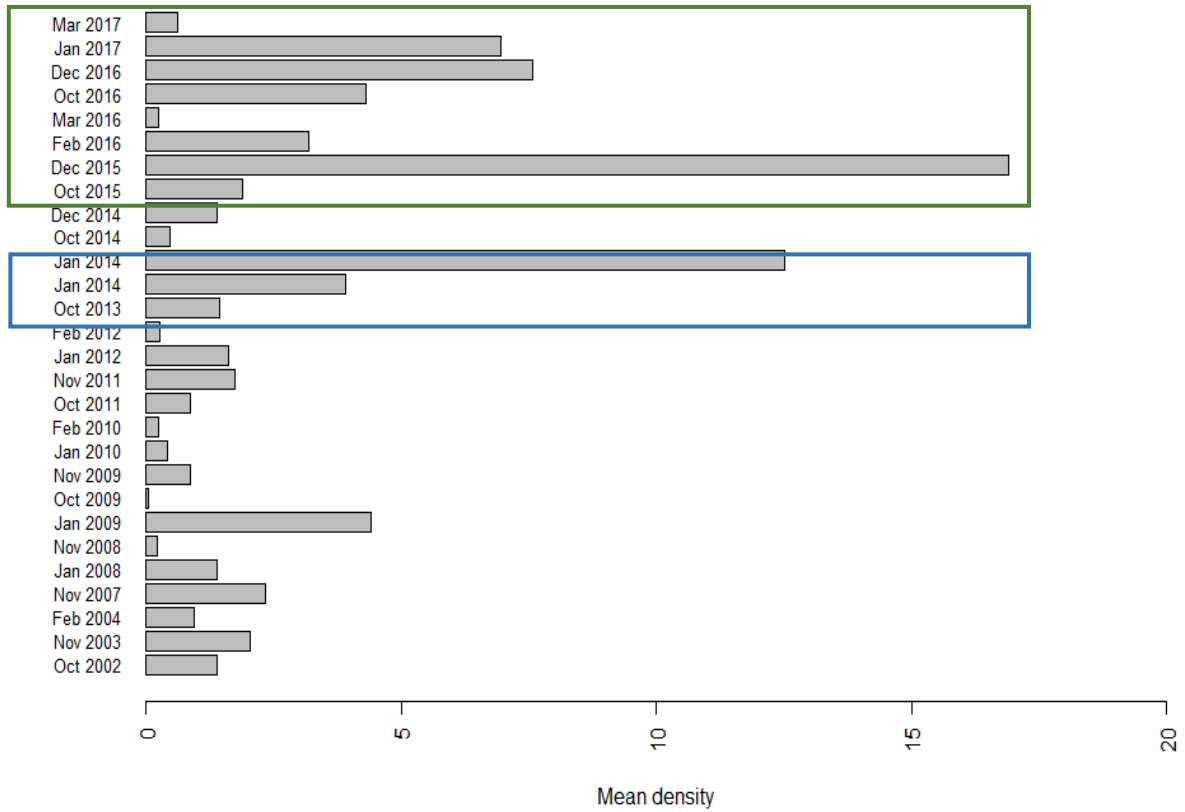


Figure 5.48. Mean observed density (birds/km²) of Common Guillemot in the entire surveyed area during LUD pre-construction surveys (indicated by a blue rectangle) and post-construction surveys (green rectangle). Densities have been corrected for distance bias.

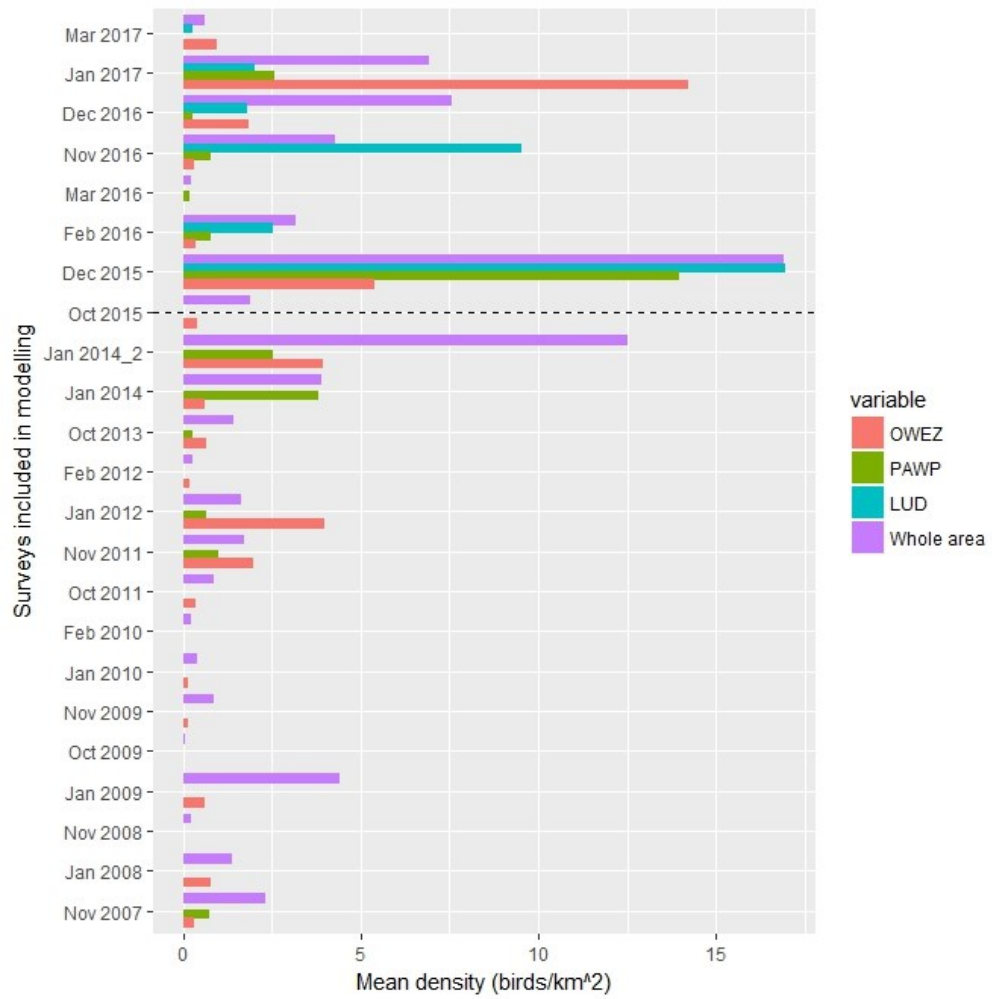


Figure 5.49. Mean density of Common Guillemot during surveys included in the modelling. The mean density within the three wind farm footprints (OWEZ, PAWP and LUD) are shown as well as the mean in the whole surveyed area.

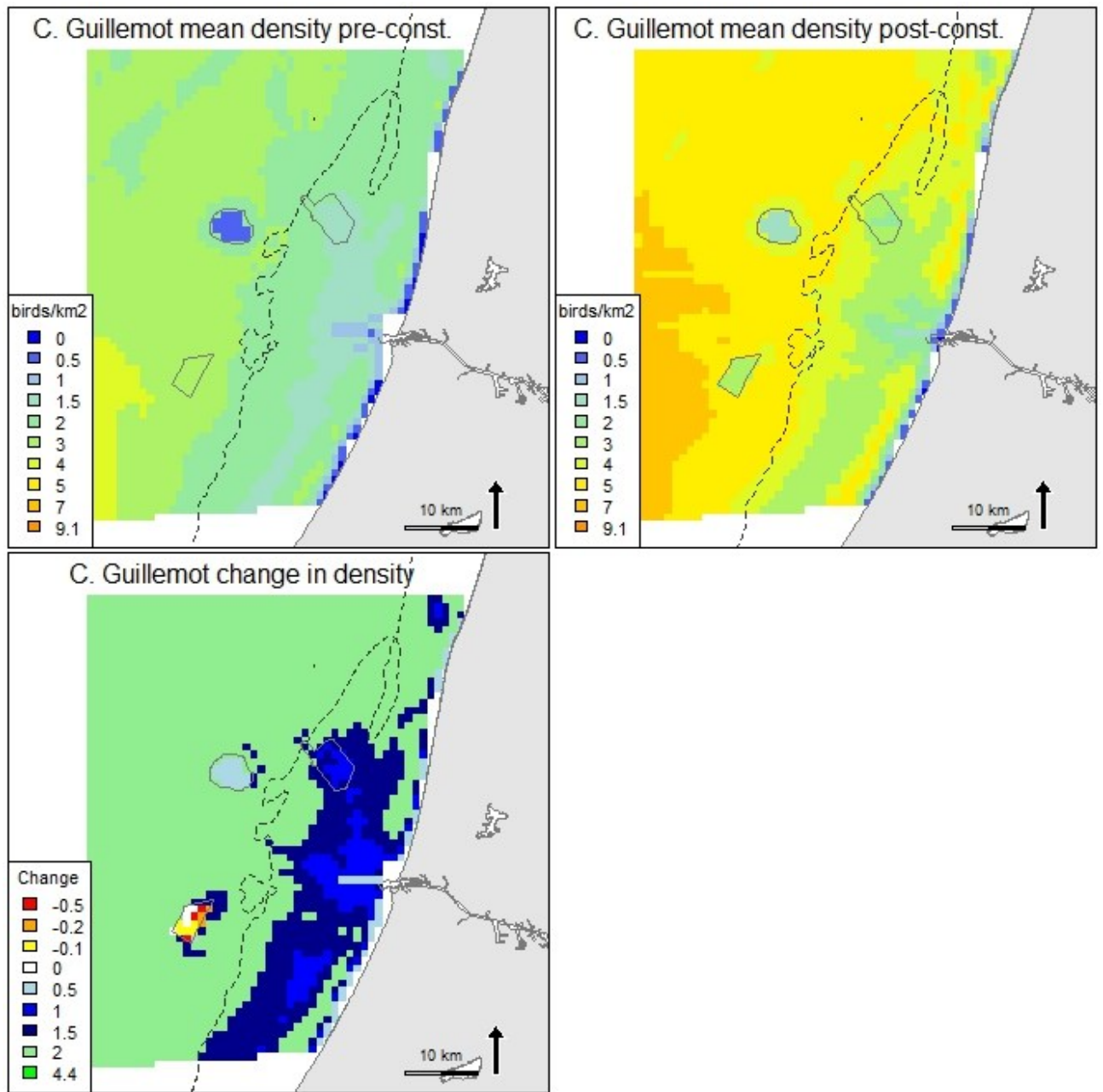


Figure 5.50. Predicted mean density (birds/km²) and distribution of wintering Common Guillemot during eight LUD pre- and eight LUD post-construction surveys, and the relative change in predicted density between the two periods. Note that all included surveys are OWEZ and PAWP post-construction surveys.

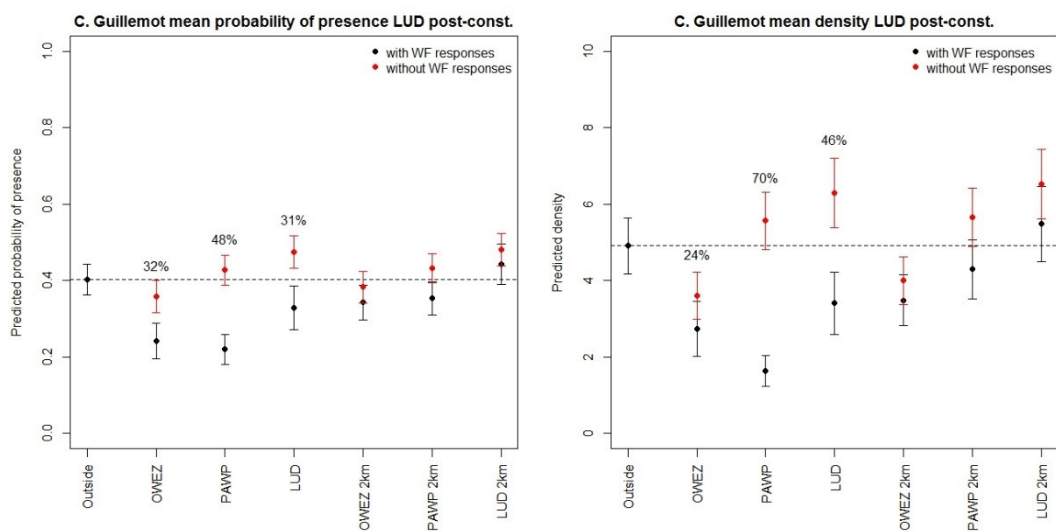


Figure 5.51. Model predictions (on model data) for Common Guillemot during the eight LUD post-construction surveys, with (fitted values) and without the response of the windfarm, when taking into account the dynamic environmental conditions. The difference indicate a mean displacement with model errors, i.e. what is the difference in probability of presence (to the left) or the density (to the right) if the windfarm(s) would not be present compared to a WF present. The mean displacement in % is indicated above the estimates for the footprints (GAMM model errors, SE, are indicated as error bars).

Simulation “power” analysis

Simulations based on the relationships modelled using GAMM reported above were refitted and simulated on the existing post-construction survey conditions using GLMM (excluding the response from LUD). The power of detecting a decline of 10-50% in LUD was assessed using 100 simulations (of which generally around 80-90% converged, Table 10, Table 11). A high power (100%) was achieved when 50% of both presence and density of Common Guillemot was reduced within windfarm (Table 10). To further assess whether 12 surveys would be sufficient for detecting a 25% reduction with a high power, we used the 2 pre-construction survey and 2 construction survey as fictional post-construction surveys and thus simulated 100 times 12 post-construction surveys with a 25 % (and 10%) displacement within the LUD windfarm. The results indicated that the power of detecting a 25% displacement of Common Guillemot following 12 surveys was rather high close to 70% while detecting only a 10% reduction was 9% (Table 11) which is still low but clearly higher than based on 8 surveys (Table 10).

Table 10. The power of a presence/absence (PA) model part and positive density model part (POS, conditional on PA) including eight post-construction surveys, with an artificial displacement of 10%, 25% and 50% from within the windfarm perimeter.

| Displacement from WF | PA | POS | N sim. |
|----------------------|-------|-------|--------|
| 10% | 0.000 | 0.035 | 86 |
| 25% | 0.500 | 0.085 | 82 |
| 50% | 1.000 | 0.817 | 93 |

Table 11. The power of a presence/absence (PA) model part and positive density model part (POS, conditional on PA) including 12 post-construction surveys, with an artificial 25% displacement from within the windfarm perimeter.

| Displacement from WF | PA | POS | N sim. |
|----------------------|-------|-------|--------|
| 25% | 0.500 | 0.690 | 100 |

| | | | |
|-----|-------|-------|----|
| 10% | 0.089 | 0.067 | 90 |
| 25% | 0.674 | 0.416 | 89 |

5.3.13 Razorbill *Alca torda*

During the LUD-T2 surveys Razorbills were frequently observed in offshore waters, including in all three windfarms (Figure 5.52). High numbers of Razorbills wintering in the area were noted during the 2015-2016 winter, and even higher densities were recorded during LUD-T2. This was especially the case during the January survey when high densities were recorded around LUD, and low densities within the windfarm (Figure 5.52, Figure 5.53). During the October-November survey in 2016 there was a higher density within the wind farm than in the whole surveyed area in average (Figure 5.54). During most other surveys the density inside the windfarm footprint were however lower than density in average, with the exceptions in OWEZ in January 2010, October 2011 and December 2015 (Figure 5.54).

Model results

Both the explanatory power of the Razorbill model was fair (Appendix A). Highest probability of presence was associated with areas with lower water depth and high current speeds found in the interface between coastal waters and the North Sea. The negative effect of PAWP on the presence of Razorbills was significant, while no significant effect was noted for the other two windfarms (Appendix A). Yet, the response levels (Appendix A) indicate a lower probability of presence within all three windfarms, including LUD and therefore a reduction in the predicted density in LUD between pre- and post-construction can be seen (Figure 5.55). When evaluating predictions, by predicting on model input data with and without the response of the wind farm the results indicate that there is in average a 39% decrease in probability of detecting a Razorbill inside the windfarm, in comparison to a case without a wind farm. However in both cases the probability is low, around 0.06 and 0.11 respectively. When both model parts are combined there is a 41% decrease in density within the wind farm when comparing model predictions including the windfarm response (factor variable) to model predictions excluding the wind farm response (Figure 5.56). This can be regarded as an indication of level of displacement, however it is important to consider the model errors as well as potential unknown uncertainties around the estimates (Figure 5.56). The response of LUD was not significant which can also be seen from the overlapping error bars (Figure 5.56).

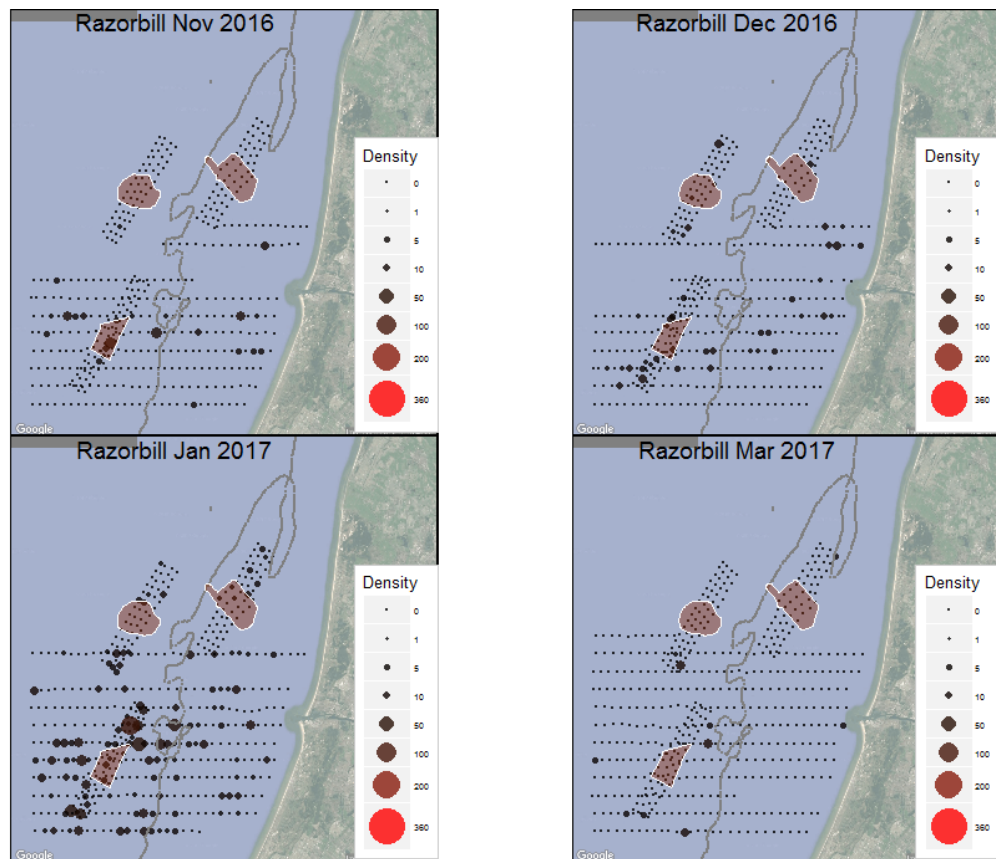


Figure 5.52. Observed density (birds/km²) of Razorbill during LUD-T2 surveys 2016-2017. Densities have been corrected for distance bias.

Razorbill, 2002-2017

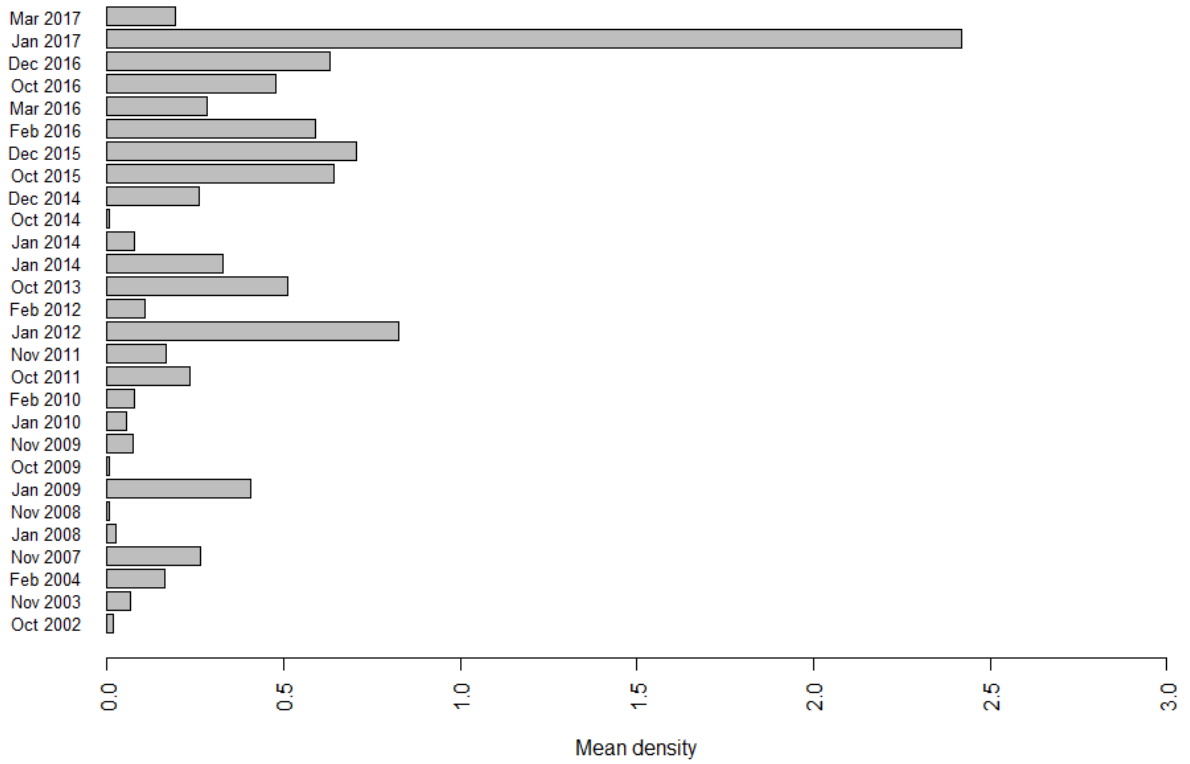


Figure 5.53. Mean observed density (birds/km²) of Razorbill in the entire surveyed area during LUD pre- and post-construction surveys. Densities have been corrected for distance bias.

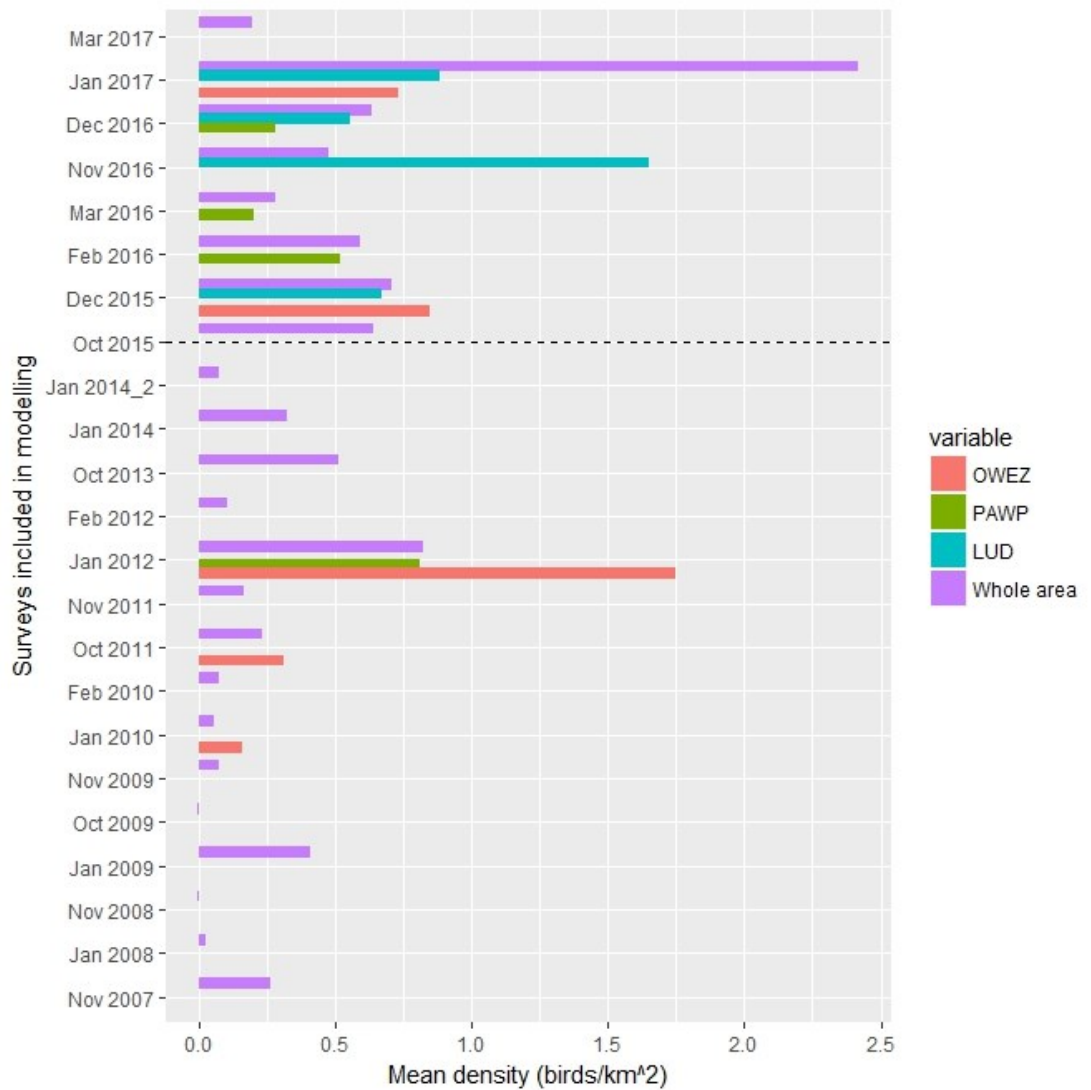


Figure 5.54. Mean density of Razorbill during surveys included in the modelling. The mean density within the three wind farm footprints (OWEZ, PAWP and LUD) are shown as well as the mean in the whole surveyed area.

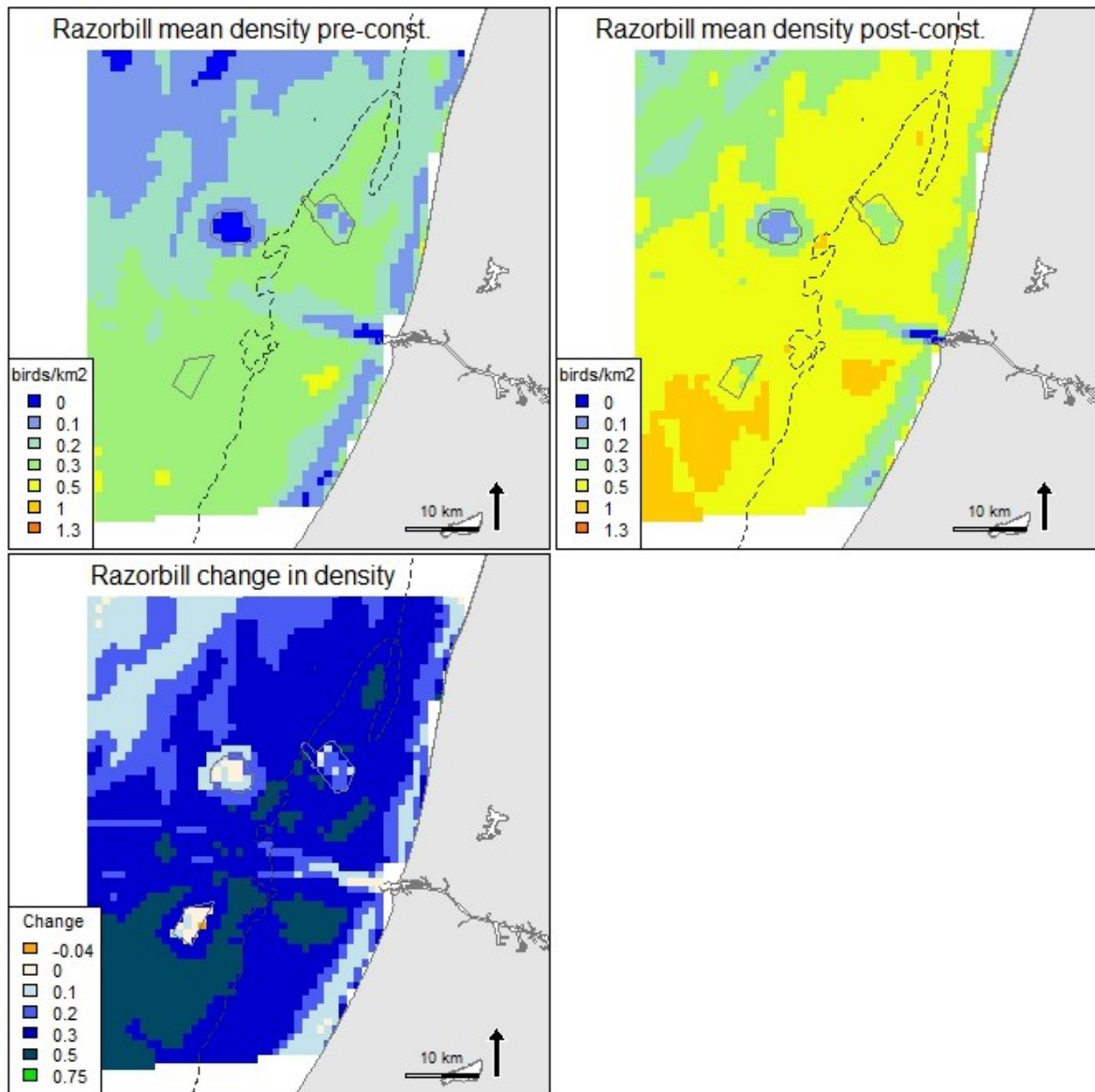


Figure 5.55. Predicted mean density (birds/km²) and distribution of wintering Razorbill during eight LUD pre- and eight LUD post-construction surveys, and the relative change in predicted density between the two periods. Note that all included surveys are OWEZ and PAWP post-construction surveys.

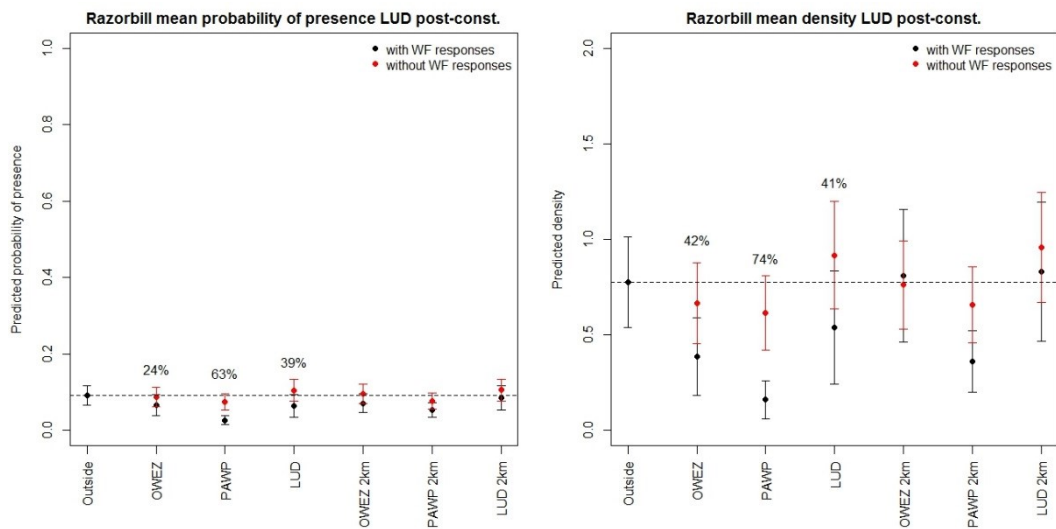


Figure 5.56. Model predictions (on model data) for Razorbill during the eight LUD post-construction surveys, with (fitted values) and without the response of the windfarm, when taking into account the dynamic environmental conditions. The difference indicate a mean displacement with model errors, i.e. what is the difference in probability of presence (to the left) or the density (to the right) if the windfarm(s) would not be present compared to a WF present. The mean displacement in % is indicated above the estimates for the footprints (GAMM model errors, SE, are indicated as error bars).

5.3.14 Marine mammal observations

With 90 sightings of 128 animals the harbour porpoise *Phocoena phocoena* was the most commonly observed marine mammal in the whole area. Most sightings of porpoises were made around LUD and PAWP and off Ijmuiden (Figure 5.47). Especially the relatively large number of sightings around and in the periphery of LUD is noteworthy.

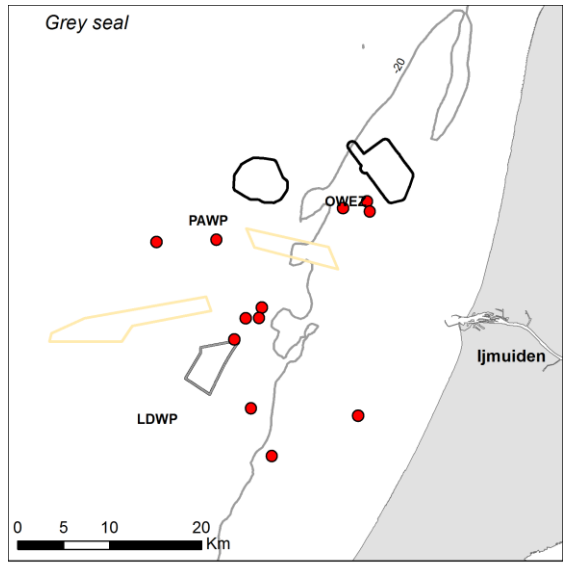
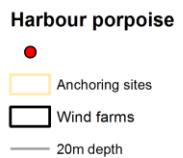
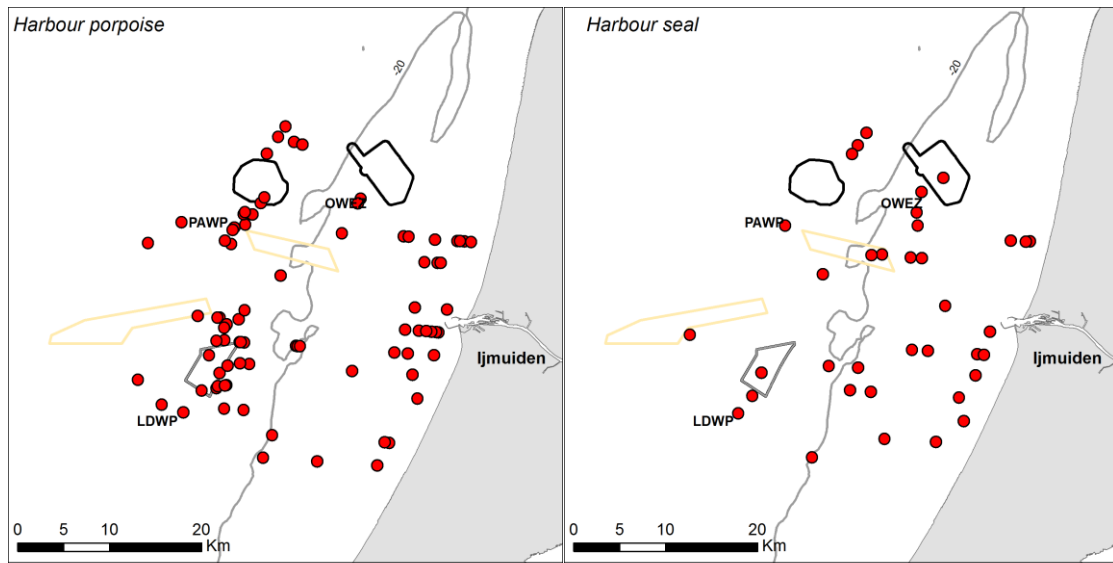


Figure 5.57. Observations of marine mammals during the LUD-T2 surveys 2016-2017. No corrections for possible double registrations have been made.

6 Discussion

The abundance and distribution of the different species of seabirds recorded during the Offshore Windfarm Eneco Luchterduinen (LUD) T2 surveys largely follow the patterns from the LUD baseline, T-Constr and T1 periods with the overall impression that the waters around LUD are mainly characterised by high densities of Common Guillemot and low to moderate densities of other species of seabirds. However, during the March 2017 survey, high abundance of Northern Gannet was also recorded. In addition, unusually high numbers of Common and Velvet Scoters were recorded during the survey in December 2016.

The T2 report provides the results from the second year of the LUD seabird monitoring program regarding displacement of seabirds from LUD as well as updated results from PAWP and OWEZ. The dynamic modelling and simulation framework, which was tested during LUD-T1 was applied on all available data from the three windfarms including the data collected during the four LUD-T2 surveys. The LUD-T1 report indicated that high power would be achievable after LUD-T2 for Common Guillemot (detection of a displacement of 50%), whereas the power of the data for Northern Gannet would be too low to detect reductions of 50% of this species from LUD after LUD-T2. The results of the updated power tests and simulations in this report corroborate these findings. The displacement of Northern Gannets at LUD is probably in the range between 50% and 75%. Since the simulations indicated that a power of 0.99 could be achieved with 75% displacement it is likely that the level of displacement will be detected following LUD-T3. As shown by the simulations, the power will however depend on the occurrence of high numbers of Northern Gannets during at least one of the T3 surveys. The degree of displacement of Common Guillemots seems to be less than for Northern Gannets. Yet due to the higher sample size the power of the data at hand from the LUD surveys is much higher for Common Guillemot. The simulations indicated that a displacement of 50% can be detected with very high power with the available data after LUD-T2. After LUD-T3 the simulations indicate that even lower levels of displacement of Common Guillemots from LUD may be detected.

The LUD-T2 results are generally in line with the results from LUD-T1 and other studies like Krijgsveld (2014) and Welcker & Nehls (2016). The LUD-T1 distribution models indicated negative responses of Northern Gannets (2 km avoidance) and Common Guillemot (2-4 km avoidance) to PAWP and OWEZ. The updated results now indicate that a 2 km avoidance zone is more realistic than 2-4 km for Common Guillemot at all three windfarms. Several species including Black-legged Kittiwake and Razorbill showed a significantly lower probability of occurrence at PAWP, while no clear effect was seen at LUD and OWEZ. It seems plausible that this difference in displacement effect is related to the shorter distance between turbines in PAWP as compared to the other two windfarms.

Based on the LUD-T2 results it seems most likely given the oceanographic variability, mobile behaviour and hence variability of abundance of Northern Gannet at LUD that detection of reductions of density at 75% of this species from this windfarm will require data from LUD-T3. It is therefore recommended to finalise surveys as planned under T3.

7 References

- Buckland, S.T., Anderson, D.R., Burnham, K.P., Laake, J.L., Borchers, D.L., and Thomas, L. 2001. Introduction to distance sampling - Estimating abundance of biological populations. Oxford University Press, Oxford. Burnham, K.P., and Anderson, D.R. 2002. Model Selection and Multimodel Inference: A Practical Information-Theoretic Approach, 2nd ed. Springer-Verlag. ISBN 0-387-95364-7. Camphuysen, C.J. & Garthe, S. 2004. Recording foraging seabirds at sea: standardised recording and coding of foraging behaviour and multi-species foraging associations. *Atlantic Seabirds* 5: 1-23.
- Burnham, K. P. & Anderson, D. R. 2002. Model selection and multimodel inference: a practical information-theoretic approach Springer.
- Camphuysen CJ, Fox TJ, Leopold MF & Petersen IK, 2004. Towards standardised seabirds at sea census techniques in connection with environmental impact assessments for offshore windfarms in the U.K. - A comparison of ship and aerial sampling methods for marine birds, and their applicability to offshore windfarm assessments. NIOZ Report to Cowrie / The Crown Estate.
- Hastie, T. & Tibshirani, R. 1990. Generalized Additive Models. Chapman & Hall, London. Leopold M.F., Camphuysen C.J., ter Braak C.J.F., Dijkman E.M., Kersting K. & van Lieshout S.M.J. 2004. Baseline studies North Sea windfarms: Lot 5 marine birds in and around the future sites Nearshore Windfarm (NSW) and Q7. Alterra-rapport 1048.
- Krijgsveld, K.L. 2014. Avoidance behaviour of birds around offshore windfarms. Overview of knowledge including effects of configuration. Bureau Waardenburg. Rijkswaterstaat Report no. 13-268.
- Leopold, M.F., van Bemmelen, R.S.A. & Zuur, A.F. 2013. Responses of Local Birds to the Offshore Windfarms PAWP and OWEZ off the Dutch mainland coast. Report number C151/12. Imares Report.
- Maclean, I.M.D., Rehfish, M. M., Skov, H. & Thaxter, C. B. 2013. Evaluating the statistical power of detecting changes in the abundance of seabirds at sea. *Ibis*: 113-126.
- Pérez-Lapenã, B. K. Wijnberg, M., Hulscher, S. J. M. H & Stein, A. 2010. Environmental impact assessment of offshore windfarms: a simulation-based approach. *Journal of Applied Ecology* 47: 1110–1118.
- Petersen I.K., Christensen T.K., Kahlert J., Desholm M. & Fox A.D. 2006. Final results of bird studies at the offshore windfarms at Nysted and Horns Rev, Denmark. NERI Report, commissioned by DONG energy and Vattenfall A/S.
- Skov, H., Leonhard, S.B., Heinänen, S., Zydalis, R., Jensen, N.E., Durinck, J., Johansen, T.W., Jensen, B.P., Hansen, B.L., Piper, W., Grøn, P.N. 2012. Horns Rev 2 Monitoring 2010-2012. Migrating Birds. Orbicon, DHI, Marine Observers and Biola. Report commissioned by DONG Energy.
- Skov, H., Heinänen, S., Nyborg, L. & Lazcny, M. 2015. Offshore Windfarm Eneco Luchterduinen Ecological monitoring of seabirds. T0 report. Commissioned by Eneco. DHI.
- Skov, H., Heinänen, S., Lazcny, M & Chudzinska, M. 2016. Offshore Windfarm Eneco Luchterduinen Ecological monitoring of seabirds. T0 report. Commissioned by Eneco. DHI.
- Tasker M.L., Jones P.H., Dixon T.J. & Blake B.F. 1984. Counting seabirds at sea from ships: a review of methods employed and a suggestion for a standardized approach. *Auk* 101: 567-577.
- Vanermen, N., Onkelinx, T. Verschelde, P., Courtens, W., Van de walle, M., Verstraete, H. & Stienen, E. W. M. 2015. Assessing seabird displacement at offshore windfarms: power ranges of a monitoring and data handling protocol. *Hydrobiologia*, 756:155-167.
- Welcker, J. & Nehls, G. 2016. Displacement of seabirds by an offshore windfarm in the North Sea. *Mar Ecol Prog Ser*, 554: 173-182.

APPENDICES

APPENDIX A – Detailed results of species distribution models for the T-2 surveys

Red-throated and Black-throated Divers

Table A.1. Smooth terms, adjusted R-squared and evaluation statistics for the Red-throated and Black-throated Diver distribution models. F statistics and the approximate significance for the smooth terms and t-statistic, estimate and the significance for the parametric terms are shown. Variables not included in either the presence/absence or positive model part are indicated with a dash. The results of the evaluation test show AUC for presence/absence and the Spearman's correlation for the density predictions. 'n.s.' indicates terms with p-values > 0.05. The significant effect of the windfarms are marked in bold.

| Smooth terms | Presence/absence | | | Positive density | | |
|-------------------------------|------------------|--------|--------|------------------|--------|-------|
| | | F | p | F | p | |
| Depth | | 12.29 | 0.01 | - | - | |
| Salinity | | 18.689 | 0 | - | - | |
| Current speed | | 14.821 | 0 | 41.111 | 0 | |
| Parametric terms | Estimate | t | p | Estimate | t | P |
| AIS | -0.016 | -4.308 | 0 | -0.006 | -1.38 | 0.169 |
| LUD WF not included | - | - | - | - | - | - |
| PAWP WF not included | - | - | - | - | - | - |
| OWEZ WF parametric | -1.8 | 0.412 | <0.001 | - | - | - |
| LUD (2 km buffer) parametric | -0.03 | -0.059 | 0.953 | - | - | - |
| PAWP (2 km buffer) parametric | -1.523 | -4.796 | 0 | - | - | - |
| OWEZ (2 km buffer) parametric | -0.753 | -2.658 | 0.008 | - | - | - |
| Survey 5 | 1.658 | 3.368 | 0.001 | 0.025 | 0.11 | 0.913 |
| Survey 6 | -0.846 | -1.401 | 0.161 | -1.233 | -4.007 | 0 |
| Survey 7 | -0.53 | -0.631 | 0.528 | 0.013 | 0.042 | 0.967 |
| Survey 8 | 2.102 | 3.27 | 0.001 | 0.199 | 0.56 | 0.576 |
| Survey 9 | 2.107 | 3.527 | 0 | 0.143 | 0.471 | 0.638 |
| Survey 10 | 2.589 | 4.707 | 0 | 0.471 | 1.885 | 0.06 |
| Survey 11 | 0.182 | 0.28 | 0.779 | -0.904 | -2.806 | 0.005 |
| Survey 12 | -0.175 | -0.266 | 0.79 | -0.821 | -2.125 | 0.034 |
| Survey 13 | 1.383 | 2.268 | 0.023 | -0.593 | -1.705 | 0.089 |
| Survey 14 | 2.094 | 3.912 | 0 | -0.246 | -0.911 | 0.363 |
| Survey 15 | 2.861 | 5.176 | 0 | 0.035 | 0.126 | 0.9 |
| Survey 16 | 1.426 | 2.261 | 0.024 | 0.593 | 1.247 | 0.213 |
| Survey 17 | -0.515 | -0.614 | 0.539 | 0.217 | 0.441 | 0.659 |
| Survey 18 | - | - | - | - | - | - |
| Survey 19 | - | - | - | - | - | - |
| Survey 20 | - | - | - | - | - | - |
| Survey 21 | - | - | - | - | - | - |
| Survey 22 | 0.209 | 0.378 | 0.705 | 0.051 | 0.104 | 0.917 |
| Survey 23 | - | - | - | - | - | - |
| Survey 24 | -0.888 | -1.558 | 0.119 | 0.045 | 0.09 | 0.928 |
| Survey 25 | - | - | - | - | - | - |
| Survey 26 | 1.571 | 2.198 | 0.028 | 0.476 | 1.498 | 0.135 |
| Survey 27 | -0.432 | -0.942 | 0.346 | 0.729 | 1.969 | 0.05 |
| Survey 28 | - | - | - | - | - | - |
| Sample size (n) | | 7608 | | | 358 | |
| Adjusted R ² | | 19.50% | | | 14.00% | |
| AUC | | 0.87 | | | | |
| Spearman's corr. | | | | | 0.48 | |

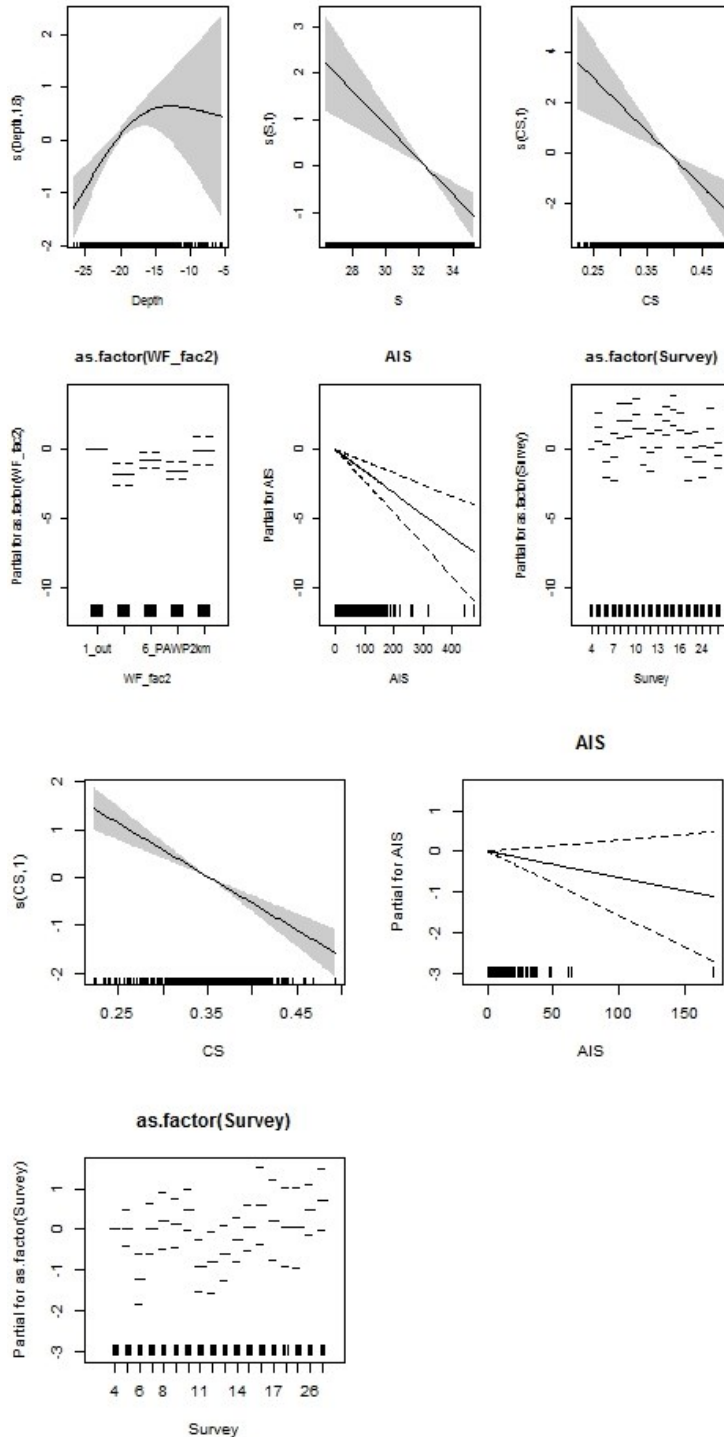


Figure A.1. Partial GAM plots for the Red-throated and Black-throated Diver distribution model – presence-absence (upper panel) and positive density (lower panel) parts. The values of the environmental variables are shown on the X-axis and the probability on the Y-axis in the scale of the linear predictor. The grey shaded areas and the dotted lines (for factors) show the 95% Bayesian confidence intervals. The degree of smoothing is indicated in the legend of the Y-axis.

Great Crested Grebe

Table A.2. Smooth terms, adjusted R-squared and evaluation statistics for the Great Crested Grebe distribution models. F statistics and the approximate significance for the smooth terms and t-statistic and the significance for the parametric terms are shown. Variables not included in either the presence/absence or positive model part are indicated with a dash. The results of the evaluation test show AUC for presence/absence and the Spearman's correlation for the density predictions. 'n.s.' indicates terms with p-values > 0.05. The significant effect of the windfarms are marked in bold.

| Smooth terms | Presence/absence | | | Positive density | | |
|---------------------------------|------------------|--------|-------|------------------|--------|-------|
| | F | p | | F | p | |
| Depth | 16.571 | 0 | | 5.343 | 0.008 | |
| Salinity | 43.787 | 0 | | 8.699 | 0.004 | |
| Current speed | 16.24 | 0 | | | | |
| Parametric terms | Estimate | t | p | Estimate | t | p |
| AIS | -0.012 | -3.752 | 0 | - | - | - |
| LUD WF not included | - | - | - | - | - | - |
| PAWP WF not included | - | - | - | - | - | - |
| OWEZ WF parametric | -0.813 | -2.063 | 0.039 | 0.218 | 0.154 | 0.878 |
| LUD (2 km buffer) not included | - | - | - | - | - | - |
| PAWP (2 km buffer) not included | - | - | - | - | - | - |
| OWEZ (2 km buffer) not included | - | - | - | - | - | - |
| Survey 5 | - | - | - | - | - | - |
| Survey 6 | - | - | - | - | - | - |
| Survey 7 | -1.117 | -1.502 | 0.133 | 0.123 | 0.277 | 0.782 |
| Survey 8 | - | - | - | - | - | - |
| Survey 9 | 1.259 | 2.46 | 0.014 | -0.525 | -0.47 | 0.639 |
| Survey 10 | 4.107 | 11.947 | 0 | 3.259 | 2.581 | 0.011 |
| Survey 11 | 1.837 | 3.585 | 0 | 3.848 | 2.944 | 0.004 |
| Survey 12 | - | - | - | - | - | - |
| Survey 13 | 1.158 | 2.18 | 0.029 | 0.547 | 0.386 | 0.7 |
| Survey 14 | 0.151 | 0.259 | 0.796 | -1.46 | -2.224 | 0.027 |
| Survey 15 | 1.546 | 2.723 | 0.006 | 2.701 | 1.796 | 0.074 |
| Survey 16 | - | - | - | - | - | - |
| Survey 17 | 1.073 | 2.194 | 0.028 | 1.134 | 1.423 | 0.157 |
| Survey 18 | 3.072 | 8.424 | 0 | -0.293 | -0.431 | 0.667 |
| Survey 19 | - | - | - | - | - | - |
| Survey 20 | - | - | - | - | - | - |
| Survey 21 | - | - | - | - | - | - |
| Survey 22 | 1.107 | 2.268 | 0.023 | -1.142 | -1.747 | 0.083 |
| Survey 23 | - | - | - | - | - | - |
| Survey 24 | - | - | - | - | - | - |
| Survey 25 | - | - | - | - | - | - |
| Survey 26 | 1.724 | 4.468 | 0 | 1.219 | 1.074 | 0.284 |
| Survey 27 | 0.194 | 0.28 | 0.779 | -2.962 | -3.473 | 0.001 |
| Survey 28 | - | - | - | - | - | - |
| Sample size (n) | 5261 | | | 188 | | |
| Adjusted R ² | 26,8% | | | 3.8% | | |
| AUC | | | | | | |
| Spearman's corr. | | | | | | |

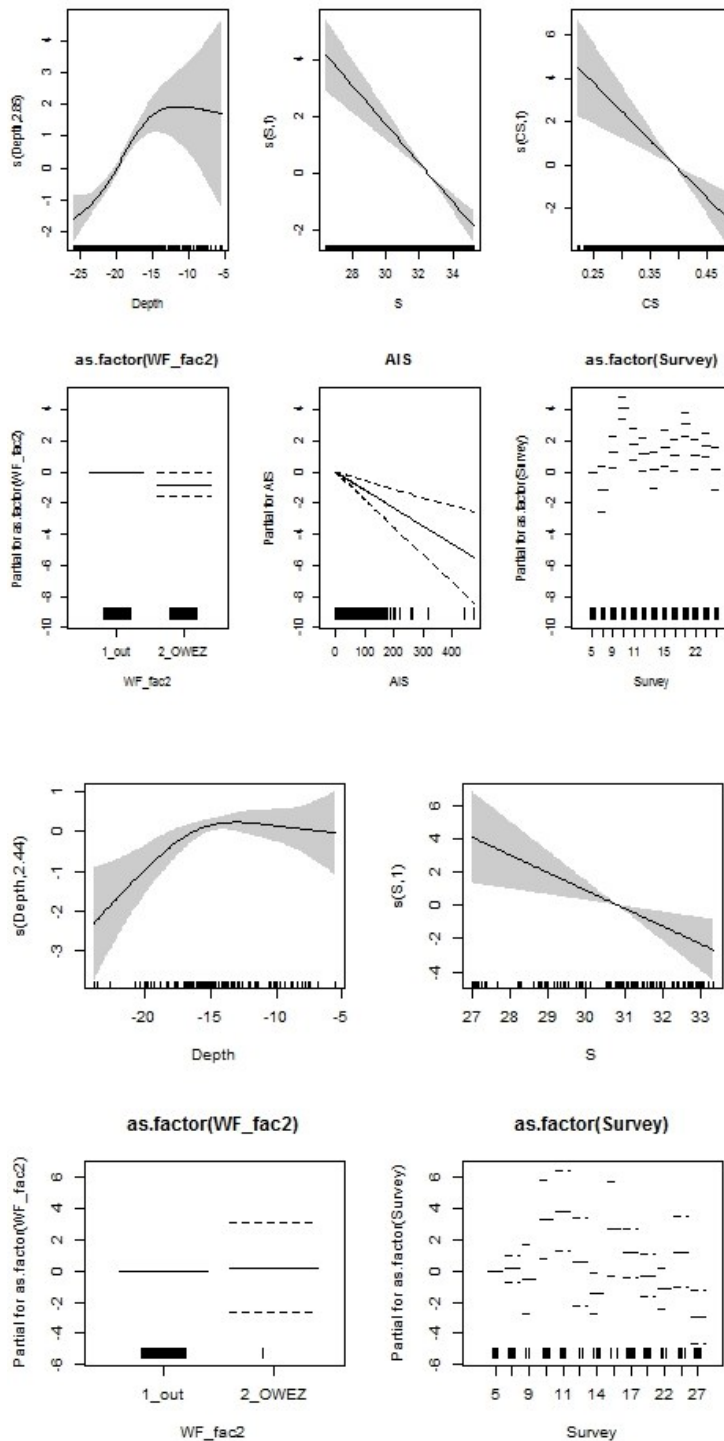


Figure A.2. Partial GAM plots for the Great Crested Grebe distribution model – presence-absence (upper panel) and positive density (lower panel) parts. The values of the environmental variables are shown on the X-axis and the probability on the Y-axis in the scale of the linear predictor. The grey shaded areas and the dotted lines (for factors) show the 95% Bayesian confidence intervals. The degree of smoothing is indicated in the legend of the Y-axis.

Northern Gannet

Table A.3. Smooth terms, adjusted R-squared and evaluation statistics for the Northern Gannet distribution models. F statistics and the approximate significance for the smooth terms and t-statistic and the significance for the parametric terms are shown. Variables not included in either the presence/absence or positive model part are indicated with a dash. The results of the evaluation test show AUC for presence/absence and the Spearman's correlation for the density predictions. 'n.s.' indicates terms with p-values > 0.05. The significant effect of the windfarms are marked in bold.

| Smooth terms | Presence/absence | | | Positive density | | |
|-------------------------------|------------------|--------|-------|------------------|--------|-------|
| | F | p | | F | p | |
| Depth | 22.718 | 0 | | 6.78 | 0.009 | |
| Salinity | 14.626 | 0 | | 27.539 | 0 | |
| Current speed | 9.639 | 0 | | | | |
| Parametric terms | Estimate | t | p | Estimate | t | p |
| AIS | | | | | | |
| LUD WF parametric | -0.889 | -3.293 | 0.001 | -0.517 | -0.994 | 0.321 |
| PAWP WF parametric | -2.574 | -11.44 | 0 | -0.136 | -0.181 | 0.857 |
| OWEZ WF parametric | -1.837 | | | | | |
| | | -7.875 | 0 | -0.209 | -0.309 | 0.758 |
| LUD (2 km buffer) parametric | -0.06 | | | | | |
| | | -0.29 | 0.772 | 0.082 | 0.304 | 0.761 |
| PAWP (2 km buffer) parametric | -0.323 | -1.855 | 0.064 | -0.167 | -0.87 | 0.384 |
| OWEZ (2 km buffer) parametric | -0.537 | | 0.001 | | | |
| | | -3.277 | | 0.046 | 0.183 | 0.855 |
| Survey 5 | -2.56 | -8.866 | 0 | -1.44 | -3.166 | 0.002 |
| Survey 6 | -0.591 | -1.748 | 0.08 | -0.407 | -2.066 | 0.039 |
| Survey 7 | -1.47 | -3.207 | 0.001 | 0.455 | 1.944 | 0.052 |
| Survey 8 | -1.503 | -4.786 | 0 | -1.587 | -4.744 | 0 |
| Survey 9 | -0.467 | -1.523 | 0.128 | -0.491 | -1.934 | 0.053 |
| Survey 10 | -2.084 | -7.889 | 0 | -1.377 | -3.723 | 0 |
| Survey 11 | -1.602 | -4.985 | 0 | -0.884 | -3.452 | 0.001 |
| Survey 12 | -0.727 | -2.375 | 0.018 | -0.795 | -2.952 | 0.003 |
| Survey 13 | -1.063 | -3.062 | 0.002 | -1.53 | -4.881 | 0 |
| Survey 14 | -1.817 | -4.99 | 0 | -1.12 | -2.827 | 0.005 |
| Survey 15 | -2.261 | -4.71 | 0 | -1.306 | -3.115 | 0.002 |
| Survey 16 | -1.124 | -1.833 | 0.067 | -1.524 | -4.823 | 0 |
| Survey 17 | -5.061 | 13.715 | 0 | -1.825 | -1.679 | 0.093 |
| Survey 18 | -3.46 | 13.195 | 0 | -1.401 | -2.586 | 0.01 |
| Survey 19 | - | - | - | - | - | - |
| Survey 20 | - | - | - | - | - | - |
| Survey 21 | -2.027 | -5.803 | 0 | -1.579 | -4.845 | 0 |
| Survey 22 | -0.609 | -2.16 | 0.031 | -0.38 | -1.361 | 0.174 |
| Survey 23 | -1.365 | -4.167 | 0 | -1.163 | -3.536 | 0 |
| Survey 24 | -3.128 | 12.794 | 0 | -1.633 | -3.62 | 0 |
| Survey 25 | -1.053 | -3.319 | 0.001 | -1.182 | -3.99 | 0 |
| Survey 26 | -1.673 | -5.276 | 0 | -1.15 | -3.487 | 0.001 |
| Survey 27 | -1.047 | -2.626 | 0.009 | -0.001 | -0.002 | 0.998 |
| Survey 28 | -1.153 | -5.062 | 0 | 0.404 | 1.487 | 0.137 |
| Sample size (n) | 10025 | | | 1336 | | |
| Adjusted R ² | 10.70% | | | 2.6% | | |

AUC
Spearman's corr.

0.78

0.10

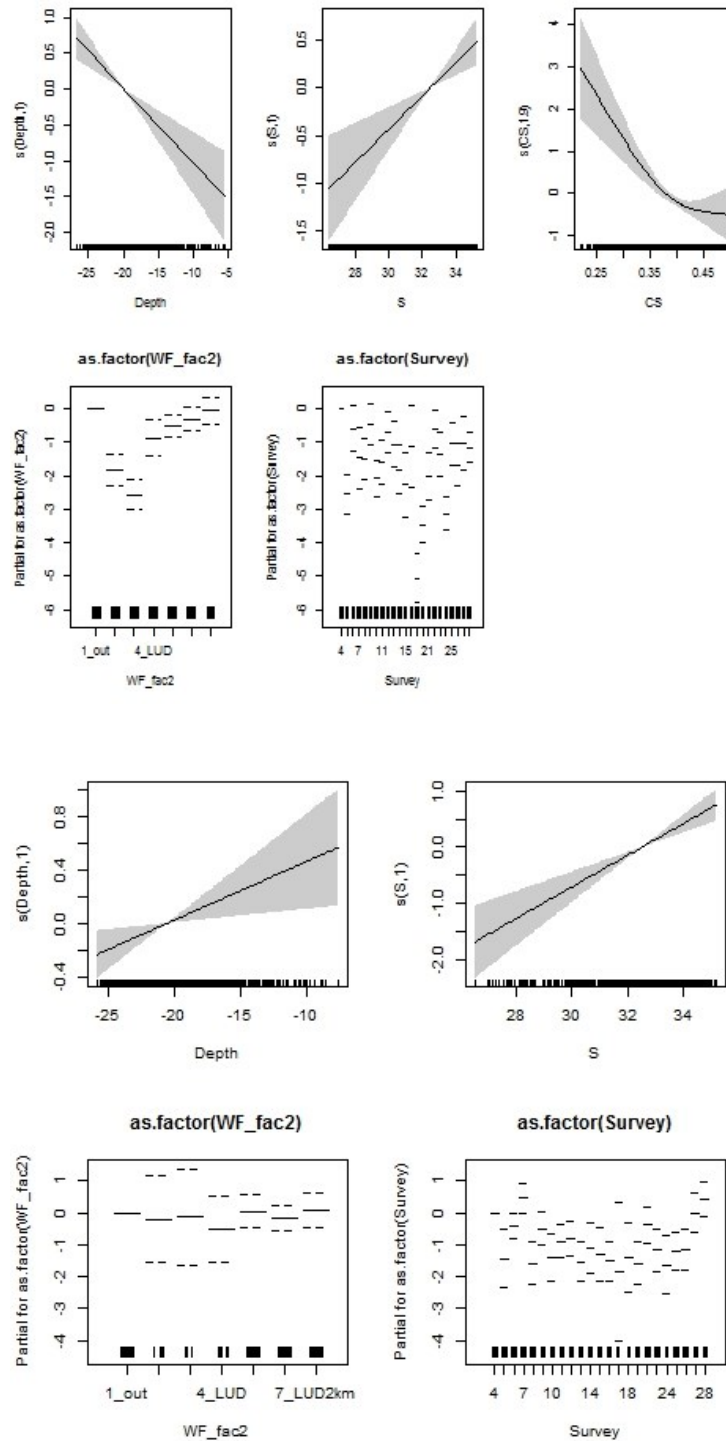


Figure A.3. Partial GAM plots for the Northern Gannet distribution model – presence-absence (upper panel) and positive density (lower panel) parts. The values of the environmental variables are shown on the X-axis and the probability on the Y-axis in the scale of the linear predictor. The grey shaded areas and the

dotted lines (for factors) show the 95% Bayesian confidence intervals. The degree of smoothing is indicated in the legend of the Y-axis. .

Great Cormorant

Table A.4. Smooth terms, adjusted R-squared and evaluation statistics for the Great Cormorant distribution models. F statistics and the approximate significance for the smooth terms and t-statistic and the significance for the parametric terms are shown. Variables not included in either the presence/absence or positive model part are indicated with a dash. The results of the evaluation test show AUC for presence/absence and the Spearman's correlation for the density predictions. 'n.s.' indicates terms with p-values > 0.05. The significant effect of the windfarms are marked in bold.

| Smooth terms | Presence/absence | | | Positive density | | |
|-------------------------------|------------------|----------|----------|------------------|----------|----------|
| | F | p | | F | p | |
| Depth | 21.411 | 0 | | 3.333 | 0.069 | |
| Salinity | 7 | 0.008 | | 3.029 | 0.082 | |
| Current speed | 7.365 | 0 | | 5.312 | 0.024 | |
| Parametric terms | Estimate | t | p | Estimate | t | p |
| AIS | -0.006 | -2.676 | 0.007 | | | |
| LUD WF parametric | 2.338 | 6.958 | 0 | 0.02 | 0.043 | 0.966 |
| PAWP WF parametric | 4.075 | 12.943 | 0 | 0.368 | 1.393 | 0.164 |
| OWEZ WF parametric | 1.598 | 5.301 | 0 | 1.486 | 5.135 | 0 |
| LUD (2 km buffer) parametric | 1.262 | 4.524 | 0 | 0.175 | 0.294 | 0.769 |
| PAWP (2 km buffer) parametric | 2.349 | 9.97 | 0 | 0.288 | 0.944 | 0.346 |
| OWEZ (2 km buffer) parametric | 1.262 | 4.524 | 0 | 0.704 | 2.99 | 0.003 |
| Survey 5 | 0.181 | 0.372 | 0.71 | -0.942 | -1.592 | 0.112 |
| Survey 6 | -1.021 | -2.109 | 0.035 | 1.511 | 2.751 | 0.006 |
| Survey 7 | -1.624 | -2.287 | 0.022 | 0.843 | 1.484 | 0.138 |
| Survey 8 | 2.134 | 4 | 0 | -0.115 | -0.18 | 0.857 |
| Survey 9 | 1.411 | 2.629 | 0.009 | -0.364 | -0.644 | 0.52 |
| Survey 10 | 0.694 | 1.449 | 0.147 | -0.692 | -1.121 | 0.263 |
| Survey 11 | -0.793 | -1.42 | 0.156 | -0.064 | -0.105 | 0.916 |
| Survey 12 | -0.406 | -0.779 | 0.436 | -0.343 | -0.56 | 0.575 |
| Survey 13 | 0.741 | 1.447 | 0.148 | -0.364 | -0.566 | 0.572 |
| Survey 14 | 0.661 | 1.295 | 0.195 | -0.678 | -0.969 | 0.333 |
| Survey 15 | 0.044 | 0.072 | 0.943 | -0.001 | -0.002 | 0.998 |
| Survey 16 | -0.38 | -0.471 | 0.638 | -1.469 | -1.854 | 0.064 |
| Survey 17 | -2.302 | -3.464 | 0.001 | -0.493 | -0.49 | 0.624 |
| Survey 18 | -1.514 | -2.955 | 0.003 | -0.634 | -0.659 | 0.511 |
| Survey 19 | - | - | - | - | - | - |
| Survey 20 | - | - | - | - | - | - |
| Survey 21 | -1.098 | -2.014 | 0.044 | -0.217 | -0.311 | 0.756 |
| Survey 22 | -0.162 | -0.312 | 0.755 | -0.25 | -0.352 | 0.725 |
| Survey 23 | 0.3 | 0.493 | 0.622 | -0.879 | -1.25 | 0.212 |
| Survey 24 | -0.627 | -1.365 | 0.172 | 0.239 | 0.361 | 0.718 |
| Survey 25 | 0.244 | 0.471 | 0.637 | -0.614 | -0.928 | 0.354 |
| Survey 26 | 0.988 | 2.129 | 0.033 | -0.545 | -0.898 | 0.369 |
| Survey 27 | 0.297 | 0.572 | 0.567 | 0.542 | 0.846 | 0.398 |
| Survey 28 | 0.298 | 0.712 | 0.477 | -0.679 | -1.137 | 0.256 |
| Sample size (n) | 10,025 | | | 523 | | |
| Adjusted R ² | 14.3% | | | -3.6% | | |
| AUC | | | | | | |
| Spearman's corr. | | | | | | |

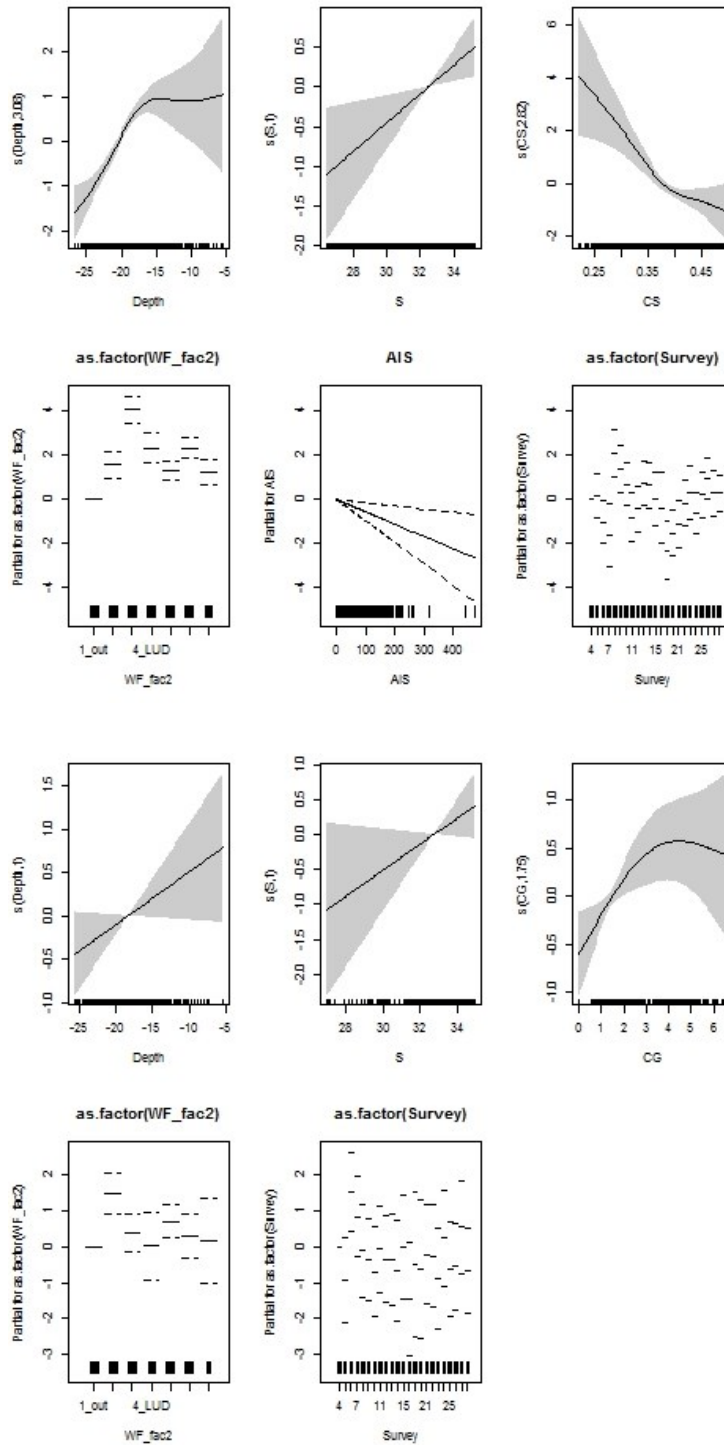


Figure A.4. Partial GAM plots for the Great Cormorant distribution model – presence-absence (upper panel) and positive density (lower panel) parts. The values of the environmental variables are shown on the X-axis and the probability on the Y-axis in the scale of the linear predictor. The grey shaded areas and the dotted lines (for factors) show the 95% Bayesian confidence intervals. The degree of smoothing is indicated in the legend of the Y-axis.

Little Gull

Table A.5. Smooth terms, adjusted R-squared and evaluation statistics for the Little Gull distribution models. F statistics and the approximate significance for the smooth terms and t-statistic and the significance for the parametric terms are shown. Variables not included in either the presence/absence or positive model part are indicated with a dash. The evaluation test did not converge due to too low sample size. 'n.s.' indicates terms with p-values > 0.05. The significant effect of the windfarms are marked in bold.

| Smooth terms | Presence/absence | | | Positive density | | |
|-------------------------------|------------------|--------|-------|------------------|--------|-------|
| | | F | p | | F | p |
| Depth | | 35.782 | 0 | | | |
| Salinity | | 11.068 | 0.001 | | - | - |
| Current speed | | 3.819 | 0.051 | | 2.893 | 0.048 |
| Current gradient | | 3.557 | 0.038 | | - | - |
| Parametric terms | Estimate | t | p | Estimate | t | p |
| AIS | -0.009 | -2.643 | 0.008 | - | - | - |
| LUD WF not included | - | - | - | - | - | - |
| PAWP WF not included | - | - | - | - | - | - |
| OWEZ WF parametric | -1.465 | -3.802 | 0 | -0.662 | -0.657 | 0.512 |
| LUD (2 km buffer) parametric | -0.026 | -0.058 | 0.954 | 0.605 | 1.073 | 0.284 |
| PAWP (2 km buffer) parametric | -0.078 | -0.272 | 0.786 | -0.612 | -1.124 | 0.262 |
| OWEZ (2 km buffer) parametric | -0.496 | -1.741 | 0.082 | -0.394 | -0.832 | 0.406 |
| Survey 5 | -0.718 | -1.025 | 0.305 | 0.055 | 0.094 | 0.925 |
| Survey 6 | 0.2 | 0.447 | 0.655 | -1.092 | -2 | 0.046 |
| Survey 7 | -0.114 | -0.13 | 0.897 | -0.779 | -0.945 | 0.345 |
| Survey 8 | -0.975 | -1.563 | 0.118 | 0.424 | 0.967 | 0.334 |
| Survey 9 | -2.365 | -4.069 | 0 | -0.002 | -0.003 | 0.998 |
| Survey 10 | -0.246 | -0.64 | 0.522 | 1.098 | 2.486 | 0.014 |
| Survey 11 | -1.122 | -2.249 | 0.025 | -0.321 | -0.431 | 0.667 |
| Survey 12 | -1.31 | -2.352 | 0.019 | -0.29 | -0.4 | 0.689 |
| Survey 13 | -0.417 | -0.825 | 0.41 | -0.12 | -0.236 | 0.814 |
| Survey 14 | -1.56 | -3.683 | 0 | -0.576 | -0.749 | 0.455 |
| Survey 15 | - | - | - | 0.431 | 0.75 | 0.454 |
| Survey 16 | -0.303 | -0.533 | 0.594 | -0.441 | -0.832 | 0.406 |
| Survey 17 | -0.291 | -0.513 | 0.608 | 0.158 | 0.335 | 0.738 |
| Survey 18 | -0.513 | -1.045 | 0.296 | 0.431 | 0.75 | 0.454 |
| Survey 19 | - | - | - | - | - | - |
| Survey 20 | - | - | - | - | - | - |
| Survey 21 | -1.443 | -2.641 | 0.008 | 0.314 | 0.449 | 0.654 |
| Survey 22 | -1.857 | -3.351 | 0.001 | -0.018 | -0.026 | 0.979 |
| Survey 23 | -2.558 | -3.943 | 0 | 0.709 | 0.852 | 0.395 |
| Survey 24 | -0.38 | -0.844 | 0.399 | 1.039 | 2.29 | 0.023 |
| Survey 25 | -2.48 | -5.126 | 0 | -0.624 | -0.773 | 0.44 |
| Survey 26 | -0.544 | -1.532 | 0.126 | 0.297 | 0.469 | 0.64 |
| Survey 27 | 0.924 | 1.709 | 0.088 | 1.139 | 2.725 | 0.007 |
| Survey 28 | -1.443 | -2.641 | 0.008 | 0.314 | 0.449 | 0.654 |
| Sample size (n) | | 9,198 | | | 297 | |
| Adjusted R ² | | 3.5% | | | 3.4% | |
| AUC | | | | | | |
| Spearman's corr. | | 0.16 | | | | |

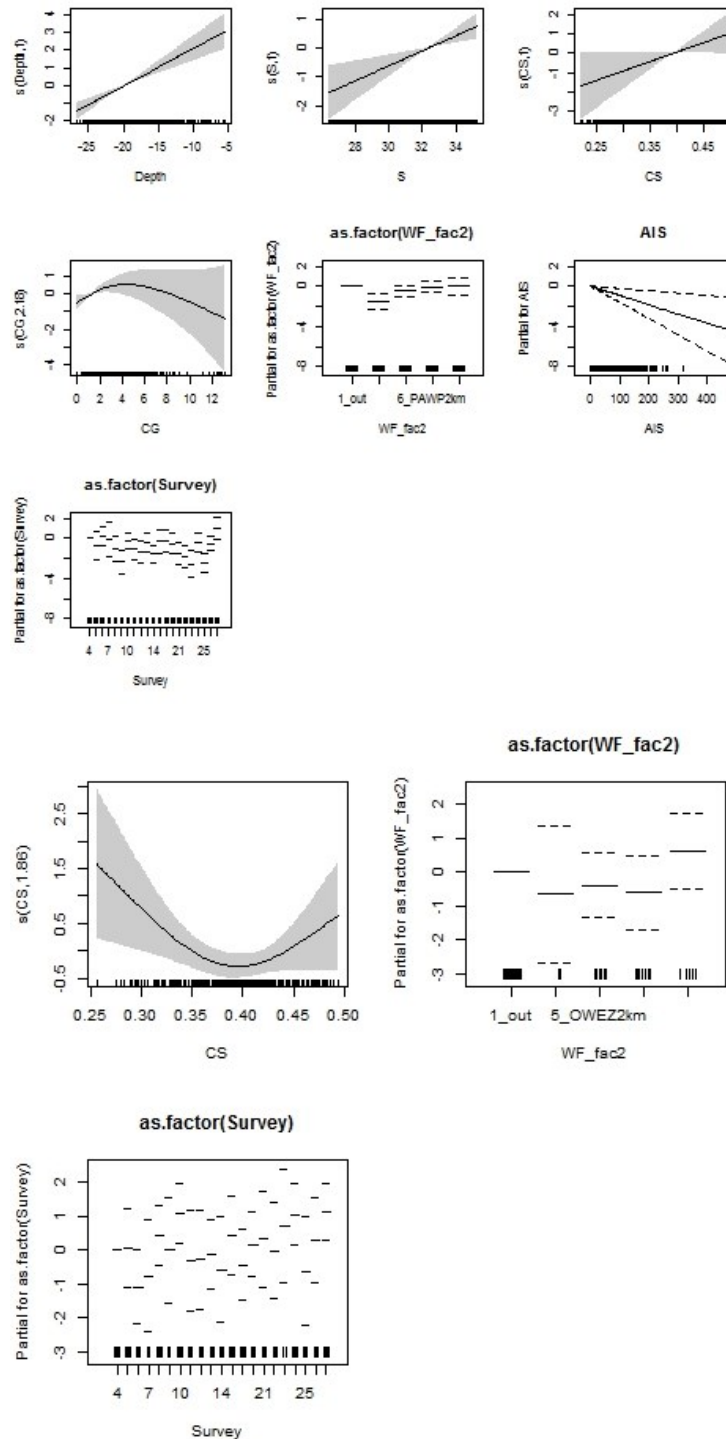


Figure A.5. Partial GAM plots for the Little Gull distribution model – presence-absence (upper panel) and positive density (lower panel) parts. The values of the environmental variables are shown on the X-axis and the probability on the Y-axis in the scale of the linear predictor. The grey shaded areas and the dotted lines (for factors) show the 95% Bayesian confidence intervals. The degree of smoothing is indicated in the legend of the Y-axis.

Black-headed Gull

Table A.6. Smooth terms, adjusted R-squared and evaluation statistics for the Black-headed Gull distribution models. F statistics and the approximate significance for the smooth terms and t-statistic and the significance for the parametric terms are shown. Variables not included in either the presence/absence or positive model part are indicated with a dash. The evaluation test did not converge due to too low sample size. 'n.s.' indicates terms with p-values > 0.05. The significant effect of the windfarms are marked in bold.

| Smooth terms | Presence/absence | | | Positive density | | |
|-------------------------------|------------------|--------|-------|------------------|--------|-------|
| | | F | p | | F | p |
| Depth | | 11.25 | 0 | | 2.674 | 0.052 |
| Salinity | | 8.175 | 0.004 | | | |
| Current speed | | 3.025 | 0.082 | | 7.346 | 0 |
| Current gradient | | 3.287 | 0.07 | | | |
| Parametric terms | Estimate | t | p | Estimate | t | p |
| AIS | 0.003 | 1.514 | 0.13 | - | - | - |
| LUD WF parametric | -1.043 | -4.123 | 0 | -1.455 | -0.952 | 0.341 |
| PAWP WF parametric | 0.003 | 0.013 | 0.989 | -0.067 | -0.201 | 0.841 |
| OWEZ WF parametric | -0.237 | -1.074 | 0.283 | -1.455 | -0.952 | 0.341 |
| LUD (2 km buffer) parametric | -0.645 | -3.103 | 0.002 | -0.624 | -0.576 | 0.565 |
| PAWP (2 km buffer) parametric | 0.069 | 0.427 | 0.67 | 0.09 | 0.395 | 0.693 |
| OWEZ (2 km buffer) parametric | -0.182 | -1.156 | 0.248 | -0.01 | -0.053 | 0.958 |
| Survey 5 | 0.63 | 1.214 | 0.225 | -0.318 | -1.51 | 0.131 |
| Survey 6 | 1.35 | 3.623 | 0 | -0.858 | -3.705 | 0 |
| Survey 7 | 1.109 | 1.471 | 0.141 | 0.002 | 0.006 | 0.995 |
| Survey 8 | 0.524 | 1.348 | 0.178 | -0.134 | -0.523 | 0.601 |
| Survey 9 | 0.271 | 0.686 | 0.493 | -0.099 | -0.351 | 0.725 |
| Survey 10 | 2.208 | 5.811 | 0 | 0.255 | 1.387 | 0.166 |
| Survey 11 | 0.417 | 0.795 | 0.427 | -1.167 | -4.419 | 0 |
| Survey 12 | -0.375 | -0.879 | 0.379 | -0.936 | -3.238 | 0.001 |
| Survey 13 | 0.761 | 1.963 | 0.05 | -0.077 | -0.329 | 0.742 |
| Survey 14 | 0.831 | 2.439 | 0.015 | 0.066 | 0.272 | 0.786 |
| Survey 15 | 1.248 | 2.988 | 0.003 | -0.177 | -0.785 | 0.433 |
| Survey 16 | -0.722 | -1.156 | 0.248 | 0.256 | 0.579 | 0.563 |
| Survey 17 | -3.701 | -8.056 | 0 | -0.905 | -0.618 | 0.537 |
| Survey 18 | -2.095 | -6.212 | 0 | 1.278 | 2.413 | 0.016 |
| Survey 19 | - | - | - | - | - | - |
| Survey 20 | - | - | - | - | - | - |
| Survey 21 | -1.315 | -2.989 | 0.003 | -0.672 | -1.588 | 0.113 |
| Survey 22 | -0.868 | -2.439 | 0.015 | -0.136 | -0.358 | 0.72 |
| Survey 23 | -2.928 | -7.47 | 0 | -1.011 | -0.937 | 0.349 |
| Survey 24 | -2.636 | -7.824 | 0 | 0.286 | 0.469 | 0.639 |
| Survey 25 | -1.322 | -3.053 | 0.002 | 0.305 | 0.63 | 0.529 |
| Survey 26 | -1.94 | -5.217 | 0 | 0.002 | 0.003 | 0.997 |
| Survey 27 | -2.195 | -3.751 | 0 | 0.703 | 1.393 | 0.164 |
| Survey 28 | -2.811 | -8.707 | 0 | 0.148 | 0.222 | 0.825 |
| Sample size (n) | | 10,025 | | | 1298 | |
| Adjusted R ² | | 23.6% | | | 6.7% | |
| AUC | | 0.77 | | | | |
| Spearman's corr. | | | | | | |

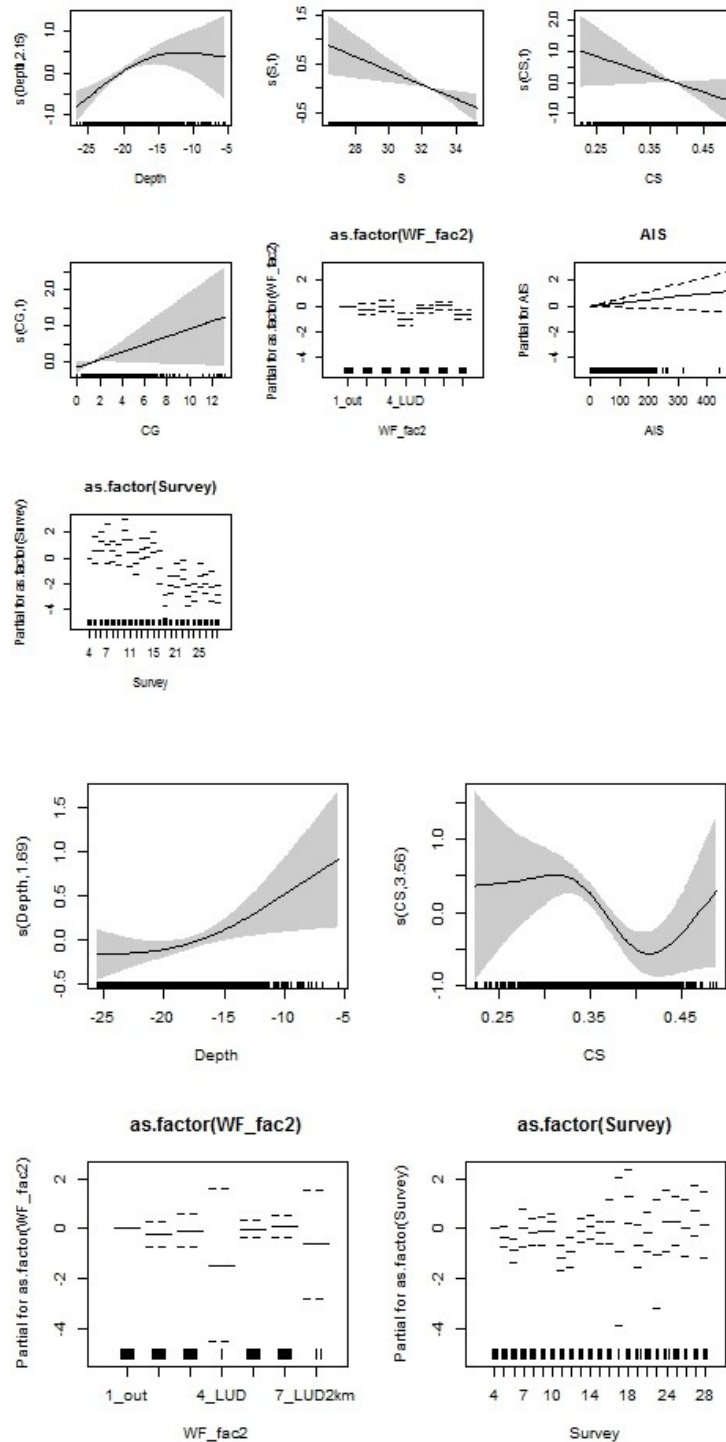


Figure A.6. Partial GAM plots for the Black-headed Gull distribution model – presence-absence (upper panel) and positive density (lower panel) parts. The values of the environmental variables are shown on the X-axis and the probability on the Y-axis in the scale of the linear predictor. The grey shaded areas and the dotted lines (for factors) show the 95% Bayesian confidence intervals. The degree of smoothing is indicated in the legend of the Y-axis.

Common Gull

Table A.7. Smooth terms, adjusted R-squared and evaluation statistics for the Common Gull distribution models. F statistics and the approximate significance for the smooth terms and t-statistic and the significance for the parametric terms are shown. Variables not included in either the presence/absence or positive model part are indicated with a dash. The evaluation test did not converge due to too low sample size. 'n.s.' indicates terms with p-values > 0.05.

| Smooth terms | Presence/absence | | | Positive density | | |
|-------------------------------|------------------|--------|-------|------------------|--------|-------|
| | F | p | | F | p | |
| Depth | 6.273 | 0 | | - | - | |
| Salinity | - | - | | 4.306 | 0.038 | |
| Current speed | 10.368 | 0.001 | | - | - | |
| Current gradient | - | - | | 31.452 | 0 | |
| Parametric terms | Estimate | t | p | Estimate | t | p |
| LUD WF | 0.001 | 0.729 | 0.466 | 0.001 | 0.379 | 0.705 |
| PAWP WF parametric | 0.332 | 1.166 | 0.244 | 0.364 | 1.163 | 0.245 |
| OWEZ WF parametric | 0.082 | 0.338 | 0.735 | -0.07 | -0.19 | 0.849 |
| OWEZ WF parametric | -0.194 | -0.764 | 0.445 | 0.164 | 0.57 | 0.569 |
| LUD (2 km buffer) parametric | 0.023 | 0.1 | 0.92 | 0.725 | 2.584 | 0.01 |
| PAWP (2 km buffer) parametric | 0.289 | 1.504 | 0.133 | 0.164 | 0.57 | 0.569 |
| OWEZ (2 km buffer) parametric | -0.217 | -1.169 | 0.243 | 0.058 | 0.217 | 0.828 |
| Survey 5 | 0.717 | 2.595 | 0.009 | -1.567 | -2.347 | 0.019 |
| Survey 6 | -0.588 | -1.158 | 0.247 | -1.232 | -1.699 | 0.09 |
| Survey 7 | 2.311 | 8.608 | 0 | -0.323 | -0.564 | 0.573 |
| Survey 8 | -0.688 | -2.18 | 0.029 | -1.351 | -1.419 | 0.156 |
| Survey 9 | 0.054 | 0.174 | 0.862 | -0.095 | -0.141 | 0.888 |
| Survey 10 | -1.138 | -1.87 | 0.061 | -1.11 | -1.131 | 0.258 |
| Survey 11 | -1.222 | -3.497 | 0 | -1.111 | -0.888 | 0.375 |
| Survey 12 | 1.781 | 4.461 | 0 | -0.716 | -1.177 | 0.24 |
| Survey 13 | 0.118 | 0.288 | 0.774 | -0.863 | -1.006 | 0.315 |
| Survey 14 | 2.163 | 5.501 | 0 | -1.234 | -1.992 | 0.047 |
| Survey 15 | 0.534 | 1.213 | 0.225 | -1.277 | -1.868 | 0.062 |
| Survey 16 | 1.926 | 7.138 | 0 | -0.176 | -0.304 | 0.761 |
| Survey 17 | 0.717 | 2.595 | 0.009 | -1.567 | -2.347 | 0.019 |
| Survey 18 | -0.588 | -1.158 | 0.247 | -1.232 | -1.699 | 0.09 |
| Survey 19 | - | - | - | - | - | - |
| Survey 20 | - | - | - | - | - | - |
| Survey 21 | 2.125 | 5.606 | 0 | -0.592 | -1.004 | 0.316 |
| Survey 22 | 2.434 | 6.006 | 0 | -0.262 | -0.446 | 0.655 |
| Survey 23 | 3.05 | 9.251 | 0 | -0.421 | -0.727 | 0.467 |
| Survey 24 | 1.82 | 6.454 | 0 | -0.712 | -1.262 | 0.207 |
| Survey 25 | 2.534 | 8.832 | 0 | -0.828 | -1.432 | 0.153 |
| Survey 26 | 3.067 | 12.315 | 0 | -0.256 | -0.449 | 0.653 |
| Survey 27 | 2.879 | 10.835 | 0 | 0.477 | 0.931 | 0.352 |
| Survey 28 | 1.263 | 4.967 | 0 | 0.273 | 0.468 | 0.64 |
| Sample size (n) | 9,259 | | | 843 | | |
| Adjusted R ² | 7.1% | | | 3.9% | | |
| AUC | | | | | | |
| Spearman's corr. | | | | | | |

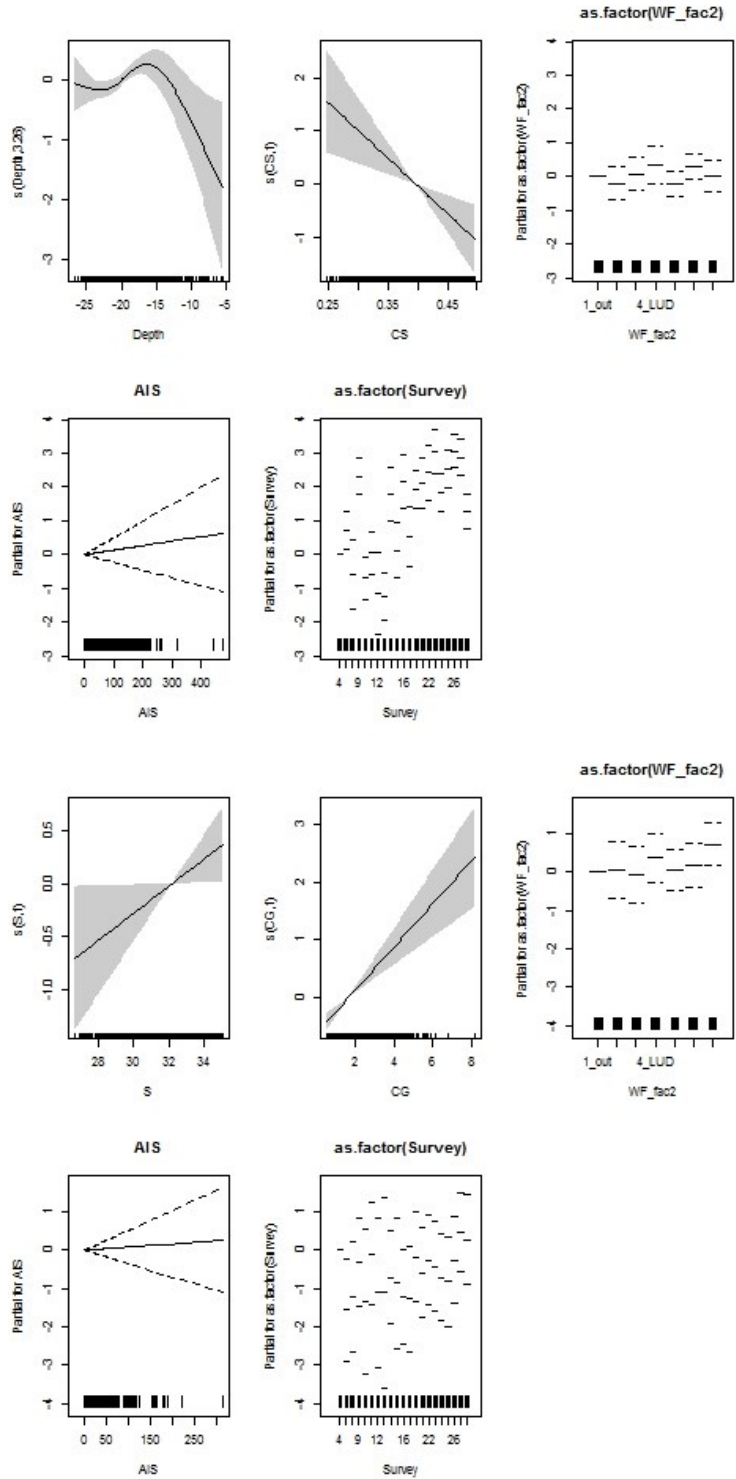


Figure A.7. Partial GAM plots for the Common Gull distribution model – presence-absence (upper panel) and positive density (lower panel) parts. The values of the environmental variables are shown on the X-axis and the probability on the Y-axis in the scale of the linear predictor. The grey shaded areas and the dotted lines (for factors) show the 95% Bayesian confidence intervals. The degree of smoothing is indicated in the legend of the Y-axis.

Lesser Black-backed Gull

Table A.8. Smooth terms, adjusted R-squared and evaluation statistics for the Lesser Black-backed Gull distribution models. F statistics and the approximate significance for the smooth terms and t-statistic and the significance for the parametric terms are shown. Variables not included in either the presence/absence or positive model part are indicated with a dash. The evaluation test did not converge due to too low sample size. 'n.s.' indicates terms with p-values > 0.05.

| Smooth terms | Presence/absence | | | Positive density | | |
|-------------------------------|------------------|--------|-------|------------------|--------|-------|
| | | F | p | | F | p |
| Depth | | 23.652 | 0 | | 2.6 | 0.046 |
| Salinity | | 14.872 | 0 | | 13.845 | 0 |
| Current speed | | | | | - | - |
| Current gradient | | 3.819 | 0.051 | | 5.595 | 0.018 |
| Parametric terms | Estimate | t | p | Estimate | t | p |
| AIS | | | | | | |
| LUD WF parametric | -0.546 | -2.699 | 0.007 | -0.447 | -0.599 | 0.549 |
| PAWP WF parametric | 0.34 | 1.83 | 0.067 | -0.584 | -1.47 | 0.142 |
| OWEZ WF parametric | 0.083 | 0.447 | 0.655 | -0.035 | -0.09 | 0.928 |
| LUD (2 km buffer) parametric | 0.066 | 0.396 | 0.692 | 0.205 | 0.435 | 0.664 |
| PAWP (2 km buffer) parametric | -0.097 | -0.668 | 0.504 | 0.005 | 0.015 | 0.988 |
| OWEZ (2 km buffer) parametric | 0.177 | 1.301 | 0.193 | 0.579 | 2.171 | 0.03 |
| Survey 5 | -0.126 | -0.483 | 0.629 | -1.076 | -2.763 | 0.006 |
| Survey 6 | 0.428 | 1.636 | 0.102 | -0.17 | -0.535 | 0.592 |
| Survey 7 | -0.404 | -0.714 | 0.475 | 0.363 | 0.862 | 0.389 |
| Survey 8 | -0.701 | -2.045 | 0.041 | -1.339 | -2.697 | 0.007 |
| Survey 9 | -1.178 | -2.854 | 0.004 | -0.931 | -2.11 | 0.035 |
| Survey 10 | -1.736 | -6.433 | 0 | -1.186 | -2.287 | 0.022 |
| Survey 11 | -1.884 | -7.223 | 0 | -1.518 | -2.711 | 0.007 |
| Survey 12 | -0.508 | -1.873 | 0.061 | -0.721 | -1.633 | 0.103 |
| Survey 13 | -0.841 | -2.847 | 0.004 | -0.67 | -1.324 | 0.186 |
| Survey 14 | -0.825 | -2.746 | 0.006 | -1.111 | -2.391 | 0.017 |
| Survey 15 | -2.045 | -4.627 | 0 | -1.405 | -2.351 | 0.019 |
| Survey 16 | -1.78 | -2.226 | 0.026 | -0.969 | -1.806 | 0.071 |
| Survey 17 | -5.534 | 14.824 | 0 | -0.894 | -0.342 | 0.732 |
| Survey 18 | -4.523 | 18.061 | 0 | -0.47 | -0.351 | 0.725 |
| Survey 19 | - | - | - | - | - | - |
| Survey 20 | - | - | - | - | - | - |
| Survey 21 | -1.147 | -4.049 | 0 | -1.055 | -2.088 | 0.037 |
| Survey 22 | -2.773 | 10.706 | 0 | -1.195 | -1.658 | 0.097 |
| Survey 23 | -2.546 | -9.143 | 0 | -0.896 | -1.353 | 0.176 |
| Survey 24 | -1.364 | -5.274 | 0 | 0.428 | 0.95 | 0.342 |
| Survey 25 | -1.002 | -3.35 | 0.001 | -0.704 | -1.539 | 0.124 |
| Survey 26 | -3.601 | 13.399 | 0 | -1.552 | -1.626 | 0.104 |
| Survey 27 | -3.716 | 15.438 | 0 | -0.628 | -0.477 | 0.634 |
| Survey 28 | -0.685 | -2.899 | 0.004 | 2.185 | 5.712 | 0 |
| Sample size (n) | | 10,025 | | | 1,714 | |
| Adjusted R ² | | 12.4% | | | 0.8% | |
| AUC | | | | | | |
| Spearman's corr. | | | | | | |

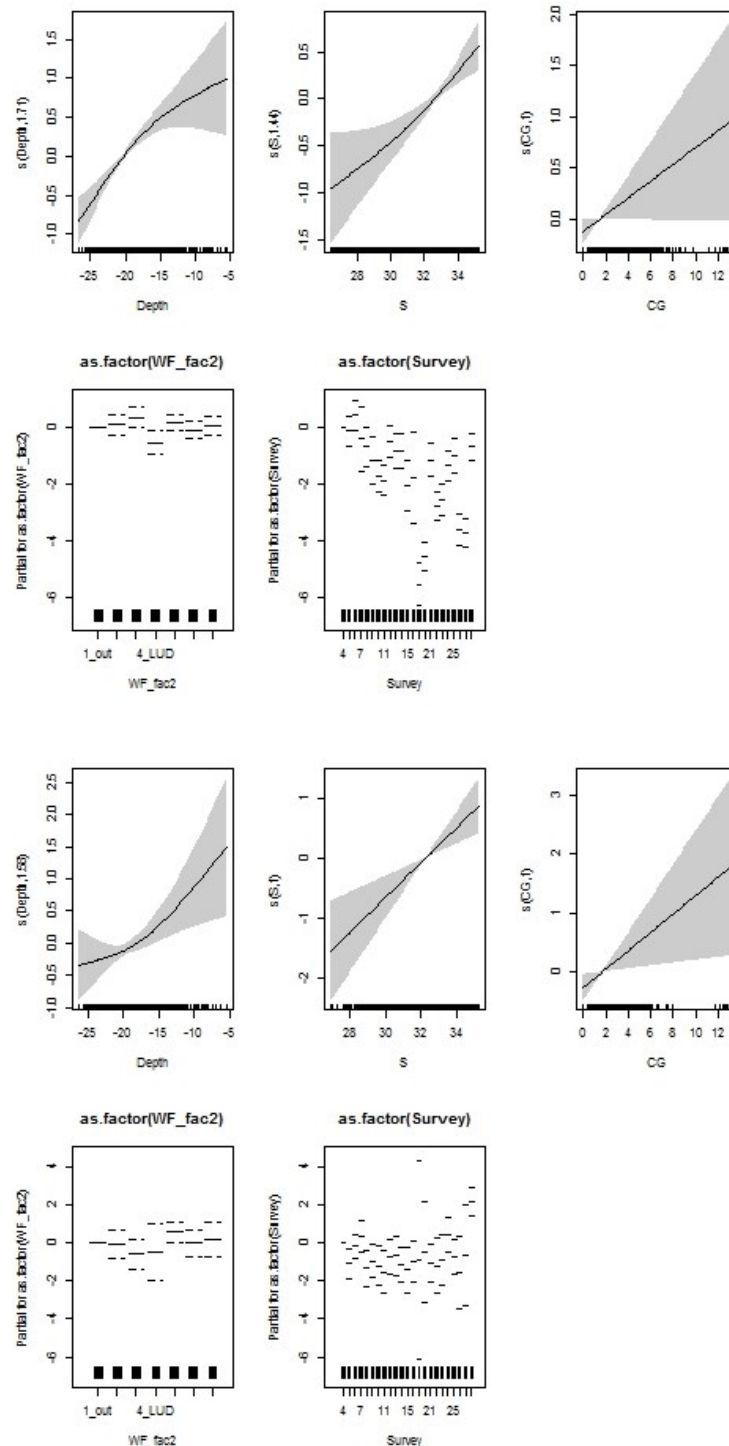


Figure A.8. Partial GAM plots for the Lesser Black-backed Gull distribution model – presence-absence (upper panel) and positive density (lower panel) parts. The values of the environmental variables are shown on the X-axis and the probability on the Y-axis in the scale of the linear predictor. The grey shaded areas and the dotted lines (for factors) show the 95% Bayesian confidence intervals. The degree of smoothing is indicated in the legend of the Y-axis.

Herring Gull

Table A.9. Smooth terms, adjusted R-squared and evaluation statistics for the Herring Gull distribution models. F statistics and the approximate significance for the smooth terms and t-statistic and the significance for the parametric terms are shown. Variables not included in either the presence/absence or positive model part are indicated with a dash. The results of the evaluation test show AUC for presence/absence and the Spearman's correlation for the density predictions. 'n.s.' indicates terms with p-values > 0.05.

| Smooth terms | Presence/absence | | | Positive density | | |
|-------------------------------|------------------|--------|-------|------------------|--------|-------|
| | F | p | | F | p | |
| Depth | - | - | | - | - | |
| Salinity | - | - | | 2.76 | 0.054 | |
| Current speed | 52.71 | 0 | | - | - | |
| Current gradient | - | - | | 41.737 | 0 | |
| Parametric terms | Estimate | t | p | Estimate | t | p |
| AIS | 0.002 | 1.059 | 0.29 | 0.003 | 1.484 | 0.138 |
| LUD WF parametric | 0.677 | 2.143 | 0.032 | 0.015 | 0.042 | 0.966 |
| PAWP WF parametric | 0.671 | 2.508 | 0.012 | -0.122 | -0.448 | 0.654 |
| OWEZ WF parametric | -0.27 | -0.974 | 0.33 | -0.019 | -0.051 | 0.959 |
| LUD (2 km buffer) parametric | 0.327 | 1.272 | 0.204 | -0.175 | -0.517 | 0.605 |
| PAWP (2 km buffer) parametric | 0.058 | 0.274 | 0.784 | -0.278 | -1.008 | 0.314 |
| OWEZ (2 km buffer) parametric | 0.25 | 1.26 | 0.208 | 0.117 | 0.533 | 0.594 |
| Survey 5 | -0.231 | -0.604 | 0.546 | -1.019 | -1.211 | 0.226 |
| Survey 6 | 0.511 | 1.254 | 0.21 | -0.623 | -1.07 | 0.285 |
| Survey 7 | | | | | | |
| Survey 8 | 3.299 | 9.06 | 0 | -0.605 | -1.009 | 0.313 |
| Survey 9 | 2.115 | 4.999 | 0 | -0.851 | -1.374 | 0.17 |
| Survey 10 | | | | | | |
| Survey 11 | 1.272 | 3.686 | 0 | -0.995 | -1.71 | 0.088 |
| Survey 12 | 2.947 | 7.416 | 0 | -0.411 | -0.732 | 0.464 |
| Survey 13 | 1.702 | 4.232 | 0 | -1.048 | -1.661 | 0.097 |
| Survey 14 | 1.041 | 2.015 | 0.044 | -0.485 | -0.635 | 0.526 |
| Survey 15 | 2.655 | 6.899 | 0 | -0.624 | -1.024 | 0.306 |
| Survey 16 | 1.864 | 4.472 | 0 | 0.179 | 0.249 | 0.803 |
| Survey 17 | 1.014 | 2.576 | 0.01 | -0.292 | -0.461 | 0.645 |
| Survey 18 | 2.554 | 6.351 | 0 | -0.19 | -0.334 | 0.739 |
| Survey 19 | - | - | - | - | - | - |
| Survey 20 | - | - | - | - | - | - |
| Survey 21 | 1.567 | 2.388 | 0.017 | -0.811 | -1.365 | 0.173 |
| Survey 22 | 3.473 | 9.18 | 0 | 0.341 | 0.609 | 0.542 |
| Survey 23 | 2.384 | 5.607 | 0 | -0.277 | -0.429 | 0.668 |
| Survey 24 | 1.1 | 3.349 | 0.001 | -0.16 | -0.263 | 0.792 |
| Survey 25 | 2.925 | 7.469 | 0 | -0.279 | -0.472 | 0.637 |
| Survey 26 | 2.073 | 5.914 | 0 | -0.5 | -0.819 | 0.413 |
| Survey 27 | 1.288 | 2.978 | 0.003 | 0.325 | 0.493 | 0.622 |
| Survey 28 | 1.896 | 4.728 | 0 | 0.806 | 1.415 | 0.157 |
| Sample size (n) | 9,315 | | | 662 | | |
| Adjusted R ² | 6.6% | | | -4.9% | | |
| AUC | | | | 0.71 | | |
| Spearman's corr. | | | | -0.004 | | |

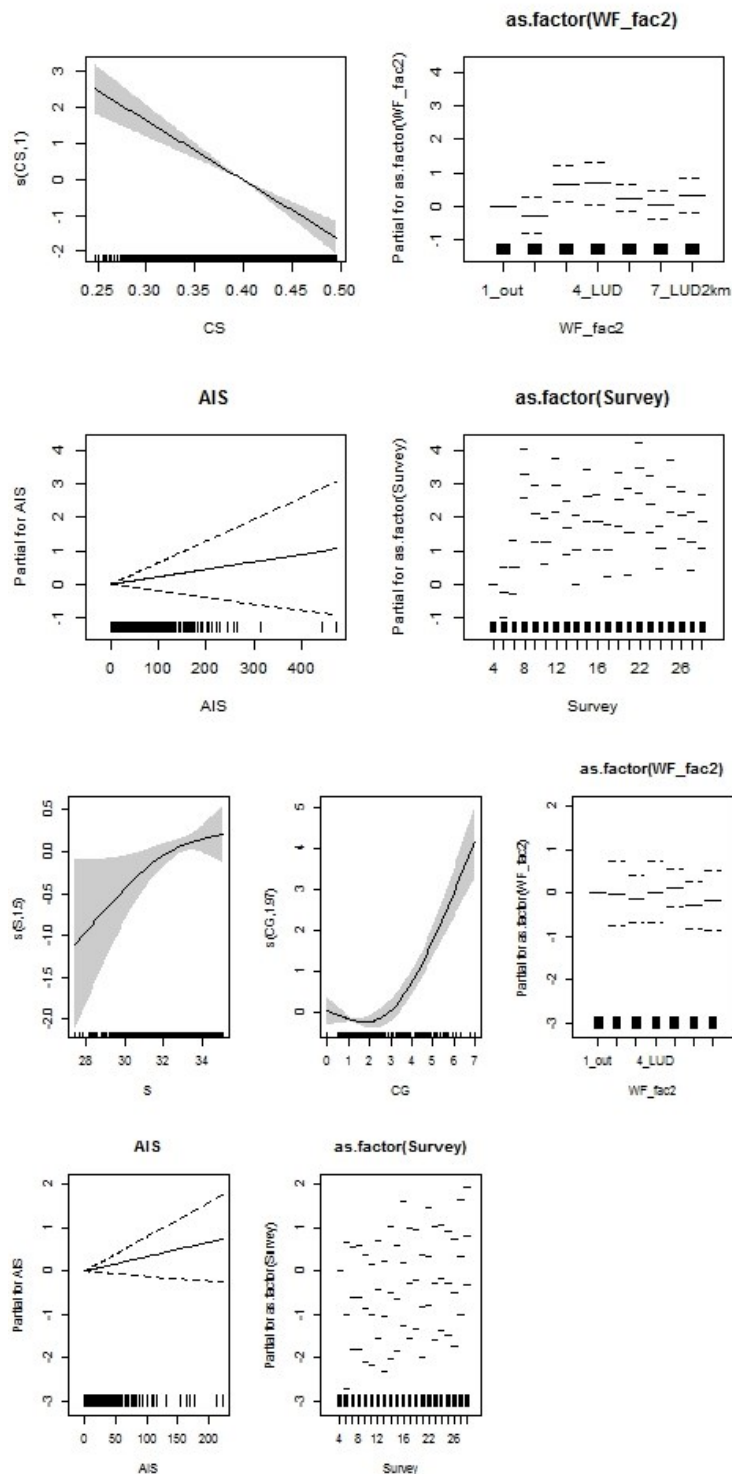


Figure A.9. Partial GAM plots for the Herring Gull distribution model – presence-absence (upper panel) and positive density (lower panel) parts. The values of the environmental variables are shown on the X-axis and the probability on the Y-axis in the scale of the linear predictor. The grey shaded areas and the dotted lines (for factors) show the 95% Bayesian confidence intervals. The degree of smoothing is indicated in the legend of the Y-axis.

Great Black-backed Gull

Table A.10. Smooth terms, adjusted R-squared and evaluation statistics for the Great Black-backed Gull distribution models. F statistics and the approximate significance for the smooth terms and t-statistic and the significance for the parametric terms are shown. Variables not included in either the presence/absence or positive model part are indicated with a dash. The results of the evaluation test show AUC for presence/absence and the Spearman's correlation for the density predictions. 'n.s.' indicates terms with p-values > 0.05. The significant effect of the windfarms are marked in bold.

| Smooth terms | Presence/absence | | | Positive density | | |
|-------------------------------|------------------|--------|-------|------------------|--------|-------|
| | | F | p | | F | p |
| Depth | | - | - | | - | - |
| Salinity | | - | - | | - | - |
| Current speed | | - | - | | - | - |
| Current gradient | | 6.109 | 0.013 | | 10.723 | 0.001 |
| Parametric terms | Estimate | t | p | Estimate | t | p |
| AIS | - | - | - | - | - | - |
| LUD WF parametric | 0.32 | 1.37 | 0.171 | 0.004 | 0.01 | 0.992 |
| PAWP WF parametric | 0.595 | 3.135 | 0.002 | -0.336 | -1.379 | 0.168 |
| OWEZ WF parametric | 0.366 | 1.866 | 0.062 | -0.088 | -0.355 | 0.722 |
| LUD (2 km buffer) parametric | 0.271 | 1.467 | 0.142 | -0.207 | -0.615 | 0.539 |
| PAWP (2 km buffer) parametric | 0.378 | 2.516 | 0.012 | -0.094 | -0.518 | 0.605 |
| OWEZ (2 km buffer) parametric | 0.185 | 1.289 | 0.198 | -0.119 | -0.651 | 0.515 |
| Survey 5 | -0.537 | -1.858 | 0.063 | -0.52 | -2.728 | 0.006 |
| Survey 6 | -2.248 | -5.427 | 0 | -1.094 | -3.988 | 0 |
| Survey 7 | -0.211 | -0.627 | 0.531 | -0.14 | -0.728 | 0.466 |
| Survey 8 | -3.553 | -10.64 | 0 | -1.036 | -2.324 | 0.02 |
| Survey 9 | -1.431 | -4.39 | 0 | -0.372 | -1.855 | 0.064 |
| Survey 10 | -3.93 | 16.265 | 0 | -1.126 | -1.966 | 0.049 |
| Survey 11 | -3.598 | 13.376 | 0 | -0.347 | -0.705 | 0.481 |
| Survey 12 | -1.642 | -6.954 | 0 | -0.439 | -1.913 | 0.056 |
| Survey 13 | -1.116 | -4.926 | 0 | -0.325 | -1.462 | 0.144 |
| Survey 14 | 0.129 | 0.562 | 0.574 | 0.348 | 1.955 | 0.051 |
| Survey 15 | -0.928 | -3.521 | 0 | -0.727 | -3.603 | 0 |
| Survey 16 | -2.173 | -6.052 | 0 | -0.642 | -2.319 | 0.02 |
| Survey 17 | -3.097 | 10.382 | 0 | -0.871 | -1.885 | 0.06 |
| Survey 18 | -3.433 | 16.854 | 0 | 0.054 | 0.131 | 0.896 |
| Survey 19 | - | - | - | - | - | - |
| Survey 20 | - | - | - | - | - | - |
| Survey 21 | -2.032 | -8.964 | 0 | -0.684 | -2.612 | 0.009 |
| Survey 22 | -1.844 | -7.314 | 0 | 0.294 | 1.213 | 0.225 |
| Survey 23 | -2.212 | -8.986 | 0 | 0.159 | 0.57 | 0.569 |
| Survey 24 | -2.549 | 12.101 | 0 | -0.571 | -2.09 | 0.037 |
| Survey 25 | -2.434 | -9.18 | 0 | -0.424 | -1.432 | 0.152 |
| Survey 26 | -2.82 | -8.633 | 0 | -0.705 | -2.101 | 0.036 |
| Survey 27 | -3.243 | 12.155 | 0 | -0.753 | -1.937 | 0.053 |
| Survey 28 | -2.764 | 12.663 | 0 | -0.513 | -1.561 | 0.119 |
| Sample size (n) | | 10,025 | | | 1,723 | |
| Adjusted R ² | | 18.5% | | | 3.4% | |
| AUC | | | | | | |
| Spearman's corr. | | | | | | |

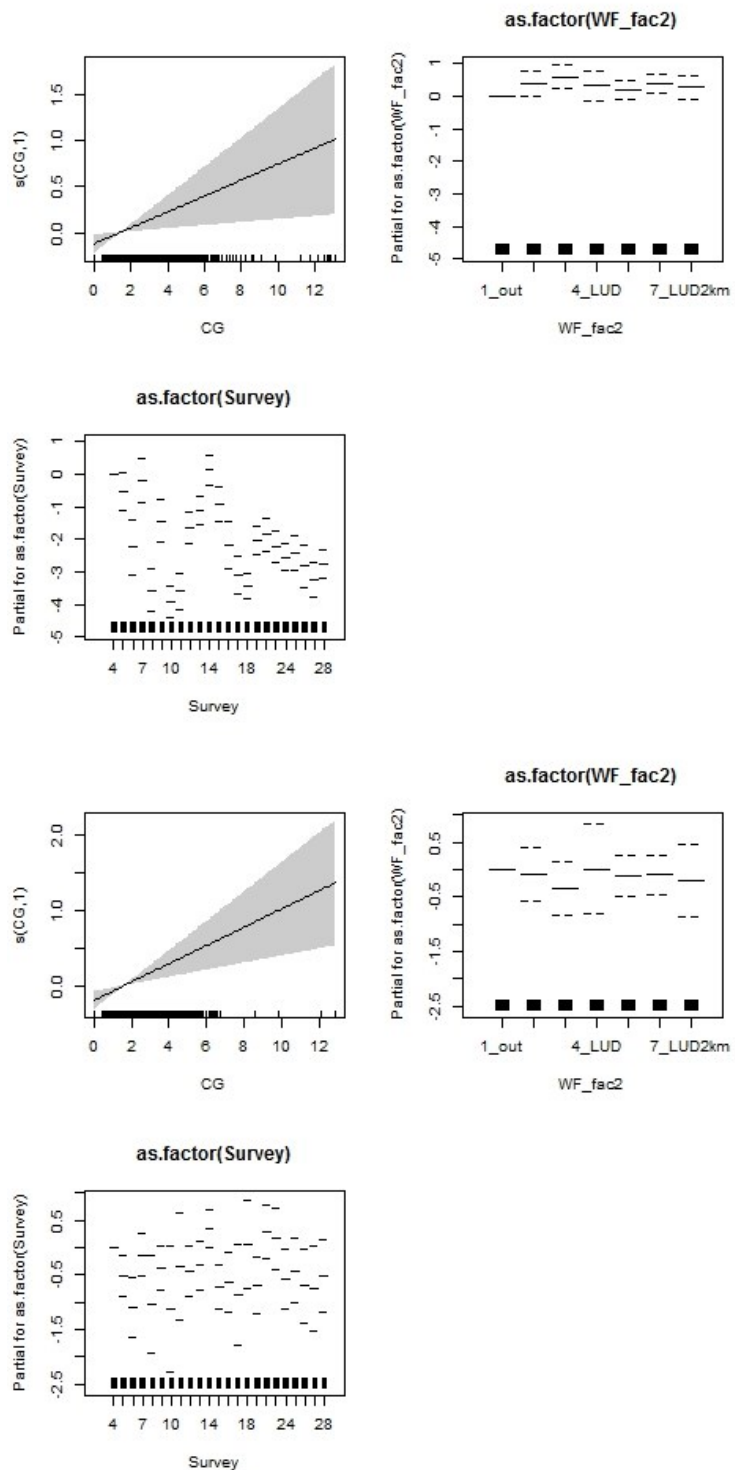


Figure A.10. Partial GAM plots for the Great Black-backed Gull distribution model – presence-absence (upper panel) and positive density (lower panel) parts. The values of the environmental variables are shown on the X-axis and the probability on the Y-axis in the scale of the linear predictor. The grey shaded areas and the dotted lines (for factors) show the 95% Bayesian confidence intervals. The degree of smoothing is indicated in the legend of the Y-axis.

Black-legged Kittiwake

Table A.11. Smooth terms, adjusted R-squared and evaluation statistics for the Black-legged distribution models. F statistics and the approximate significance for the smooth terms and t-statistic and the significance for the parametric terms are shown. Variables not included in either the presence/absence or positive model part are indicated with a dash. The evaluation test did not converge due to low sample size. 'n.s.' indicates terms with p-values > 0.05. The significant effect of the windfarms are marked in bold.

| Smooth terms | Presence/absence | | | Positive density | | |
|-------------------------------|------------------|----------|----------|------------------|----------|----------|
| | F | p | | F | p | |
| Depth | 33.625 | 0 | | - | - | |
| Salinity | 16.134 | 0 | | 10.215 | 0.001 | |
| Current speed | 5.153 | 0.002 | | 7.939 | 0 | |
| Current gradient | - | - | | - | - | |
| Parametric terms | Estimate | t | p | Estimate | t | p |
| AIS | -0.003 | -1.977 | 0.048 | - | - | - |
| LUD WF parametric | 0.299 | 1.246 | 0.213 | 0.359 | 0.749 | 0.454 |
| PAWP WF parametric | -0.518 | -2.543 | 0.011 | 1.244 | 2.164 | 0.031 |
| OWEZ WF parametric | -0.3 | -1.393 | 0.164 | -0.336 | -0.662 | 0.508 |
| LUD (2 km buffer) parametric | 0.204 | 1.054 | 0.292 | 0.303 | 0.779 | 0.436 |
| PAWP (2 km buffer) parametric | -0.239 | -1.458 | 0.145 | -0.074 | -0.174 | 0.862 |
| OWEZ (2 km buffer) parametric | -0.254 | -1.642 | 0.101 | -0.041 | -0.114 | 0.909 |
| Survey 5 | 0.872 | 2.315 | 0.021 | -1.042 | -2.47 | 0.014 |
| Survey 6 | -0.078 | -0.198 | 0.843 | -1.607 | -3.172 | 0.002 |
| Survey 7 | 0.067 | 0.14 | 0.888 | -2.038 | -3.244 | 0.001 |
| Survey 8 | -1.238 | -3.036 | 0.002 | -0.24 | -0.427 | 0.669 |
| Survey 9 | -1.635 | -4.504 | 0 | -0.697 | -1.139 | 0.255 |
| Survey 10 | -1.239 | -3.362 | 0.001 | -1.216 | -1.956 | 0.051 |
| Survey 11 | -1.653 | -3.541 | 0 | -2.892 | -3.936 | 0 |
| Survey 12 | -0.952 | -1.942 | 0.052 | -1.948 | -3.297 | 0.001 |
| Survey 13 | -1.974 | -4.177 | 0 | -0.047 | -0.055 | 0.956 |
| Survey 14 | -1.416 | -3.347 | 0.001 | -0.951 | -1.263 | 0.207 |
| Survey 15 | -1.476 | -3.776 | 0 | -1.274 | -1.88 | 0.06 |
| Survey 16 | -2.742 | -6.721 | 0 | -0.646 | -0.671 | 0.502 |
| Survey 17 | -0.197 | -0.487 | 0.626 | -1.57 | -2.7 | 0.007 |
| Survey 18 | -0.269 | -0.763 | 0.445 | -0.208 | -0.448 | 0.655 |
| Survey 19 | - | - | - | - | - | - |
| Survey 20 | - | - | - | - | - | - |
| Survey 21 | -1.95 | -4.797 | 0 | -1.858 | -2.474 | 0.013 |
| Survey 22 | 0.736 | 1.936 | 0.053 | 2.153 | 4.515 | 0 |
| Survey 23 | -0.965 | -2.455 | 0.014 | -0.301 | -0.464 | 0.643 |
| Survey 24 | -1.648 | -4.976 | 0 | -0.258 | -0.395 | 0.693 |
| Survey 25 | -1.06 | -2.789 | 0.005 | -0.338 | -0.563 | 0.573 |
| Survey 26 | 0.134 | 0.341 | 0.733 | -0.07 | -0.151 | 0.88 |
| Survey 27 | 0.789 | 2.021 | 0.043 | 0.598 | 1.296 | 0.195 |
| Survey 28 | -1.978 | -5.328 | 0 | -0.697 | -0.846 | 0.398 |
| Sample size (n) | 10,025 | | | 1,287 | | |
| Adjusted R ² | 10.8% | | | 0.3% | | |
| AUC | | | | | | |
| Spearman's corr. | | | | | | |

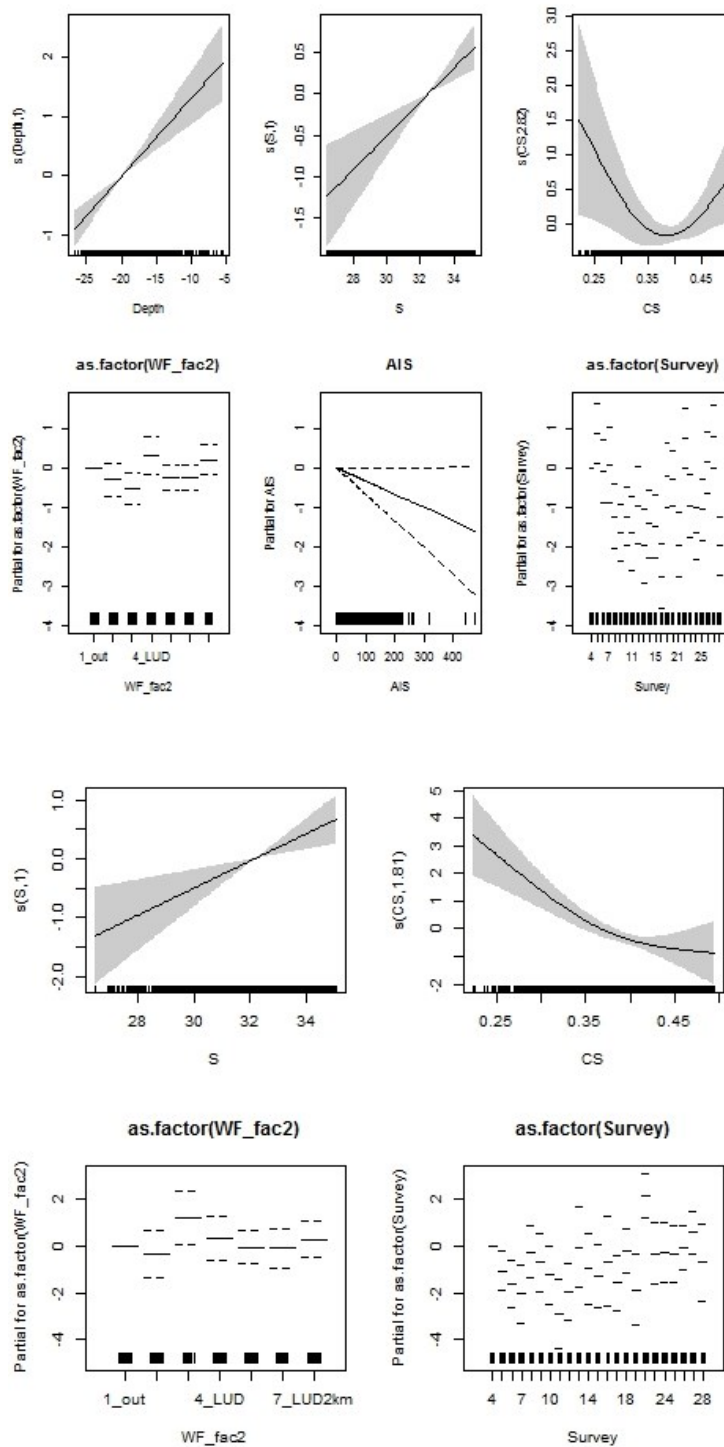


Figure A.11. Partial GAM plots for the Kittiwake distribution model – presence-absence (upper panel) and positive density (lower panel) parts. The values of the environmental variables are shown on the X-axis and the probability on the Y-axis in the scale of the linear predictor. The grey shaded areas and the dotted lines (for factors) show the 95% Bayesian confidence intervals. The degree of smoothing is indicated in the legend of the Y-axis.

Common Guillemot

Table A.12. Smooth terms, adjusted R-squared and evaluation statistics for the Common Guillemot distribution models. F statistics and the approximate significance for the smooth terms and t-statistic and the significance for the parametric terms are shown. Variables not included in either the presence/absence or positive model part are indicated with a dash. The results of the evaluation test show AUC for presence/absence and the Spearman's correlation for the density predictions. 'n.s.' indicates terms with p-values < 0.05. The significant effect of the windfarms are marked in bold.

| Smooth terms | Presence/absence | | | Positive density | | |
|-------------------------------|------------------|--------|-------|------------------|--------|-------|
| | F | p | | F | p | |
| Depth | 1.844 | 0.127 | | 2.154 | 0.071 | |
| Salinity | 21.271 | 0 | | 5.246 | 0.022 | |
| Current speed | 7.704 | 0 | | 6.41 | 0.001 | |
| Current gradient | | | | 7.341 | 0.007 | |
| Parametric terms | Estimate | t | p | Estimate | t | p |
| AIS | -0.003 | -1.997 | 0.046 | -0.001 | -0.767 | 0.443 |
| LUD WF parametric | -0.8 | -3.452 | 0.001 | -0.31 | -2.012 | 0.044 |
| PAWP WF parametric | -1.28 | -7.548 | 0 | -0.657 | -4.297 | 0 |
| OWEZ WF parametric | -0.706 | -3.942 | 0 | 0.085 | 0.571 | 0.568 |
| LUD (2 km buffer) parametric | -0.208 | -1.156 | 0.248 | -0.108 | -1.059 | 0.289 |
| PAWP (2 km buffer) parametric | -0.458 | -3.482 | 0 | -0.109 | -1.111 | 0.267 |
| OWEZ (2 km buffer) parametric | -0.228 | -1.789 | 0.074 | -0.04 | -0.407 | 0.684 |
| Survey 5 | -0.393 | -1.614 | 0.107 | -0.669 | -3.263 | 0.001 |
| Survey 6 | -1.779 | -6.031 | 0 | -1.102 | -3.856 | 0 |
| Survey 7 | 0.48 | 1.192 | 0.233 | -0.588 | -1.652 | 0.099 |
| Survey 8 | -4.18 | 13.513 | 0 | -1.432 | -3.466 | 0.001 |
| Survey 9 | -1.272 | -4.834 | 0 | -0.924 | -4.254 | 0 |
| Survey 10 | -1.532 | -5.748 | 0 | -1.031 | -4.426 | 0 |
| Survey 11 | -2.752 | -8.238 | 0 | -0.649 | -1.825 | 0.068 |
| Survey 12 | -1.311 | -4.393 | 0 | -0.815 | -3.365 | 0.001 |
| Survey 13 | -0.157 | -0.546 | 0.585 | -0.784 | -3.594 | 0 |
| Survey 14 | -0.175 | -0.602 | 0.547 | -0.699 | -3.419 | 0.001 |
| Survey 15 | -2.037 | -7.289 | 0 | -1.437 | -5.45 | 0 |
| Survey 16 | -1.822 | -5.936 | 0 | -0.904 | -3.442 | 0.001 |
| Survey 17 | 0.107 | 0.341 | 0.733 | -0.296 | -1.248 | 0.212 |
| Survey 18 | 1.455 | 5.998 | 0 | 0.441 | 2.442 | 0.015 |
| Survey 19 | - | - | - | - | - | - |
| Survey 20 | - | - | - | - | - | - |
| Survey 21 | -0.668 | -2.18 | 0.029 | -0.58 | -2.414 | 0.016 |
| Survey 22 | 1.289 | 4.557 | 0 | 0.724 | 3.641 | 0 |
| Survey 23 | -0.812 | -2.464 | 0.014 | -0.662 | -2.69 | 0.007 |
| Survey 24 | -2.206 | -9.584 | 0 | -0.918 | -3.848 | 0 |
| Survey 25 | -0.518 | -1.912 | 0.056 | -0.024 | -0.114 | 0.909 |
| Survey 26 | 0.517 | 1.156 | 0.248 | 0.239 | 1.232 | 0.218 |
| Survey 27 | 2.098 | 7.035 | 0 | 0.3 | 1.882 | 0.06 |
| Survey 28 | -1.398 | -6.325 | 0 | -0.505 | -2.367 | 0.018 |
| Sample size (n) | 10,025 | | | 3,091 | | |
| Adjusted R ² | 26.7% | | | 14.9% | | |
| AUC | | | | | | |
| Spearman's corr. | | | | | | |

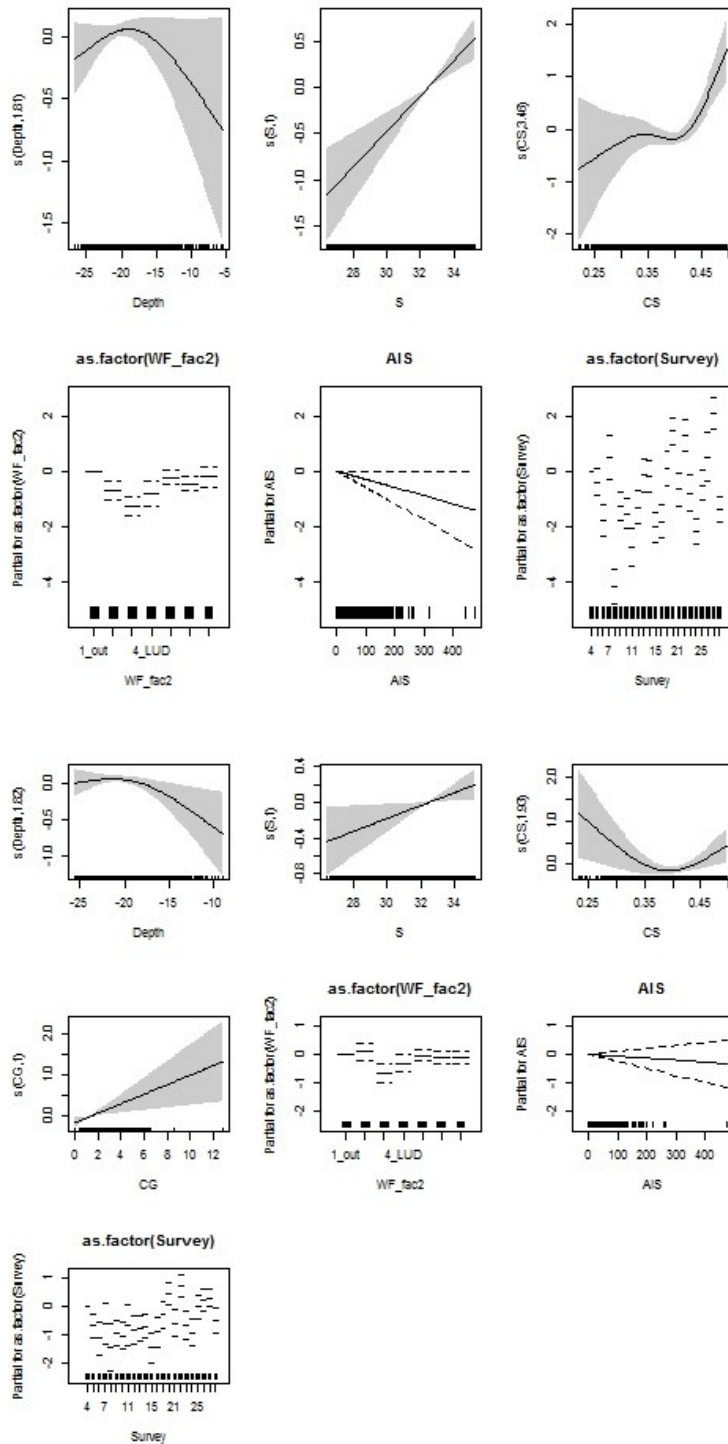


Figure A.12. Partial GAM plots for the Common Guillemot distribution model – presence-absence (upper panel) and positive (lower panel) parts. The values of the environmental variables are shown on the X-axis and the probability on the Y-axis in the scale of the linear predictor. The grey shaded areas and the dotted lines (for factors) show the 95% Bayesian confidence intervals. The degree of smoothing is indicated in the legend of the Y-axis.

Razorbill

Table A.13. Smooth terms, adjusted R-squared and evaluation statistics for the Razorbill distribution models. F statistics and the approximate significance for the smooth terms and t-statistic and the significance for the parametric terms are shown. Variables not included in either the presence/absence or positive model part are indicated with a dash. The evaluation test did not converge due to low sample size. 'n.s.' indicates terms with p-values < 0.05. The significant effect of the windfarms are marked in bold.

| Smooth terms | Presence/absence | | | Positive density | | |
|-------------------------------|------------------|--------|-------|------------------|--------|-------|
| | F | p | | F | p | |
| Depth | 9.113 | 0.003 | | - | - | |
| Salinity | 0.09 | 0.764 | | - | - | |
| Current speed | 16.364 | 0 | | 3.939 | 0.048 | |
| Current gradient | - | - | | - | - | |
| Parametric terms | Estimate | t | p | Estimate | t | p |
| AIS | -0.003 | -1.131 | 0.258 | -0.003 | -1.71 | 0.088 |
| LUD WF parametric | -0.58 | -1.38 | 0.168 | -0.037 | -0.134 | 0.893 |
| PAWP WF parametric | -1.094 | -3.641 | 0 | -0.33 | -0.809 | 0.419 |
| OWEZ WF parametric | -0.314 | -0.978 | 0.328 | -0.273 | -0.969 | 0.333 |
| LUD (2 km buffer) parametric | -0.257 | -0.782 | 0.434 | 0.077 | 0.402 | 0.688 |
| PAWP (2 km buffer) parametric | -0.391 | -1.644 | 0.1 | -0.251 | -1.079 | 0.281 |
| OWEZ (2 km buffer) parametric | -0.34 | -1.473 | 0.141 | 0.077 | 0.402 | 0.688 |
| Survey 5 | -1.224 | -3.047 | 0.002 | -0.951 | -1.416 | 0.157 |
| Survey 6 | -1.563 | -3.128 | 0.002 | -1.459 | -1.588 | 0.113 |
| Survey 7 | 2.389 | 4.658 | 0 | -0.1 | -0.283 | 0.777 |
| Survey 8 | -2.926 | -6.032 | 0 | -1.804 | -1.93 | 0.054 |
| Survey 9 | -1.58 | -4.254 | 0 | -0.644 | -1.305 | 0.193 |
| Survey 10 | -0.38 | -1.01 | 0.312 | -1.355 | -3.202 | 0.001 |
| Survey 11 | -0.059 | -0.114 | 0.909 | -0.13 | -0.255 | 0.799 |
| Survey 12 | 1.06 | 2.21 | 0.027 | -0.482 | -1.446 | 0.149 |
| Survey 13 | 0.844 | 2.101 | 0.036 | -1.108 | -3.16 | 0.002 |
| Survey 14 | 1.951 | 4.931 | 0 | -1.055 | -3.62 | 0 |
| Survey 15 | 0.147 | 0.299 | 0.765 | -1.512 | -4.078 | 0 |
| Survey 16 | -0.206 | -0.361 | 0.718 | -0.547 | -1.43 | 0.153 |
| Survey 17 | 0.966 | 1.569 | 0.117 | -0.104 | -0.29 | 0.772 |
| Survey 18 | -0.747 | -1.658 | 0.097 | -1.127 | -2.766 | 0.006 |
| Survey 19 | - | - | - | - | - | - |
| Survey 20 | - | - | - | - | - | - |
| Survey 21 | 1.922 | 3.99 | 0 | -0.223 | -0.785 | 0.433 |
| Survey 22 | 1.069 | 2.401 | 0.016 | -0.823 | -2.583 | 0.01 |
| Survey 23 | 0.161 | 0.333 | 0.739 | -0.708 | -1.896 | 0.059 |
| Survey 24 | 0.479 | 1.385 | 0.166 | -0.399 | -1.259 | 0.209 |
| Survey 25 | 0.086 | 0.203 | 0.84 | -0.451 | -1.296 | 0.196 |
| Survey 26 | 1.195 | 1.913 | 0.056 | -0.679 | -2.293 | 0.022 |
| Survey 27 | 2.192 | 5.979 | 0 | -0.364 | -1.277 | 0.202 |
| Survey 28 | -0.352 | -0.64 | 0.522 | -0.226 | -0.59 | 0.556 |
| Sample size (n) | 10,025 | | | 519 | | |
| Adjusted R ² | 7.5% | | | 3.4% | | |
| AUC | | | | | | |
| Spearman's corr. | | | | | | |

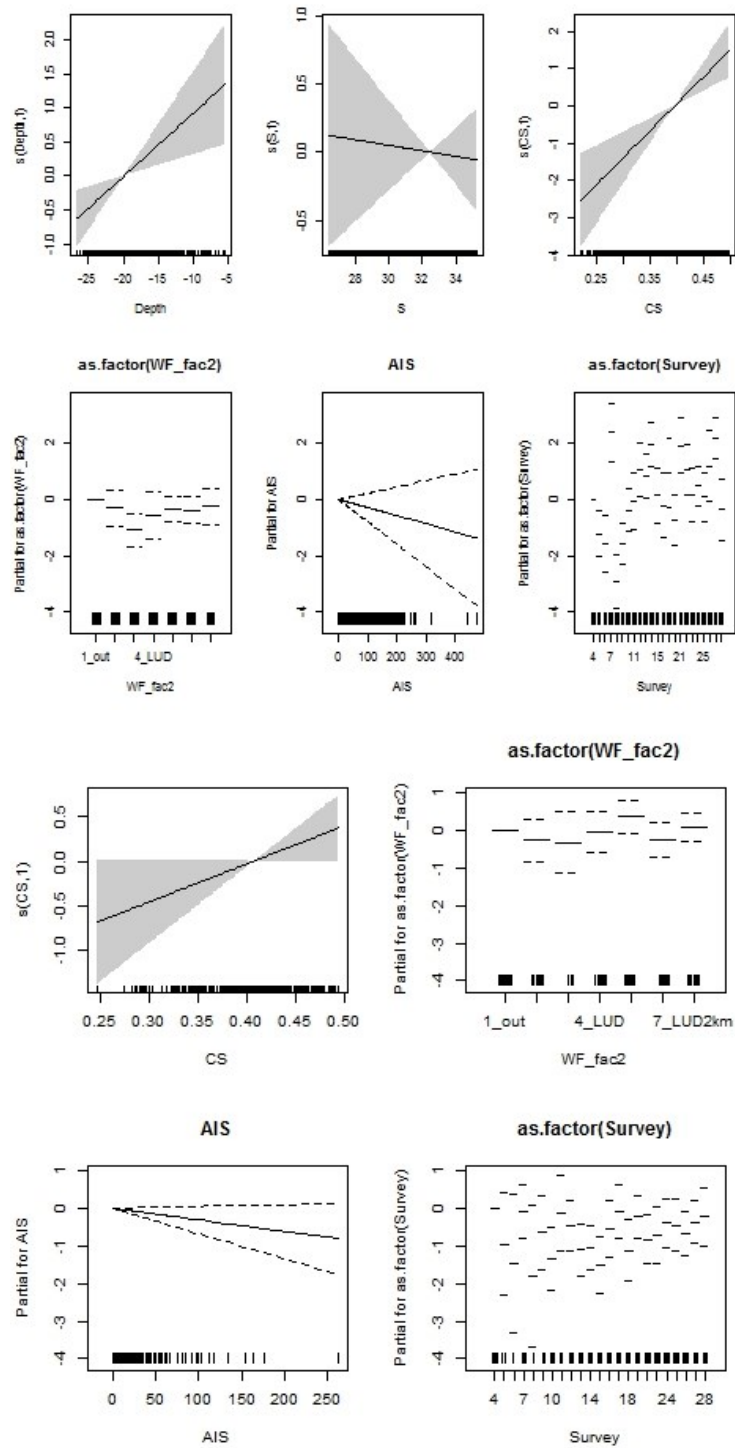


Figure A13. Partial GAM plots for the Razorbill distribution model – presence-absence (upper panel) and positive density (lower panel) parts. The values of the environmental variables are shown on the X-axis and the probability on the Y-axis in the scale of the linear predictor. The grey shaded areas and the dotted lines (for factors) show the 95% Bayesian confidence intervals. The degree of smoothing is indicated in the legend of the Y-axis.

